Title
A New Statistical Framework for Estimating Carbon Monoxide Impacts at Intersections

Author
Meng, Yu

Publication Date
1998-03-01

A New Statistical Framework for Estimating Carbon Monoxide Impacts at Intersections

By

Yu Meng
B.S. (Xian University of Technology, China) 1991
M.S. (China Academy of Railway Science, China) 1994

DISSERTATION

Submitted in partial satisfaction of the requirements for the degree of

DOCTOR OF PHILOSOPHY

In

Civil and Environmental Engineering
in the
OFFICE OF GRADUATE STUDIES
of the
UNIVERSITY OF CALIFORNIA
DAVIS

Approved:

_____

_____

_____

_____

Committee in Charge

1998

Yu Meng
March 1998
Civil and Environmental Engineering

A New Statistical Framework for Estimating Carbon Monoxide Impacts at Intersections

Abstract

The computer program CAL3QHCR has been recommended by the U.S. Environmental Protection Agency (EPA) for modeling carbon monoxide (CO) concentrations at intersections. EPA's guidelines for modeling CO concentration ([CO]) levels at roadway intersections outline a procedure to identify intersections that should undergo a more detailed CO analysis by running CAL3QHCR, and this procedure uses intersection level-of-service (LOS) as one of its major defining factors.

However, it is possible that intersections can exhibit the same intersection LOS but different levels of [CO], depending on factors such as intersection orientation, intersection geometry, total traffic volume, local meteorological condition (e.g. wind speed and wind direction), and emission factors.

A new statistical framework for determining whether an intersection should be modeled for CO emission impact using CAL3QHCR and for estimating [CO] levels is presented for use at the intersection design level. The proposed statistical framework is based on not only the intersection LOS (as EPA's current criterion) but also on other major modeling factors, such as intersection orientation, intersection geometry, traffic volume, wind speed, wind direction, and vehicle emission factors, to predict [CO] levels.

The proposed statistical model is much simpler than CAL3QHCR so that it can be used by traffic engineers at the intersection design level to approximate the [CO] level. Ideally then any potential exceedance could be mitigated at the design level. In addition, the new statistical model better represents the potential of CO exceedance than EPA's current LOS D criterion.

The dependent variable, modeled [CO] level, used in this study is the output of the computer program CAL3QHCR rather than actual measured field [CO]. Thus, we are assuming that CAL3QHCR is a "perfect" model for estimating [CO] at intersections. In addition, a hypothetical typical urban traffic pattern rather than real traffic data was used in developing the statistical models. Therefore, the proposed models might not be applicable to areas that have a different traffic pattern from the one used in this study.

_____

Major Advisor

Debbie A. Niemeier

TABLE OF CONTENTS

LIST OF FIGURES

LIST OF TABLES

1.0 BACKGROUND

The Federal Clean Air Act of 1970 produced a legislative mandate to improve air quality in certain metropolitan areas by controlling emissions, among others, produced by vehicles (41). As a follow-up, the Federal Clean Air Act Amendments (CAAA) of 1990 and the Intermodal Surface Transportation Efficiency Act (ISTEA) of 1991 contain provisions requiring the coordination of transportation investments and air quality standards (32&36). Over the past twenty years, coordination between transportation planning and air quality modeling has improved both in terms of policy and practice.

Many studies have focused on developing vehicular emission rate models and vehicular emission dispersion models. In terms of vehicular emission rate models, one of the major developments has been a better understanding of the relationship among different quantities of pollutant emissions and the factors related to different vehicle technological and maintenance characteristics (34). It is now clear that the vehicle pollutant emission levels are dependent not only on the number of trips and the number of miles traveled, but also on other factors as well. These other important determinants include many well known characteristics such as travel speed, ambient temperature, emissions control technology, vehicle type, and vehicle operating characteristics (1&34). Many recent studies have improved the ability of vehicular emission rate models to characterize emissions from vehicles operating in real world conditions. The recent studies include: driver variability's impacts on vehicular emission rates (15) and a better estimation of emissions directly related to vehicle operating modes (1) such as idle, steady-state cruise, and various levels of acceleration/deceleration. Currently, the on-road

vehicular composite emission rates are estimated by the California EMFAC series models (within California) and the MOBILE series models (for the remaining 49 states).

In terms of vehicular emission dispersion models, one of the most widely used models is the CALINE series model. The vehicular pollutant dispersion models estimates air pollutant concentrations resulting from vehicles on traffic roadways, given the on-road vehicular composite emission rates, meteorology and site geometry. The CALINE series models assume that vehicular emissions from traffic roadways can be represented by a "line source" and disperse in a Gaussian distribution (2 & 3). The California Department of Transportation (Caltrans) published the first CALINE series model in 1972, and it was replaced by CALINE2 in 1975. Because of the over-predictions by CALINE2 under certain situations (e.g. stable, parallel wind directions) (2), CALINE3 was released in 1980. CALINE3 uses the same Gaussian dispersion methodology but different vertical and horizontal dispersion curves modified for the effects of surface roughness, averaging time, and vehicle-induced turbulence (2). Also, the concepts of mixing zone and equivalent finite line source were introduced into CALINE3 (2). The latest released version of CALINE models is CALINE4, which is an updated and expanded version of CALINE3. The real differences between CALINE3 and CLINE4 are in the areas of improved input/output flexibility and expanded capabilities (e.g. special options for street canyon/bluff effects and parking facilities are provided in CALINE4). There are still many studies underway to improve the dispersion models. A recent study conducted by UC Davis (16) states that under slight wind or calm and stable conditions, CALINE3 or CALINE4 cannot fully account for the "extent of the vertical dispersion or the buoyant

rise of the plume" and is believed to over-predict ground level carbon monoxide concentration ([CO]) near congested traffic roadways as a result.

In addition to CALINE series models, several other models have been developed to estimate [CO] near intersection in the last decade. These models include IMM (Intersection Middle-block Model), GIM (Georgia Intersection Model), EPAINT (EPA Intersection), FHWAINT (FHWA Intersection) and TEXIN2 (Texas Intersection) (6, 23, 24, 28, 30, 31, and 39). These models and CALINE series models differ in their analysis of emission rate and CO dispersion algorithm along roadway segments (28). More detailed comparison of these models can be found in Table V of Reference 28 and Reference 39. A recent evaluation study of CO intersection modeling techniques using a New York City database conducted by the U.S. EPA indicates that CALINE requires less user inputs and produces more accurate [CO] levels at intersection (39).

CAL3QHC and CAL3QHCR are computer programs that incorporate the CALINE3 line source dispersion model and a traffic algorithm for estimating the number of vehicles queued at an intersection (10). CAL3QHCR has been recommended by EPA for modeling [CO] at intersections. CAL3QHCR accepts large meteorological data files and also requires substantial user inputs: emission factors, hourly traffic volume, signalization data, intersection geometry, receptor locations, and hourly meteorological data such as wind speed, wind direction, ambient temperature, and atmospheric stability class. CAL3QHCR has been used in many project level analyses in accordance with State Implementation Plans (SIPs) and conformity analyses. Because of its input complexity, in EPA's Guideline for Modeling CO from Roadway Intersections, CO impact analyses by CAL3QHCR are not required for the intersections operating at Level

of Service (LOS) A, B, or C. The Guideline states that "…the delay and congestion [at intersections that are LOS A, B, or C] would not likely cause or contribute to a potential exceedance of the NAAQS (National Ambient Air Quality Standards)" (38). Intersection LOS is a measure of traffic volume, signal timing, and related congestion and delay. It is only dependent on the averaged stopped delay (ASD) per vehicle at the intersection (35). That is, in determining "critical" intersections in terms of CO impacts, EPA uses LOS/ASD as one of the major defining characteristics. However, a recent study conducted by UC Davis (17&18) showed that there are other major factors beyond LOS/ASD that have significant impacts on the modeled [CO] at intersections. These factors include intersection orientation, intersection geometry, and traffic volume. Very few studies have been conducted to develop an appropriate framework for determining critical intersections in terms of CO impacts. It is clear now that EPA's current LOS criterion for determining the critical intersections in terms of CO impacts is not appropriate under certain situations as will be discussed in Section 4.3.

In addition, there has been an increasing need for a linkage between the transportation planning and design process and the transportation air quality conformity process (11&12). The risk of the lack of this linkage is that a transportation project could move through the project approval process from the traffic perspective by Metropolitan Planning Organization (MPO) or Regional Transportation Planning Agency (RTPA) but fails the subsequent air quality conformity test. The failure may generate additional analyses and potential project redesign costs. The risk of additional costs leads to a call for a method of detecting the potential air quality conformity failure at the transportation project planning and design level. The Pennsylvania Department of Transportation

(PennDOT) developed a firm linkage between the planning and design process and the air quality conformity process for ozone analyses (12). To date, however, there has been no comprehensive study to develop a method for CO analyses at the transportation project planning and design level.

2.0 INTRODUCTION

2.1 Preface

Level of Service (LOS) at signalized intersections is defined in the Highway Capacity Manual (HCM) as " the average stopped delay per vehicle for a 15-min analysis period (35)." It is a measure of "driver discomfort and frustration and lost travel time (35)." The LOS criteria for intersections are based upon the average stopped delay (ASD) per vehicle. Many transportation agencies have identified a specific LOS that is considered acceptable and these values are part of the general plans, ordinances and other regulations, although local standards for guiding the development of the transportation system may vary.

Recently, the LOS measures have also been used to determine the intersections required for modeling of carbon monoxide (CO) conformity impacts. Specifically, the Environmental Protection Agency's (EPA) guidelines for modeling [CO] levels at roadway intersections states that (38):

> …As part of the procedure for determining critical intersections, those intersections [operating] at LOS D, E, F or those that have changed to LOS D, E, or F because of increased volumes of traffic or construction related to a new project in the vicinity should be considered for modeling. Intersections that are LOS A, B, or C probably do not require further analysis, i.e., the delay and congestion would not likely cause or contribute to a potential CO exceedence of the NAAQS [National Ambient Air Quality Standards].

The application of this rationale is shown in Figure 2.1. This rationale assumes that for intersections operating at LOS A, B, or C there is no need to model [CO] with CAL3QHCR. Further, there is also another important, but implicit assumption made

when intersection LOS is used as a defining characteristic. This assumption is that the ASD is the only major factor contributing to the [CO] modeled near roadway intersections. However, as we will show the ASD is not always representative of CO emission impacts (Section 4.3). It is possible that intersections can exhibit relatively similar ASDs but different [CO] levels, depending on such factors as traffic volume, the orientation of the intersection, intersection geometry, emission factors and meteorological factors such as wind speed and atmospheric stability class. It is also possible that an intersection operating at LOS C with the potential for exceeding the NAAQS is approved under the current EPA's guideline (Step 3 in Figure 2.1). Moreover, the use of LOS criteria for CO modeling implies a point estimate of the ASD rather than the range estimate it actually represents. That is, for a certain LOS we can have a range of ASD (e.g., ASD ranges from 25 seconds to 40 seconds for LOS D). It is possible that intersections operating at the same LOS but different ASD may result in different CO emission levels. Additionally, at Step 3 in Figure 2.1, if an intersection design exhibits a potential exceedence of the NAAQS after running CAL3QHCR, the intersection must be redesigned (Step 1). The iteration of Step 1 and Step 2 will likely cost a substantial amount of time and money. Or vice versa, considerable resources could be spent in detailed modeling of an intersection operating at LOS D (Step 3) that will not exceed NAAQS.

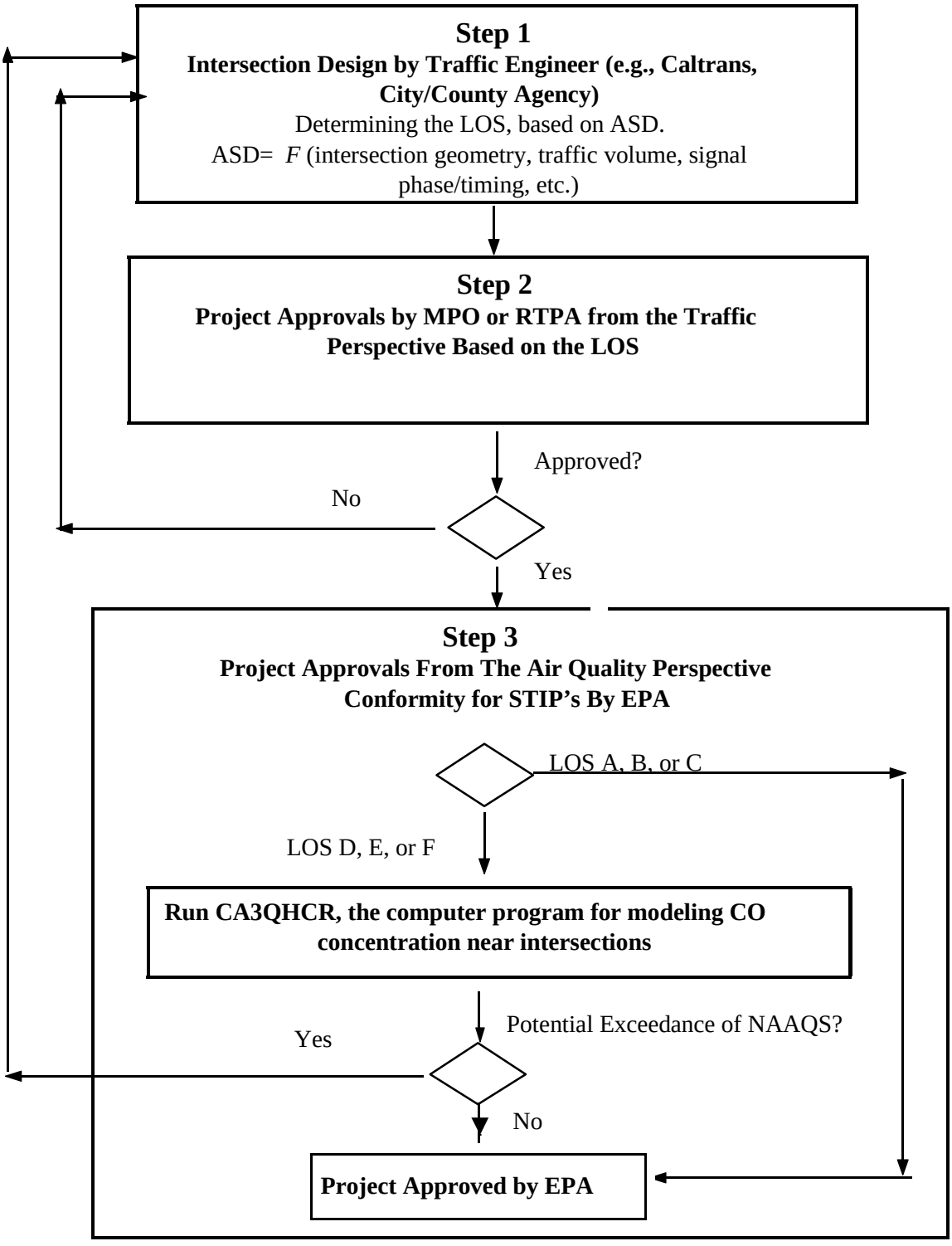

Figure 2.1 Application of EPA's LOS Criterion

2.2 Research Objectives and Hypotheses

As concern over air quality increases, there is a need for a better theoretical and empirical framework for determining whether a certain intersection should be modeled for the potential CO exceedence of the NAAQS. This framework should take into account impacts from not only the ASD but also other major factors that contribute to the predicted [CO] at intersections. This new method should provide more precise information on the potential for CO exceedence of the NAAQS. In addition, the proposed framework should be relatively simple to use so that any potential exceedence of the NAAQS could be detected by traffic engineers at Step 1 (the design process) rather than being detected at Step 3 (Figure 2.1).

The major objectives of this study are:

- to define the relationship between the modeled [CO] and each individual major factor that contributes to the predicted [CO] near roadway intersections;
- to develop a new statistical model expressing the relationship between the [CO] predicted by CAL3QHCR and the major modeling factors such as ASD, orientation of the intersection, intersection geometry, emission factors and meteorological factors, such as wind speed, surface roughness length, stability class, and ambient temperature.

The study hypotheses are stated as:

- There are other major factors beyond the ASD such as orientation of the intersection, intersection geometry, emission factors, and meteorological factors that contribute to the modeled [CO] at intersections;

- The proposed statistical model will better represent the potential exceedence of NAAQS than EPA's current LOS criterion.

2.3 Contributions of This Study

This study will contribute to air quality-transportation research by developing an improved framework for determining whether an intersection should be modeled for CO emission impact (Step 3 in Figure 2.1). This study will identify the major modeling factors that contribute to the modeled [CO] at intersections and based on these factors, develop a new statistical model to predict [CO] at intersections.

The study will also contribute to the literature by improving our understanding of the relationship between the modeled [CO] and each individual factor by identifying the sensitivity of modeled [CO] to each factor (Section 4.3 and 5.1), thereby assessing the degree of accuracy to which factors need to be estimated. A better understanding of the degree of accuracy to which factors need to be estimated will avoid the waste of time and effort at the input data collection level.

The final contribution is that the new statistical model developed in this study can be used by traffic engineers at the intersection design level (Step 1 in Figure 2.1) to predict the potential exceedence of the NAAQS. This development effort could save a substantial amount of effort and money often wasted in the iteration of Step 1 and Step 2 in Figure 2.1.

2.4 Organization of This Dissertation

The remainder of this dissertation is divided into six chapters. Chapter 3 conducts a review of the algorithm used in the Highway Capacity Software (HCS) Release 3.0, a

computer program to implement the procedures contained in the 1994 HCM, for calculating the ASD and LOS and the algorithm used in CAL3QHCR for estimating queue length and predicting [CO]. Chapter 4 begins with a presentation of the data setting in the preliminary study and the limitations of EPA's current rationale for determining whether a certain intersection should be modeled for CO emission impact. This is followed by a presentation of the preliminary results of examining the possible relationships between the modeled [CO] and several different factors. Chapter 5 represents the relationship between the modeled [CO] and each individual factor. Chapter 6 describes the approach for the statistical modeling and the discussion of the development of the new statistical models. Chapter 7 presents a discussion of model choice between the proposed statistical models, model validation, and study limitations. Finally, conclusions are given in Chapter 8.

3.0 CALCULATING THE ASD AND MODELING [CO]

In the first section of this chapter, the algorithm used in HCM for calculating the ASD is presented. In the second section, the discussion turns to the algorithm used in CAL3QHCR to estimate vehicle queue length at signalized intersections. The third section focuses on CALINE3, the dispersion algorithm used in CAL3QHCR to model [CO]. Finally, a discussion on the additional input requirements by CAL3QHCR, beyond those required in computing ASD by HCS and estimating queue length by CAL3QHCR, are presented.

3.1 HCM Algorithm for Calculating the ASD

The HCM computation of ASD depends on a number of variables. These variables are summarized in Table 3.1.

Table 3.1 Input Requirements by HCS

Traffic volume/arrival rate	Intersection geometry (e.g. # of lanes and lane width)
Right turns on red	Signalization data (signal type, phase, and timing)
Progression rate	the mix (classification of vehicles by size) of vehicles
Adjacent parking lane	bus stop and conflicting pedestrian activities per hour

Intersection LOS is directly related to the ASD using the criteria specified in HCM 1994 and summarized in Table 3.2.

Table 3.2 LOS Criteria for Signalized Intersection (35)

Level of Service	ASD Per Vehicle (Sec.)
A	< = 5.0
B	> 5.0 and < = 15.0
C	> 15.0 and < = 25.0
D	> 25.0 and < = 40.0
E	> 40.0 and < = 60.0
F	> 60.0

In the modeling of [CO] in CAL3QHCR, a *link* is defined as a group of lanes having a constant width and emission source strength (10). This may differ slightly from the *lane group* concept used by HCM, which is defined as a group of lanes having a common stop line and capacity shared by all vehicles (35). For the purpose of this study, we will consider links and lane groups as interchangeable. In the LOS module of HCM (1994), the ASD per vehicle is estimated for each lane group (link) and averaged first for approaches and then for the intersection as a whole. For example, in the intersection depicted in Figure 4.1 there are nine links: EB left (link 1), EB through (thru) (link 2), EB right (link 3), WB left (link 4), WB through and right (link 5), NB left (link 6), NB through and right (link 7), SB left (link 8), and SB through and right (link 9).

The ASD per vehicle for a given lane group is given by Equation 3.1 (35):

$$d = d_1 \times DF + d_2 \tag{3.1}$$

$$d_1 = 0.38C[1-(g/C)]^2 / \{1-(g/C)[Min(X,1.0)]\}$$

$$d_2 = 173X^2\{(X-1)+[(X-1)^2+mX/c]^{0.5}\}$$

where:

d = the ASD per vehicle
d_1 = uniform delay, an estimate of delay assuming perfectly uniform arrivals and stable flow
d_2 = incremental delay, an estimate of the incremental delay due to non - uniform arrivals
DF = delay adjustment factor, accounts for the impact of control type and signal progression on delay
X = volume to capacity ratio (v/c) for lane group
C = cycle length
c = capacity of lane group
g = effective green time for lane group
m = an incremental delay calibration term representing the effect of arrival type and degree of platooning

3.2 Algorithm for Estimating Queue Length

Micro-scale [CO] analysis is conducted using CAL3QHCR. The model combines the "CALINE3 line source dispersion model and a traffic algorithm for estimating vehicle queue length at signalized intersections (10)." In this section, the traffic algorithm for estimating queue length is presented. The inputs required for estimating queue length in CAL3QHCR include:

- traffic volume/vehicle arrival rate;
- intersection geometry;
- saturation flow rate; and
- signalization data.

Estimating the queue length in CAL3QHCR does not require *right turns on red*, *the mix of vehicles*, *adjacent parking lane*, or *bus stop and conflicting pedestrian activities* as inputs, but instead requires *saturation flow rate*. In contrast, HCS automatically adjusts the ideal saturation flow rate, 1900 veh/hour-lane, by the adjustment

factors based on right turns on red, the mix of vehicles, adjacent parking lane, and bus stop and conflicting pedestrian activities. Therefore, in estimating queue length in CAL3QHCR, the task of adjusting the saturation flow rate is left for the user and the adjusted saturation flow rate the required direct input from the user. This difference in input requirement between HCS in computing ASD and CAL3QHCR in estimating queue length partially accounts for the fact that the impact of ASD, rather than the queue length, on the modeled [CO] will be examined in CAL3QHCR modeling.

For under-saturated conditions (i.e., volume to capacity ratio, *v/c*, is less than one, the queue is estimated by Equation 3.2 (35):

$$N_u = Max[q \times D + (r/2) \times q, q \times r] \tag{3.2}$$

$$D = d \times F_c$$

where:

N_u = average number of vehicles queued per lane at the beginning of green phase
q = vehicle arrival rate per lane
D = the average approach delay
r = the length of the red phase
d = the ASD per vehicle, as specified in equation 1
F_c = stopped delay to approach delay conversion factor (1.3)

For over-saturated conditions (i.e., volume to capacity greater than one), the queue is estimated by Equation 3.3 (35):

$$N_o = Max[q^* \times D^* + (r/2) \times q^*, r \times q^*] + \tfrac{1}{2}(v - c) \tag{3.3}$$

where:

N_0 = average number of vehicles queued per lane at the beginning of the green phase
q^* = vehicle arrival rate per lane during at - capacity operating conditions (i.e., v/c = 1)
D^* = average approach delay during at - capacity operating conditions (i.e., v/c = 1)
v = lane group traffic volume
c = lane capacity
r = the length of the red phase

3.3 Dispersion Algorithm in CAL3QHCR - CALINE3

There are some additional input requirements in CAL3QHCR, beyond those required to estimate queue length, to model [CO]. These additional input requirements include:

- emission factors for the vehicle mix being modeled;
- receptor locations; and
- meteorological data, such as wind speed, wind direction, stability class, surface roughness, and ambient temperature.

3.3.1 Emission Sources

The dispersion module in CAL3QHCR, CALINE3, treats the roadway links as linearly distributed emissions and processes them as "line sources." Separate user-specified emission factors for free-flow links and queue links are required in CAL3QHCR. Emissions from free-flow vehicles are computed using a composite free-flow emission rate for the length of the link, which is dependent on the average link speed and percent of cold/hot start. Emissions from queued vehicles are computed using the duration of the idling time and the idling emission rate, which is dependent on the percent of cold/hot starts. Both the free-flow emission rate in grams per vehicle-mile and queue emission rate in grams per vehicle-hour are usually estimated by EMFAC series models in California or MOBILE series models in other states.

The total line source strength for a free-flow link is given by Equation 3.4 (35):

$$q_1 = 0.1726 \times VPH \times EF \tag{3.4}$$

where:

q_1 = total free - flow line source strength, in micrograms per meter - second
0.1726 = conversion factor from grams per mile - hour to micrograms per meter - second
VPH = traffic volume, in vehicles per hour
EF = free - flow emission factor, in grams per vehicle - mile

The total line source strength for queue link is given by Equation 3.5 (35):

$$q_2 = 21.6 \times N \times n \times EF \times (r/C) \tag{3.5}$$

where:

q_2 = total idling line source strength, in micrograms per meter - second
21.6 = conversion factor from grams per vehicle - hour to micorgrams per meter - second
N = average number of vehicles queued per lane, as specified in equation 3.2 and 3.3
n = number of lanes
EF = idling emission factor, in grams per vehicle - hour
r = red time during the signal cycle
C = signal cycle length

3.3.2 Predicting [CO] by Finite Line Source Gaussian Formula

In CALINE3, each individual link is divided into a series of elements and each element is processed as an equivalent (i.e., the emission rate is assumed to be uniform throughout the element) finite line source (FLS). The concentration attributable to each FLS is computed by Gaussian formulation and the program automatically sums the concentration from each FLS to each receptor (3). The first element is a square with sides equal to link width. Subsequent elements are formed as rectangles with the width equal to the link width. The length of the rectangle increases as the distance from the receptor increases (3). So the elements further away from the receptor become less important.

The determination of lengths of elements of an individual link is given by Equation 3.6 (3):

$$EL = W \times BASE^{NE} \tag{3.6}$$

where:

EL = element length
W = link width
NE = element number (0 for the first element)
$BASE$ = element growth factor

$$BASE = 1.1 + (PHI^{3} / 2.5 \times 10^{5})$$

PHI = relative angle between roadway link direction and wind direction in degrees

Figure 3.1 is an illustration of dividing an individual link into elements.

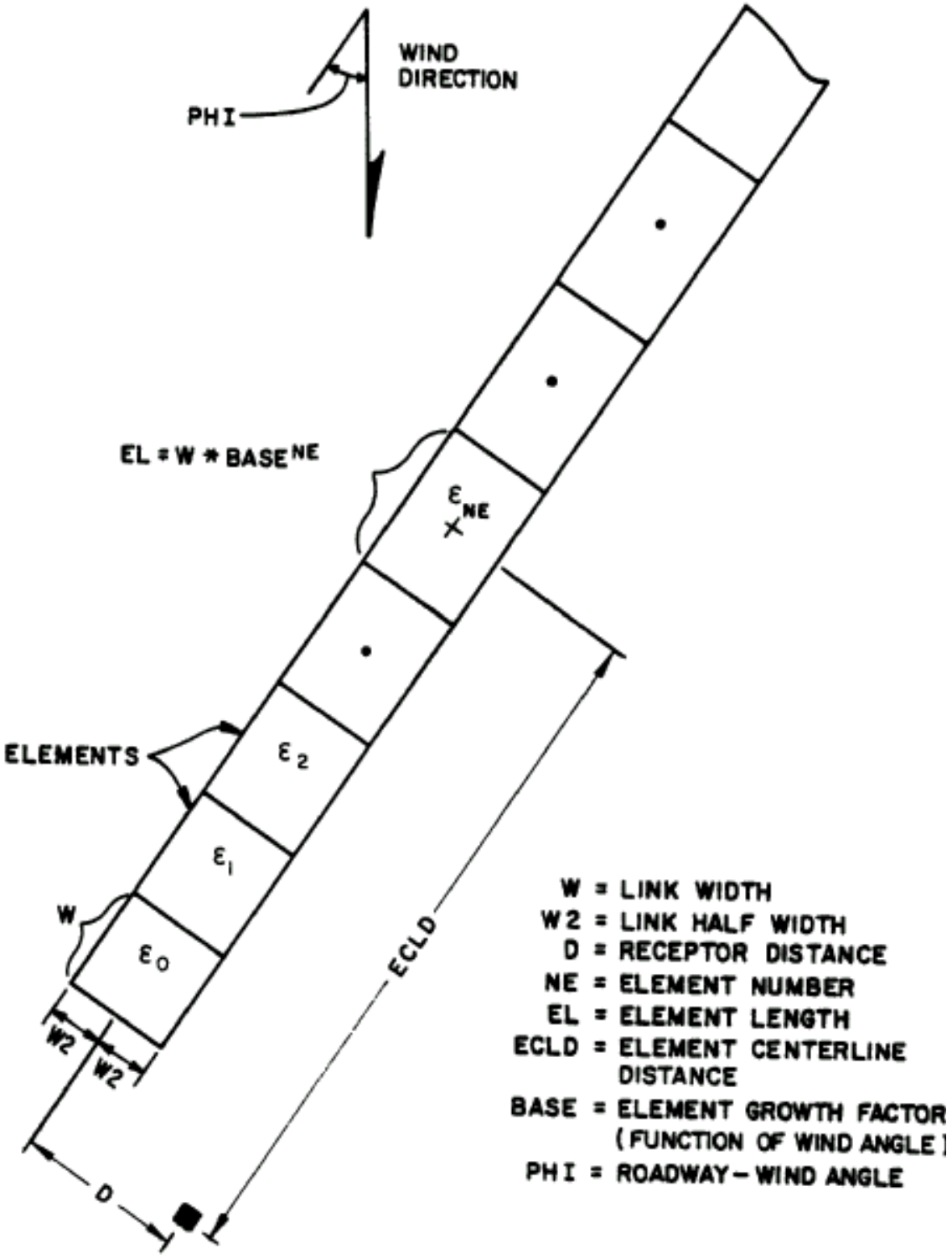

Figure 3.1 Element Series Used by CALINE3 (Source: reference 3)

Each element is processed as an equivalent FLS, and each FLS is centered at the midpoint of the element and perpendicular to the wind direction (3) as shown in Figure 3.2. In addition, “the emissions occurring within an element are assumed to be released along the FLS representing the element (3).” The length and orientation of each FLS are dependent on the element size and the relative angle between element direction and wind direction (3) as shown in Figure 3.3.

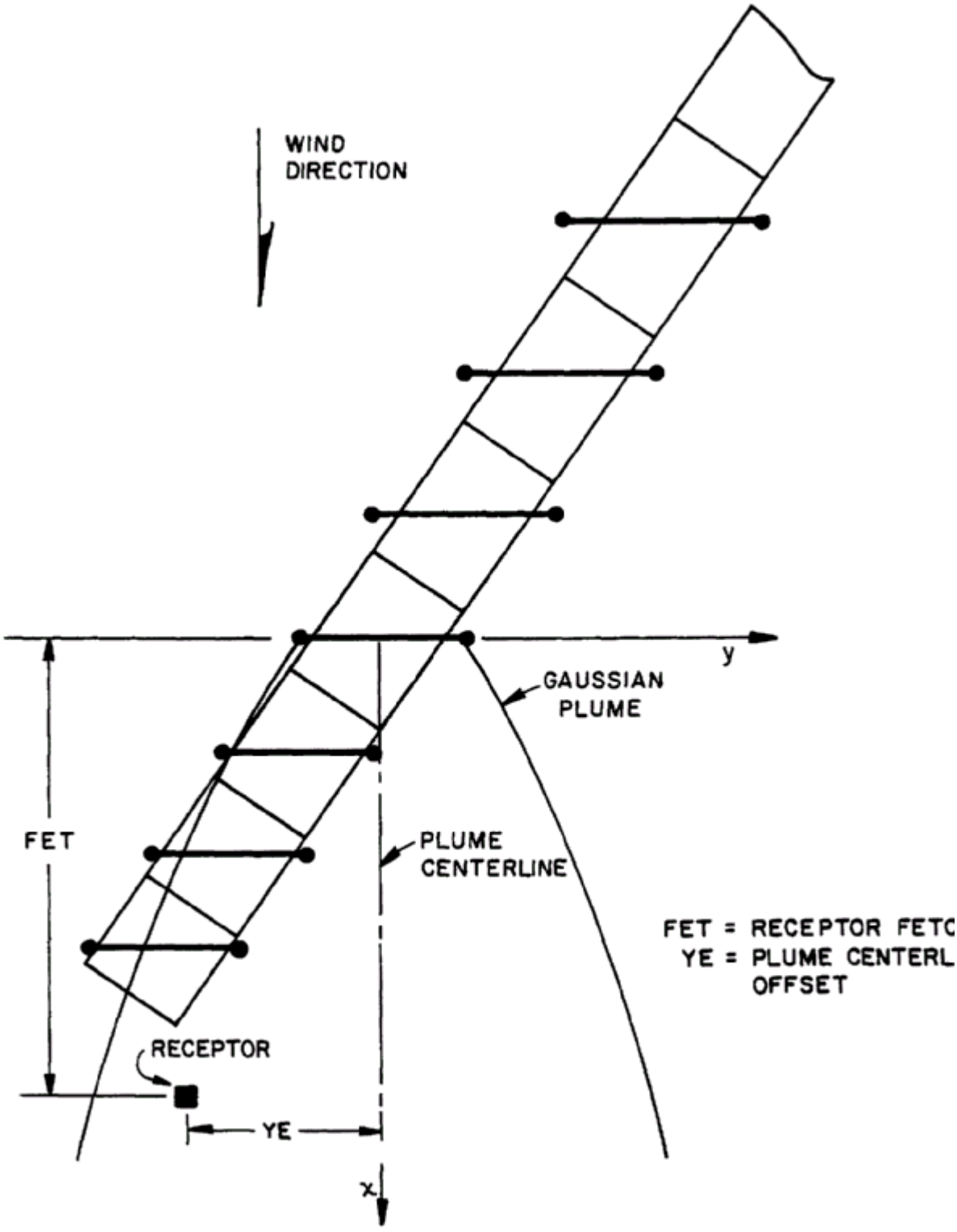

Figure 3.2 Element Series Represented by Series of FLS (Source: reference 3)

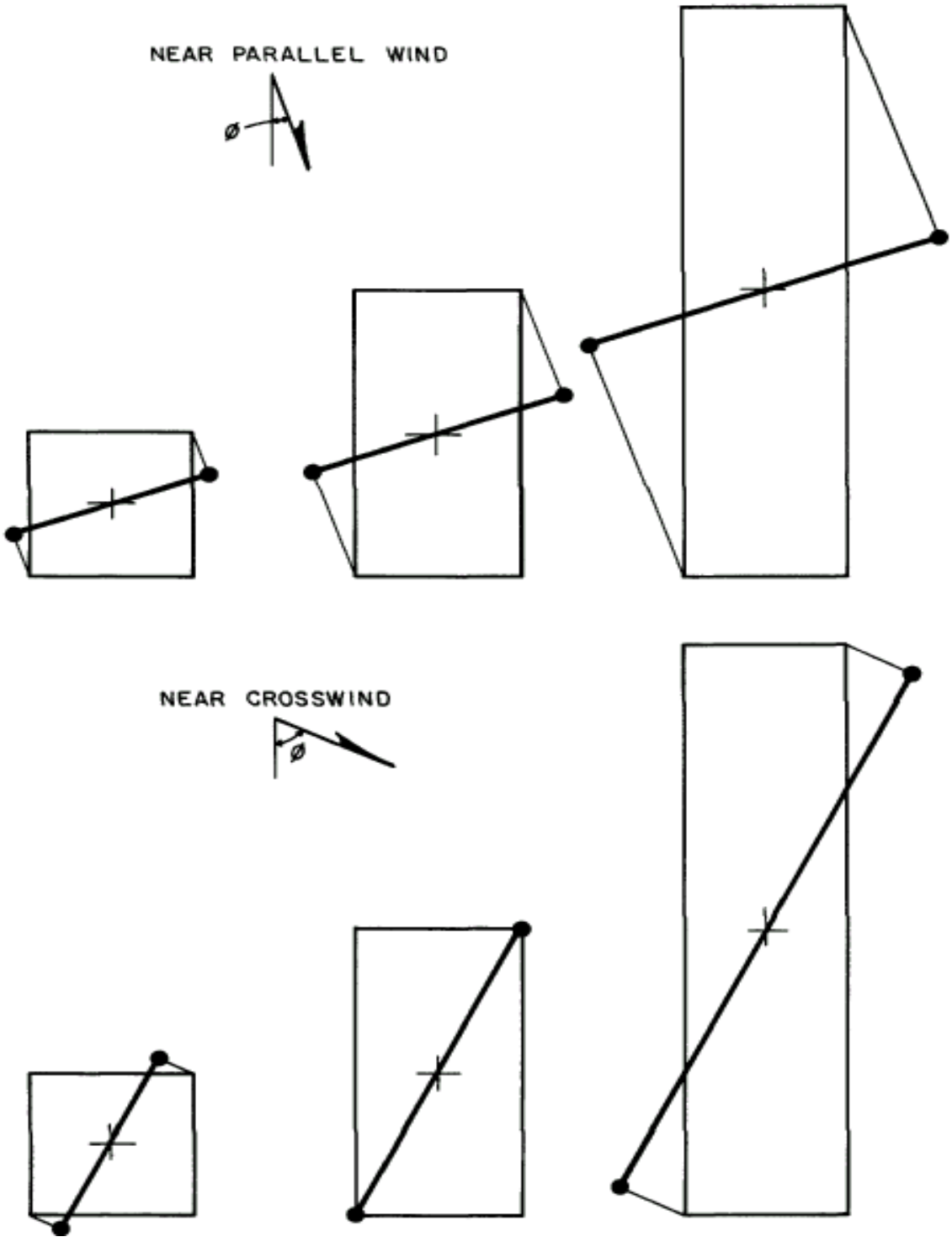

Figure 3.3 Equivalent FLS Presentation (Source: reference 3)

The modeled [CO] at a receptor, C(x, y, z), attributable to each FLS is given by the cross wind FLS Gaussian formulation (Equation 3.7) and shown in Figure 3.4 (3):

$$C = \frac{q}{2\pi\sigma_z u}\{\exp[\frac{-(Z-H)^2}{2\sigma_z^{\,2}}] + \exp[\frac{-(Z+H)^2}{2\sigma_z^{\,2}}]\}\int_{y_1/\sigma_y}^{y_2/\sigma_y} \exp(\frac{-p^2}{2})dp \qquad (3.7)$$

where:

$C(x, y, z)$ = concentration attributable to each FLS

q = uniform line source strength, as specified in Equation 3.4 and Equation 3.5

σ_z = vertical dispersion parameter

σ_y = horizontal dispersion parameter

u = wind speed

Z = receptor height

H = emission source height

y_1 = y coordinate of the staring point of FLS

y_2 = y coordinate of the ending point of FLS

$p = {}^{y}\!/_{\sigma_y}$

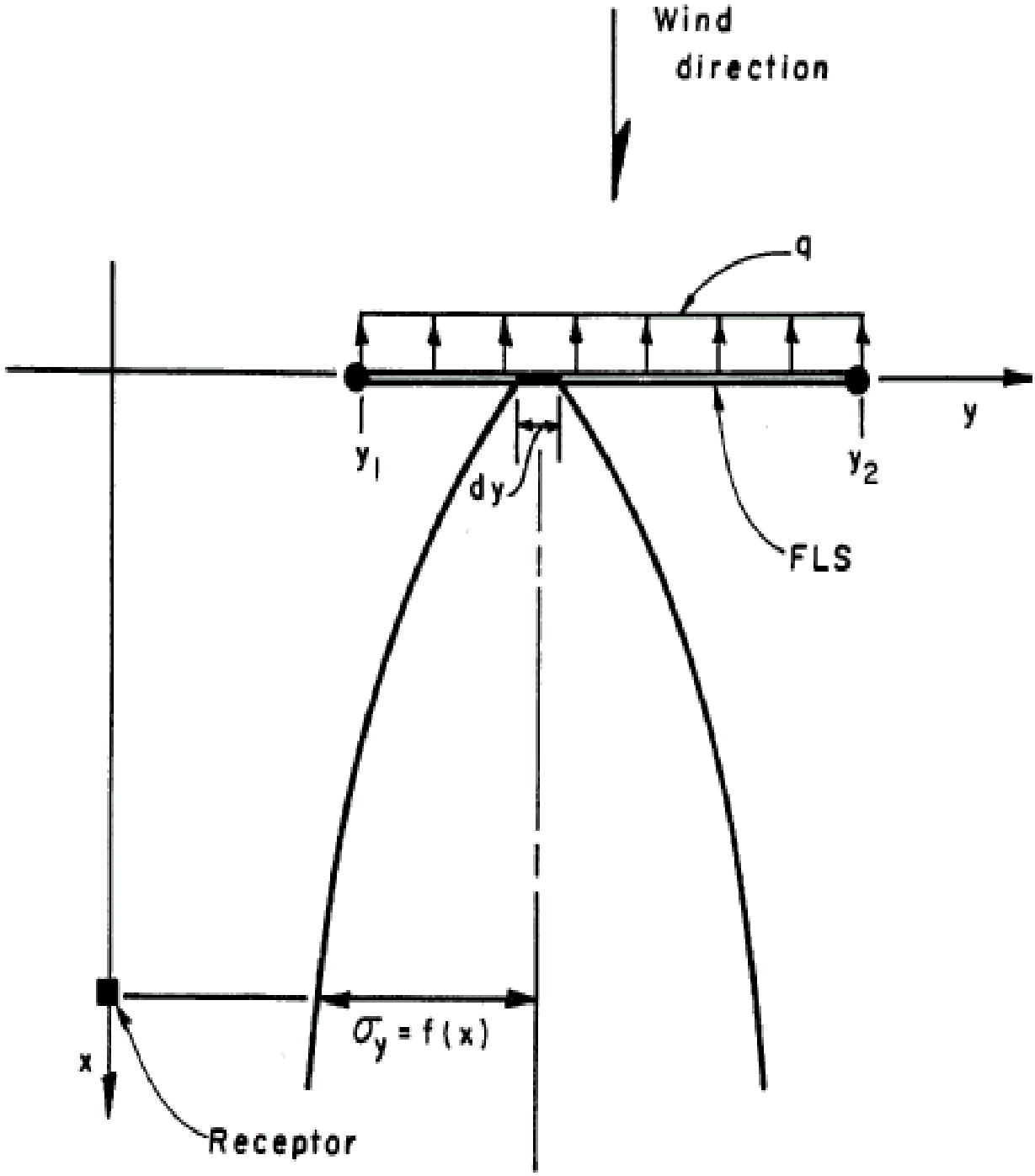

q = uniform line source strength

σ_y = horizontal dispersion parameter

x = receptor distance, measured along a perpendicular from the receptor to FLS centerline

Figure 3.4 Generalized Finite Line Source (Source: reference 2)

3.4 Additional Inputs Required in CAL3QHCR to Model [CO]

The input requirements for HCS and CAL3QHCR (the algorithm discussed in Section 3.1, Section 3.2, and Section 3.3) are summarized in Figure 3.5. Some additional inputs are required, beyond those required in estimating queue length or computing ASD, to model [CO]. These additional inputs include: emission factors required for computing line source strength, and wind speed, the relative angle between link direction and wind direction, surface roughness length, and ambient stability class required for estimating [CO] attributable to each FLS by Gaussian dispersion formulation. Each of these inputs will be discussed in more details in Section 4.3 and Section 5.1.

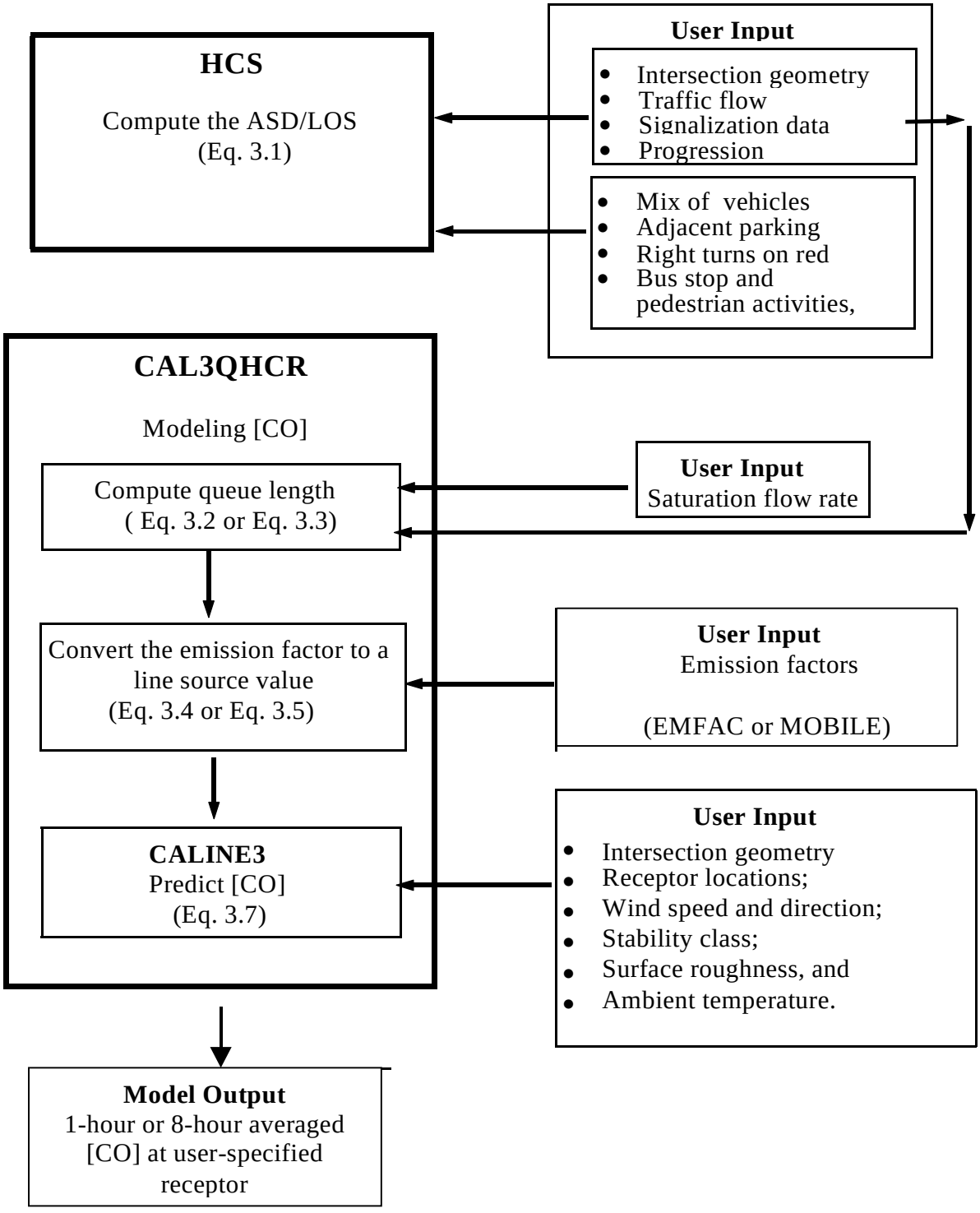

Figure 3.5 Additional User's Inputs to HCS and CAL3QHCR

4.0 DATA SETTING AND LIMITATIONS OF EPA's CURRENT RATIONALE - PRELIMINARY EVIDENCE

In the first section of this chapter, the user inputs to CAL3QHCR and HCS are discussed. The computation of ASD and the prediction of [CO] are discussed in the second section. Some limitations of EPA's current LOS criterion for determining whether an intersection should be modeled for CO impacts are presented in the third section. The preliminary findings are given in the last section of this chapter.

4.1 Data Setting in the Preliminary Study

The data inputs to the CAL3QHCR program include intersection geometry, receptor locations, emission factors, traffic data, signalization data, and location specific meteorological data. In this section, each of the major data input variables is discussed. Table 4.1 provides a summary of user inputs to CAL3QHCR. The table identifies the required input variables and the recommended (default) values specified in the CAL3QHCR User's Guide (10). In addition, the preliminary study input data values assigned to each variable are presented.

Table 4.1 Study Inputs to CAL3QHCR

User Input	CAL3QHCR Value	Study Value	Data Source
Meteorological Variables			
Wind Speed (m/s)	>= 1.0	local met. data	Worst-case for region
Stability Class	1 to 6 = A to F	local met. data	Worst-case for region
Gregorian Start Date	In month, day, year format	local met. data	Worst-case for region
Gregorian End Date	In month, day, year format	local met. data	Worst-case for region
Met. Data Surface ID	Year must equal End year	local met. data	Worst-case for region
Met. Data Upper Air ID	Year must equal Start year	local met. data	Worst-case for region
Background [CO] Flag	Included = 1, excluded = 0	0	3 ppm (assumed)
Intersection Variables			
Traffic Patterns	day of week pattern	CAL3QHCR	CAL3QHCR
Number of Links	maximum allowed = 20	17	HCM
Hourly Ave. Traffic Vol.	any real number	Table 4.4	HCM
Signal Cycle Length (Sec.)	any real number	92	LOS D Maintained
Red Phase Duration (Sec.)	any real number	Table 4.5	HCM
Lost Yellow Time	1 second	1 second	HCM
Saturation Flow Rate	1600 (veh/hr/lane)	1600 (veh/hr/lane)	CAL3QHCR
Signal Type	Pretimed=1;act.=2;semi-act.=3	1	HCM, conservative
Lane Width	10-12 ft.	12 ft.	CAL3QHCR
Arrival Rate	1~5=worst to best progression	3	HCM, conservative
Emission Factors			
Idle Emission Factor	Dependent on % of cold start	426.0 g/veh-hour	EMFAC, conservative
Free-Flow Emission Factor	Dependent on free-flow speed	23.0 g/veh-mile	EMFAC, conservative
General Variables			
Rural / Urban Switch	rural = R, urban = U	U	CAL3QHCR
Tier I II Approach Switch	Tier I = 1, Tier II = 2	2	CAL3QHCR
CO/PM Switch	CO = C, PM = P	C	CAL3QHCR
Number of Receptors	maximum allowed = 60	20	CAL3QHCR
Link Type	free-flow = 1, queue = 2	1, 2	CAL3QHCR
Source Height (m)	between -10 and 10	0	CAL3QHCR
Averaging Time (Minute)	30 or 60	60	CAL3QHCR
Surface Roughness (cm)	321 for CBD	321	CAL3QHCR
Settling Velocity (cm/s)	0	0	CAL3QHCR
Deposition Velocity (cm/s)	0	0	CAL3QHCR
Mixing Height (m)	1000	1000	CAL3QHCR

4.1.1. Intersection Geometry

In the preliminary study, a hypothetical four-leg, five-phase, fixed time intersection was simulated. The physical geometry of the hypothetical intersection is summarized in Table 4.2 and Figure 4.1. Note that only queue links are shown in Figure 4.1, while Table 4.2 covers both queue links and free-flow links. The origin (0,0) of the intersection coordinate system has been defined at the center of the intersection. The positive Y-axis is aligned due north and the positive X-axis is aligned due east.

There are two types of link that can be specified in CAL3QHCR: *free-flow* links where vehicles are assumed to be traveling without delay and *queue* links where vehicles are assumed to be in an idling mode of operation during some specified period of time. Consistent with the CAL3QHCR recommended coding, the starting point of each queue link is coded at the intercept of the centerline of the link with the respective approach stop-line and the starting point of each free-flow link is coded at the intercept of the centerline of the link with either the Y-axis or X-axis. The mixing zone width has been defined as the width of the traveled roadway (width of the lanes on which vehicles are idling) for *queue* links and the roadway width plus three meters on each side for *free-flow* links.

A total of seventeen roadway links were specified: nine queue links and eight free-flow links. There are three queue links for the east-bound (EB) approach, and two queue links for each of the west-bound (WB), north-bound (NB), and south-bound (SB) approaches. A separate queue link is assigned to the left-turn movement for all approaches. With the exception of the EB approach, all the right-turn movements share the right-most lane of the through link. One free-flow link has been assigned for each of

the intersection’s approach and departure legs.

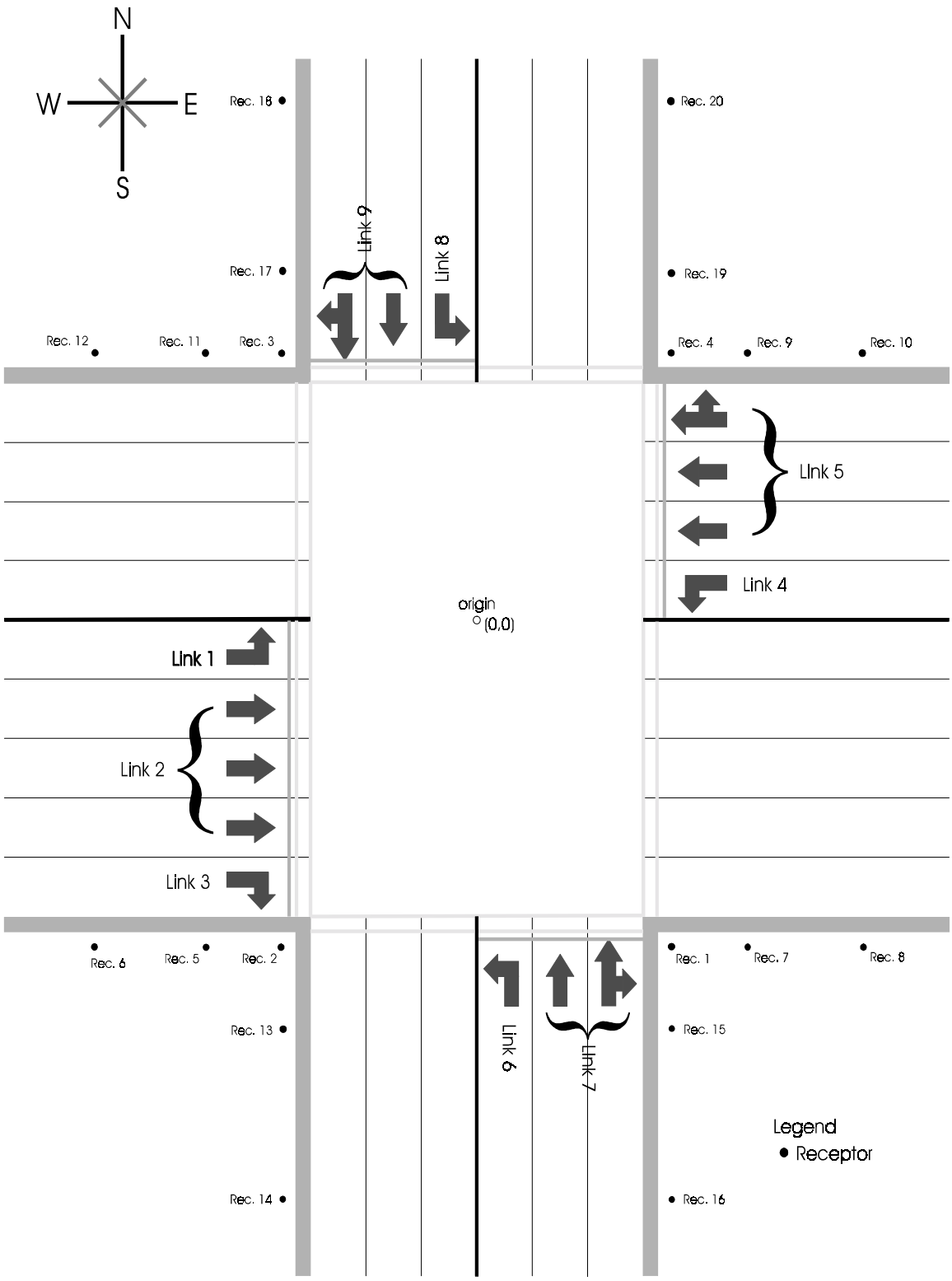

Figure 4.1 Intersection Geometry

Table 4.2 Intersection Geometry

Link	Link Type	# of Lanes	Mixing Zone Width	Origin (x,y)	End (x,y)
1. EB LEFT	queue	1	12.0 ft	(-36, -6)	(-1000, -6)
2. EB THROUGH	queue	3	36.0 ft	(-36, -30)	(-1000, -30)
3. EB RIGHT	queue	1	12.0 ft	(-36, -54)	(-1000, -54)
4. WB LEFT	queue	1	12.0 ft	(36, 6)	(1000, 6)
5. WB THRU&RIGHT	queue	3	36.0 ft	(36, 24)	(1000, 24)
6. NB LEFT	queue	1	12.0 ft	(6, -60)	(6, -1000)
7. NB THRU&RIGHT	queue	2	24.0 ft	(18, -6)	(18 -1000)
8. SB LEFT	queue	1	12.0 ft	(-6 48	(-6 1000)
9. SB THRU&RIGHT	queue	2	24.0 ft	(-18, 48)	(-18, 1000)
10. EB APPROACH	free-flow	5	79.6 ft	(-1000, -30)	(0, -30)
11. EB DEPARTURE	free-flow	5	79.6 ft	(0, -30)	(1000, -30)
12. WB APPROACH	free-flow	4	67.6 ft	(1000, 24)	(0, 24)
13. WB DEPARTURE	free-flow	4	67.6 ft	(0, 24)	(-1000, 24)
14. NB APPROACH	free-flow	3	55.6 ft	(18, -1000)	(18, 0)
15. NB DEPARTURE	free-flow	3	55.6 ft	(18, 0)	(18, 1000)
16. SB APPROACH	free-flow	3	55.6 ft	(-18, 1000)	(-18, 0)
17. SB DEPARTURE	free-flow	3	55.6 ft	(-18, 0)	(-18, -1000)

4.1.2 Receptor Location

The general principals in locating receptors include:

- "Receptors should be located where the maximum total project concentration is likely to occur and where the general public is likely to have access (38)." In this study, a hypothetical intersection was used for modeling purposes. Prior knowledge of the "general public access" was not available, so receptors were located adjacent to each side of the traffic roadways (see Figure 4.1).
- The maximum number of receptors allowed in CAL3QHCR is 60. A standard of 3 meters away from the traveled roadway is applied. The height (*z* coordinate) of the receptors are set to be 6.00 feet, which is generally considered typical of the general public's breathing height (38).

A total of 20 receptors were used and the locations of the receptors are summarized in Table 4.3 and also shown in Figure 4.1. A single receptor was located at each corner of the intersection (SE corner, SW corner, NE corner, and NW corner), and four receptors were located on both sides of each approach (EB, WB, NB, and SB).

Table 4.3 Receptor Location

Receptor	*x* coordinate (ft)	*y* coordinate (ft)	*z* coordinate (ft)
1 (SE corner)	45.8	-69.8	6.0
2 (SW corner)	-45.8	-69.8	6.0
3 (NW corner)	-45.8	57.8	6.0
4 (NE corner)	45.8	57.8	6.0
5	-96.0	-69.8	6.0
6	-482.0	-69.8	6.0
7	96.0	-69.7	6.0
8	482.0	-69.8	6.0
9	96.0	57.8	6.0
10	482.0	57.8	6.0
11	-96.0	57.8	6.0
12	-482.0	57.8	6.0
13	-45.8	-120.0	6.0
14	-45.8	-485.0	6.0
15	45.8	120.0	6.0
16	45.8	-485.0	6.0
17	45.8	110.0	6.0
18	-45.8	488.0	6.0
19	45.8	110.0	6.0
20	45.8	488.0	6.0

4.1.3 Emission Factors

As discussed in Section 4.1, nine queue links and eight free-flow links were specified in the hypothetical intersection. The program requires user-specified queue link and free-flow link emission factors. The queue link emission factors are dependent on the percent of cold/hot starts. The queue emission factor assuming 30% cold start was used in the preliminary study. The free-flow link emission factors are dependent on the

free-flow speed and percent of cold/hot start. The free-flow emission factor for a 20 mph free-flow speed and 30% cold start was used in the preliminary study. By using EMFAC7F and 1997 California vehicle fleet characteristics, the queue link emission factor for 30% cold starts is 426.0 grams/vehicle-hour and the free-flow link emission factor with a speed of 20 mph and 30% cold starts is 23.0 grams/vehicle-mile.

4.1.4 Traffic Data

The Tier II approach in CAL3QHCR is capable of reflecting the traffic conditions on an hourly basis. A set of 24-hour hourly traffic and signal timing data is called a pattern. A pattern can be used to represent the traffic flow and signal timing for a given day, group of days, or non-sequential group of days (10). CAL3QHCR is capable of processing up to seven patterns, one for each day of the week. In this study, only one pattern was applied to both weekday and weekend. Inferring from Figure 2 - "24-hour hourly traffic volume at an intersection" in CAL3QHCR User's Guide (10), a hypothetical traffic pattern was assigned to the study intersection. The hourly traffic pattern is summarized in Table 4.4 and Figure 4.2.

Table 4.4 Hourly Traffic Volume by Link

Ending Hour	Link 1	Link 2	Link 3	Link 4	Link 5	Link 6	Link 7	Link 8	Link 9	Link 10	Link 11	link 12	Link 13	Link 14	Link 15	Link 16	Link 17
1	12	290	74	12	280	36	160	24	136	376	344	292	272	196	202	160	206
2	6	145	37	6	140	18	80	12	68	188	172	146	136	98	101	80	103
3	6	145	37	6	140	18	80	12	68	188	172	146	136	98	101	80	103
4	6	145	37	6	140	18	80	12	68	188	172	146	136	98	101	80	103
5	12	290	74	12	280	36	160	24	136	376	344	292	272	196	202	160	206
6	30	725	185	30	700	90	400	60	340	940	860	730	680	490	505	400	515
7	45	1088	278	45	1050	135	600	90	510	1410	1290	1095	1020	735	758	600	773
8	60	1450	370	60	1400	180	800	120	680	1880	1720	1460	1360	980	1010	800	1030
9	60	1450	370	60	1400	180	800	120	680	1880	1720	1460	1360	980	1010	800	1030
10	60	1450	370	60	1400	180	800	120	680	1880	1720	1460	1360	980	1010	800	1030
11	45	1088	278	45	1050	135	600	90	510	1410	1290	1095	1020	735	758	600	773
12	45	1088	278	45	1050	135	600	90	510	1410	1290	1095	1020	735	758	600	773
13	45	1088	278	45	1050	135	600	90	510	1410	1290	1095	1020	735	758	600	773
14	45	1088	278	45	1050	135	600	90	510	1410	1290	1095	1020	735	758	600	773
15	45	1088	278	45	1050	135	600	90	510	1410	1290	1095	1020	735	758	600	773
16	45	1088	278	45	1050	135	600	90	510	1410	1290	1095	1020	735	758	600	773
17	60	1450	370	60	1400	180	800	120	680	1880	1720	1460	1360	980	1010	800	1030
18	60	1450	370	60	1400	180	800	120	680	1880	1720	1460	1360	980	1010	800	1030
19	60	1450	370	60	1400	180	800	120	680	1880	1720	1460	1360	980	1010	800	1030
20	36	870	222	36	840	108	480	72	408	1128	1032	876	816	588	606	480	618
21	24	580	148	24	560	72	320	48	272	752	688	584	544	392	404	320	412
22	24	580	148	24	560	72	320	48	272	752	688	584	544	392	404	320	412
23	24	580	148	24	560	72	320	48	272	752	688	584	544	392	404	320	412
24	12	290	74	12	280	36	160	24	136	376	344	292	272	196	202	160	206

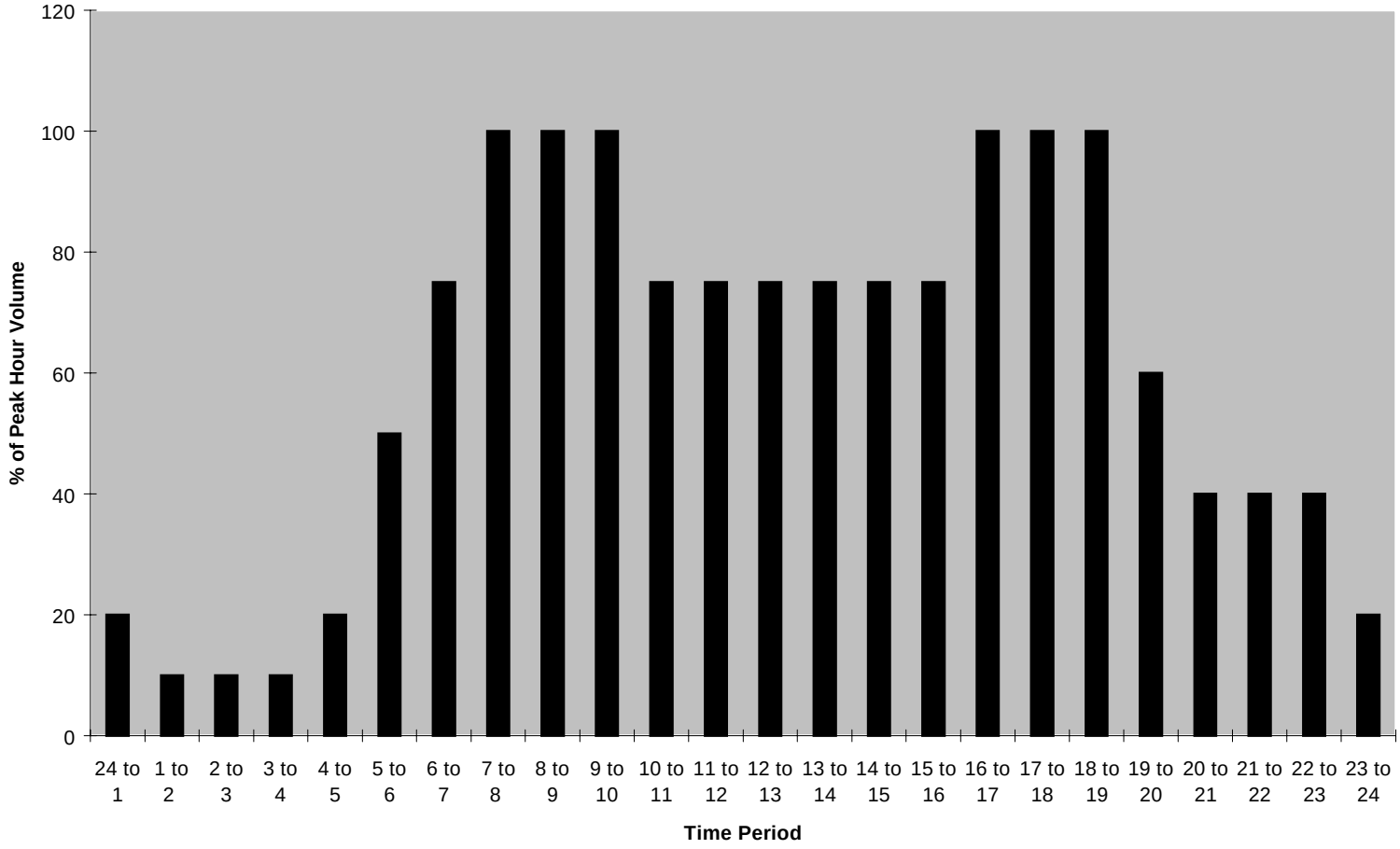

Figure 4.2 Hourly Traffic Pattern

4.1.5 Signalization Data

The intersection operations are assumed to be controlled by a pre-timed signal with five phases and a cycle length of 92 seconds. There are five types of *arrival rates* which can be specified in CAL3QHCR: the worst progression (dense platoon at the beginning of red time); below average progression (dense platoon during the middle of red time); average progression (random arrivals); above average progression (dense platoon during the middle of green time); and the best progression (dense platoon at the beginning of green time) (35). The traffic operations are assumed to improve as progression improves. In this study, the default arrival rate in CAL3QHCR, average progression, was used. In addition, one second of lost yellow time (i.e., yellow time that is not used for vehicle movement) is applied to all phases. The signalization data are summarized in Table 4.5.

Table 4.5 Signalization Data

Phasing	**Green Time (Sec.)**	**Yellow plus Red (Sec.)**
1. *EB* left and *WB* left	7.0	4.0
2. *EB* thru, right; *WB* thru, right	30.0	4.0
3. *NB* left and *SB* left	12.0	4.0
4. *NB* thru, right, left	4.0	0.0
5. *NB* thru, right; *SB* thru, right	23.0	4.0

The input file to CAL3QHCR incorporating the traffic pattern, signalization data, and intersection geometry specified above is given in Appendix I.

4.1.6 Meteorological Data

On-site collected meteorological data for a single year was provided by Caltrans for four locations: Sacramento (1989) (representative of inland cities), Redlands (1981) (representative of slightly inland cities), West Los Angeles (1981) (representative of

coastal cities), and San Jose (1988) (representative of slightly coastal cities). The meteorological data includes:

- wind flow vector (deg.), the direction the wind is blowing toward (i.e., 90 degrees is to the east);
- wind speed (m/s), which should be at least 1 m/s, since the CALINE3 dispersion model has not been validated for wind speeds less than 1 m/s;
- ambient temperature (K);
- stability class (A=1, F=6), on which the spreading parameters in CALINE3 are dependent; and
- mixing height (m) (CAL3QHCR User's Guide recommends a mixing height of 1000m, since the mixing height used in developing the dispersion parameters in CAL3QHCR was about 1000m).

4.1.7 Miscellaneous Input Variables

The remaining input variables required by CAL3QHCR for completion of this analysis include:

- source height equals 0;

  Recommended in CAL3QHCR User's Guide, "in most applications (at-grade), a source height of 0 m should be used."
- saturation flow rate equals 1,600 vehicles per hour per lane;

  This value is consistent with EPA's recommendation for an urban intersection in CAL3QHCR, even though in the third edition of the Highway Capacity Manual, 1,900 vehicles per hour per lane is recommended.
- average model running time equals 60 minutes; and

The 8-hour average predictions are based on a one-hour period.

- surface roughness length equals 321.00 cm.

Recommended CALINE3 value for central business district (CBD).

4.2 Computation of ASD and Modeling [CO]

As discussed in Section 3.1, the LOS for lane groups, approaches or intersections is defined in HCM as "the average stopped delay per vehicle for a 15-min analysis period". The LOS is directly related to the ASD using the criteria specified in HCM (1994) and summarized in Table 3.2. The computation of average stopped delay depends on a number of variables:

- vehicle arrival rate;
- number of lanes of each lane group;
- signal type, phase, and timing;
- the mix (classification of vehicles by size) of vehicles using the facility;
- peak hour factor (PHF);
- pedestrian, bus, and parking activities;
- turning vehicles; and
- progression type.

The intersection geometry, traffic data and signalization data discussed in this section, together with the following hypothetical values of the other input variables summarized in Table 4.6 were used in the simulation of the LOS.

Table 4.6 Other Input Variable to HCS

Input Variable	Analysis Value
PHF	0.9

Area Type	CBD
Percent Grade	0
Percentage of Heavy Vehicles	2
Number of Bus Stops	0
Arrival Type	3
Adjacent Parking	No
Pedestrians Button	No
No. of Conflicting Pedestrians	0

The computed lane group delays and approach delays are summarized in Table 4.7.

Table 4.7 Calculation of LOS by Lane Groups and Approaches

Lane Group		v/c ratio	g/C ratio	ASD by lane group	Lane Group LOS	ASD by approach	Approach LOS
EB	left	0.484	0.087	32.5	D		
	thru	0.951	0.337	31.6	D	31.6	D
	right	0.856	0.337	31.5	D		
WB	left	0.484	0.087	32.5	D		
	thru/right	0.948	0.337	31.5	D	31.5	D
NB	left	0.679	0.185	30.8	D		
	Thru/right	0.897	0.304	30.9	D	30.9	D
SB	left	0.591	0.141	31.1	D		
	Thru/right	0.880	0.261	32.2	D	32.0	D

Cycle length = 92 seconds, Intersection ASD = 31.5 sec/veh, Intersection LOS = D

This hypothetical intersection is operating around the middle of LOS D with a 31.5 sec/veh intersection delay time. Each individual lane group and approach also operates around the middle of LOS D. The number of vehicles queued at each lane group is summarized in Table 4.8. The number of vehicles queued, together with the predominant wind direction and receptor location account for the impacts of the orientation of intersection on the modeled [CO] levels, as will be discussed in Section 4.3.2.

Table 4.8 The Queue Length for Each Lane Group

Lane	Group	Number of Vehicles in Queue	Queue Length (meters)
EB	left	2.4	14.4
	thru	24.3	145.8
	right	6.9	41.1
WB	left	2.4	14.4
	thru/right	13.1	78.6
NB	left	4.5	27
	thru/right	10.7	64.2
SB	left	3.2	19.2
	thru/right	10.4	62.4

4.3 CAL3QHCR Modeling Results

Micro-scale CO analysis was conducted using CAL3QHCR. In this study, the highest maximum 8-hour averaged concentration was selected for analysis.

As discussed in Section 2.1, EPA's current LOS rationale for determining whether an intersection should be modeled for CO impacts is only dependent on the ASD at signalized intersections. In this section, the impacts of some other modeling factors on the modeled [CO], such as meteorological data, intersection orientation, and intersection geometry, are presented.

4.3.1 Modeled [CO] with Different Meteorological Data

Four different runs were made, in which the same intersection geometry, traffic data, and signalization data were applied to all four runs so that the ASD was held constant at 31.5 seconds, but meteorological data was varied by location: Sacramento (1989), Redlands (1981), West Los Angeles (1981), and San Jose (1988). The highest maximum 8-hour [CO], the receptor where the highest maximum [CO] occurs, and the ending day and hour of this occurrence are summarized in Table 4.9.

Table 4.9 The highest 8-hour maximum [CO]

City	[CO] (ppm)	Receptor	Ending Day (Julian)	Ending Hour
Sacramento	4.18	2	31	14:00
Redlands	7.68	2	88	15:00
West LA	8.67	2	354	12:00
San Jose	5.89	2	10	13:00

Even though the ASDs for these four runs were held constant at 31.5 seconds, the modeled highest maximum [CO] still varied from 4.18 ppm (Sacramento) to 8.67 ppm (West Los Angeles) due to different meteorological conditions. This difference implies that local meteorological conditions have a significant impact on the modeled [CO] levels. It is generally believed that the worst meteorological conditions from an air-quality perspective (the conditions under which the NAAQS is most likely violated) for CO occur from midnight to early morning during the winter months. We have provided, as an example, the winter time (November through February) 6-hour averaged (12:00 AM to 6:00 AM) wind direction, wind speed, and atmospheric stability class for Redlands (representative of slightly inland cities) and San Jose (representative of coastal cities) in Figure 4.3 and Figure 4.4, respectively. As shown in Table 4.9, Redlands has a higher tendency for CO violations than San Jose. This difference can be partially attributed to the different meteorological conditions that exist between these two areas. Compared to San Jose, Redlands tends to have lower wind speeds, less variability in wind direction, and greater atmospheric stability during the worst meteorological conditions used for this analysis. The impacts of meteorological conditions on modeled [CO] levels will be examined thoroughly in Section 5.

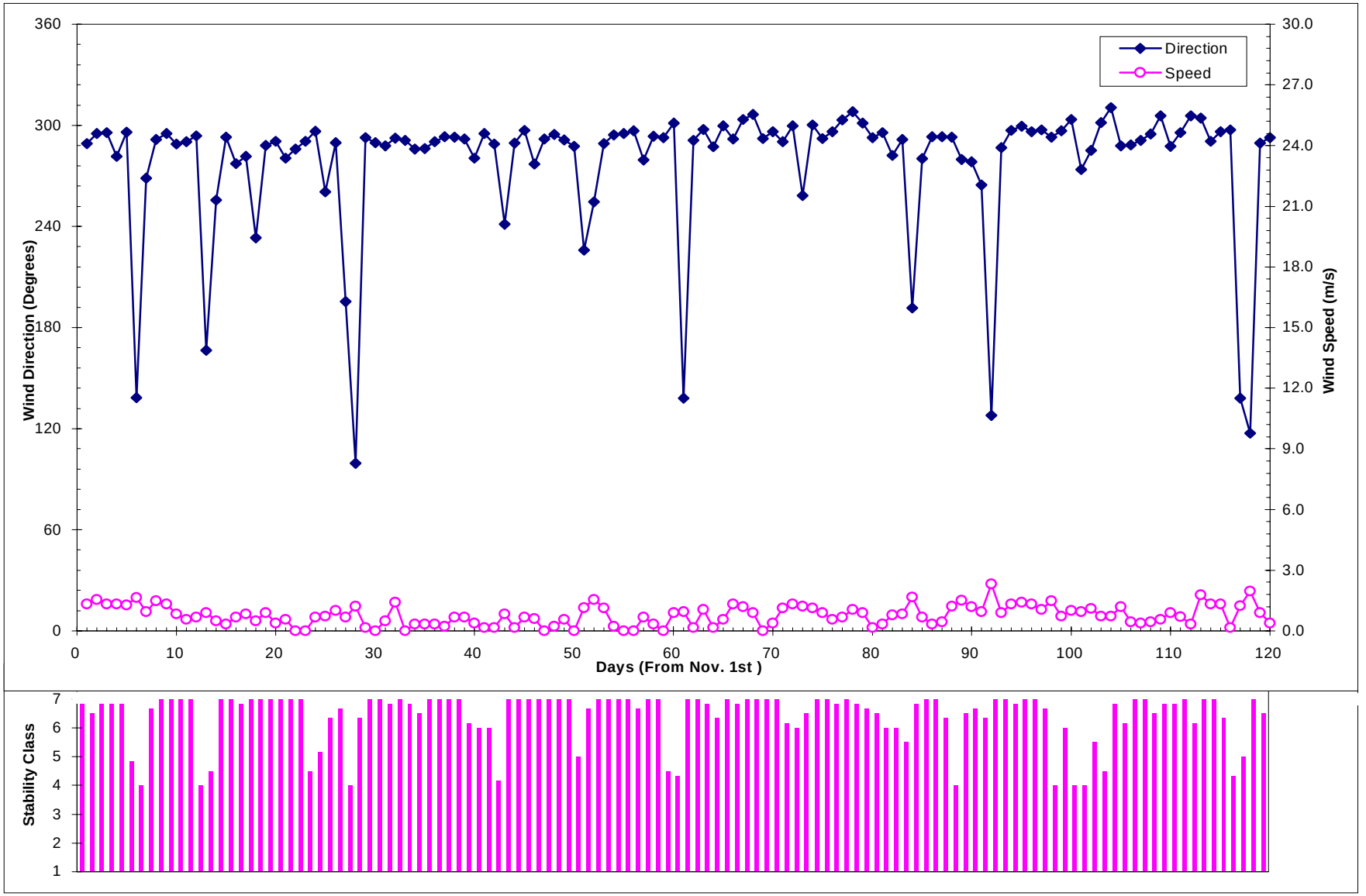

Figure 4.3 Example of Meteorological Conditions for Redlands, CA (12:00 AM to 6:00 AM, Nov. 1st to Feb. 28th, 1981)

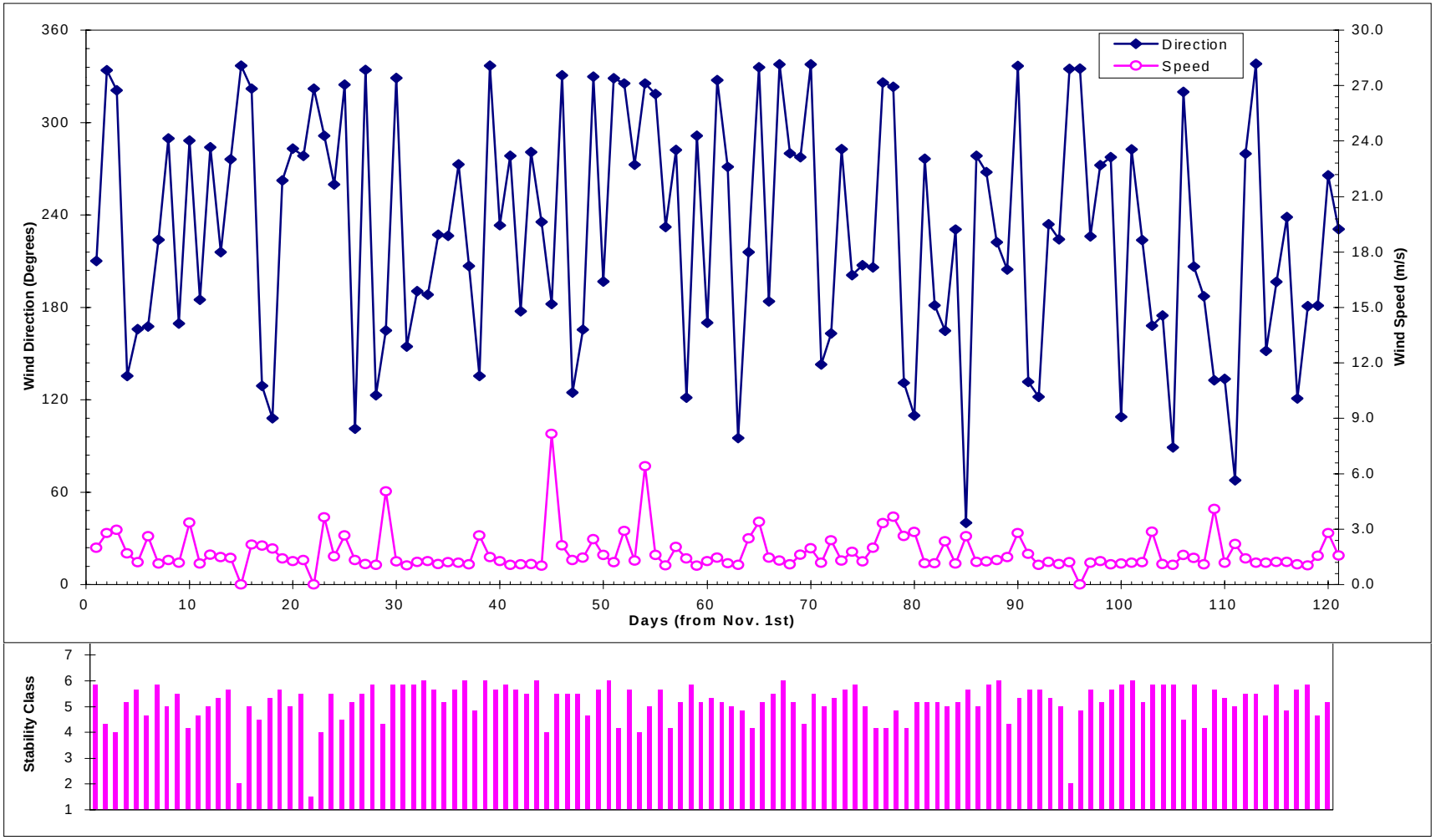

Figure 4.4 Example of Meteorological Conditions for San Jose, CA (12:00 AM to 6:00 AM, Nov. 1st to Feb. 29th, 1988)

4.3.2 Modeled [CO] with Different Intersection Orientations

As noted earlier, the intersection developed for this simulation is hypothetical but the meteorological data represents real conditions. Thus, the orientation of the intersection, defined as the relative angle between the dominant wind direction and the traffic link with the longest queue (i.e. EB through in this study, as shown in Table 4.8), will make a substantial difference in modeled 8-hour [CO] levels. In the real world, both the orientation of existing intersections may vary as well as the orientation of new designs. The intersection was rotated counter-clockwise in a 5 degrees increments, using West LA meteorological data and holding emission factors, traffic and signalization (ETS) data constant, each time computing the maximum 8-hour concentration (a total of 72 runs). The modeling results due to intersection orientation are summarized in Table 4.10 and Figure 4.5. The C program for calculating the (x, y) coordinates of each intersection rotation is provided as Appendix II.

Table 4.10 Intersection Orientation[1]

Orientation (deg.)	[CO] (ppm)	Orientation (deg.)	[CO] (ppm)
5	8.57	185	8.02
10	8.33	190	8.05
15	8.05	195	8.10
20	7.73	200	8.08
25	***7.30***	205	8.03
30	7.32	210	8.13
35	7.40	215	8.43
40	7.67	220	8.70
45	7.85	225	8.98
50	8.10	230	9.07
55	8.17	235	9.13
60	8.28	240	9.17
65	8.28	245	9.15
70	8.12	250	9.35
75	7.82	255	10.06
80	7.46	260	10.61
85	7.54	***265***	***10.94***
90	7.54	270	10.64
95	7.95	275	10.81
100	8.23	280	10.45
105	8.42	285	10.01
110	8.73	290	9.48
115	9.43	295	8.89
120	9.92	300	8.29
125	10.38	305	8.12
130	10.58	310	8.32
135	10.58	315	8.47
140	10.43	320	8.57
145	10.17	325	8.70
150	10.10	330	8.80
155	9.82	335	8.88
160	9.47	340	9.00
165	9.10	345	9.00
170	8.68	350	8.98
175	8.12	355	8.82
180	7.85	360	8.67

[1]: The background concentration is not included in this study.

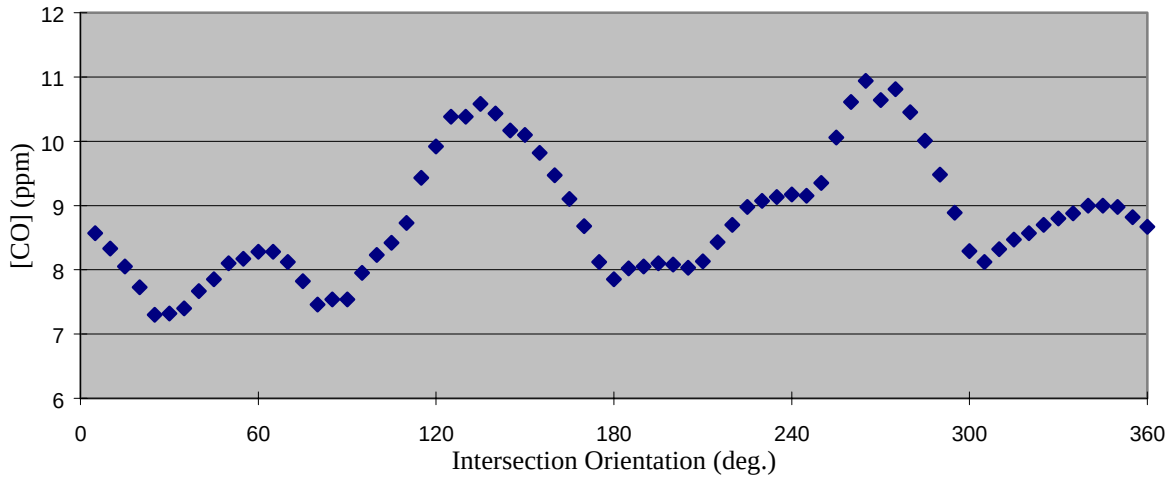

Figure 4.5 Modeled [CO] vs. Intersection Orientation

The highest [CO] among all receptors varied from 7.3 ppm to 10.94 ppm with the orientation of the intersection. The worst orientation occurred at 265 degrees, with the highest [CO] at 10.94ppm. The California State and national standard for 8-hour averaged [CO] is 9 ppm. In these 72 runs, there were 26 runs with the modeled [CO] over the standard: the intersections rotated counter-clock wise between 115 degrees and 165 degrees and between 230 and 290 degrees. That is, even though the ASDs for these 72 runs were held constant, the highest modeled [CO] with different intersection orientations still varied from 7.30 ppm (at 25 degrees), which is below the standard, to 10.94 ppm (at 265 degrees), which exceeds the standard.

After rotation, the intersection geometry and receptor locations at 265 degrees are shown in Figure 4.6 and summarized in Table and Table 4.12. The CAL3QHCR output file is presented in Appendix III.

Table 4.11 Intersection Geometry (at 265 deg.)

Link	# of Lanes	Link Type	Link Width	Origin (x,y)	End (x,y)
EB LEFT	1	queue	12 ft	(-2.84, 36.39)	(81.18, 996.72)
EB THR.	3	queue	36 ft	(-26.75, 38.48)	(57.27, 998.81)
EB RIGHT	1	queue	12 ft	(-50.66, 40.57)	(33.36, 1000.9)
WB LEFT	1	queue	12 ft	(2.84, -36.39)	(-81.18, -996.72)
WB THR&R	3	queue	36 ft	(20.77, -37.95)	(-63.24, -998.29)
NB LEFT	1	queue	12 ft	(-60.29, -0.75)	(-996.72, 81.18)
NB THR&R	2	queue	24 ft	(-61.34, -12.70)	(-997.76 ,69.22)
SB LEFT	1	queue	12 ft	(48.34, 1.79)	(996.72,-81.18)
SB THR&R	2	queue	24 ft	(49.39, 13.75)	(997.76, -69.22)

Table 4.12 Receptor Location (at 265 deg.)

Receptor	*x* coord. (ft)	*y* coord. (ft)	*z* coord. (ft)
1 (SE corner)	-73.52	-39.54	6.0
2 (SW corner)	-65.54	51.71	6.0
3 (NW corner)	61.57	40.59	6.0
4 (NE corner)	53.59	-50.66	6.0
5	-61.17	101.72	6.0
6	-27.52	486.25	6.0
7	-77.90	-89.55	6.0
8	-111.54	-474.08	6.0
9	49.21	-100.67	6.0
10	15.57	-485.20	6.0
11	65.95	90.59	6.0
12	99.59	475.13	6.0
13	-115.55	56.08	6.0
14	-479.16	87.89	6.0
15	-123.54	-35.17	6.0
16	-487.15	-3.36	6.0
17	113.57	36.04	6.0
18	490.13	3.09	6.0
19	105.59	-55.21	6.0
20	482.15	-88.15	6.0

As discussed in Section 4.1.6, the wind flow vector in the meteorological data is coded as the direction the wind is blowing toward (i.e., 270 degrees represents a wind blowing *to* the west). However, when calculating [CO] by CALINE3, the dispersion

model in CAL3QHCR, wind angle input to the model follows the accepted meteorological convention (i.e., 270 degrees represents a wind *from* the west). Note that there is a 180-degree difference between the coding in meteorological data and the input requirement of CALINE3. The highest modeled [CO], 10.94 ppm, occurred between 7am and 2pm, on Dec. 28th, 1981. In this 8-hour period, most of the hourly wind *flow* vectors were between 270 and 300 degrees. That is, by adding 180 degrees to convert to the accepted meteorological convention, during this 8-hour period the dominant wind *direction* was between 90 degrees and 120 degrees (approximately from the East).

The highest modeled [CO] occurred at receptor 2, and the x, y coordinates of receptor 2 after rotating 265 degrees are -65.5 and 51.7, respectively. The contribution to the predicted [CO] at receptor 2 by each link is summarized in Table 4.13. The links contributing the most to the total predicted concentration at receptor 2 are links 2 and 3. Link 3 accounts for about 60% of the total concentration predicted at receptor 2 (6.5 ppm out of 10.94 ppm) and link 2 accounts for about 24% (2.64 ppm out of 10.94 ppm). Referring to the queue length of each link in Table 4.8 and a West LA wind direction from 7 am to 2 pm, Dec. 28th, 1981, and the intersection geometry and the location of receptor 2 in Figure 4.6, link 2 and link 3 are closer to receptor 2 and the highest modeled [CO] occurs when the wind is almost perpendicular to these two links. Although somewhat less intuitive, the results are consistent with the CAL3QHCR User's Guide expectation that "if the receptor is very close to the intersection, with a larger number of lanes under cross-wind conditions, higher CO levels may be predicted; but if the receptor is further away from the intersection, a smaller number of lanes (a longer queue) under near parallel winds will result in higher predicted [CO] levels (10)."

Table 4.13 Eight-hour Averaged Link Contributions at Receptor 2

Link	Contribution (ppm)	% of Contribution
1	0.38	3
2	2.64	24
3	6.50	60
4	0.01	0
5	0.20	2
6	0.00	0
7	0.10	1
8	0.20	2
9	0.91	8
Total	10.94	100

Figure 4.6 Intersection Geometry at 265 degrees

4.3.3 Modeled [CO] with Different Intersection Geometry

In this Section, two additional runs were made, in which the ASD was held constant at 31.5 seconds, but different intersection geometry was specified for each run.

In the first run, the separated EB right-turn movement was dropped and forced to share the right-most lane of the EB-through link. By doing so, for all the approaches in this intersection the right turn movement shared the right-most lane of the through link. The signal phase and timing data were held constant (at the level depicted in Table 4.5), but traffic volumes were adjusted so that intersection ASD was again held constant at 31.5 seconds. The total number of links was sixteen, since the link for the EB right turn was dropped. The intersection geometry and receptor locations are shown in Figure 4.7 and also summarized in Table 4.14 and Table 4.15, respectively.

.

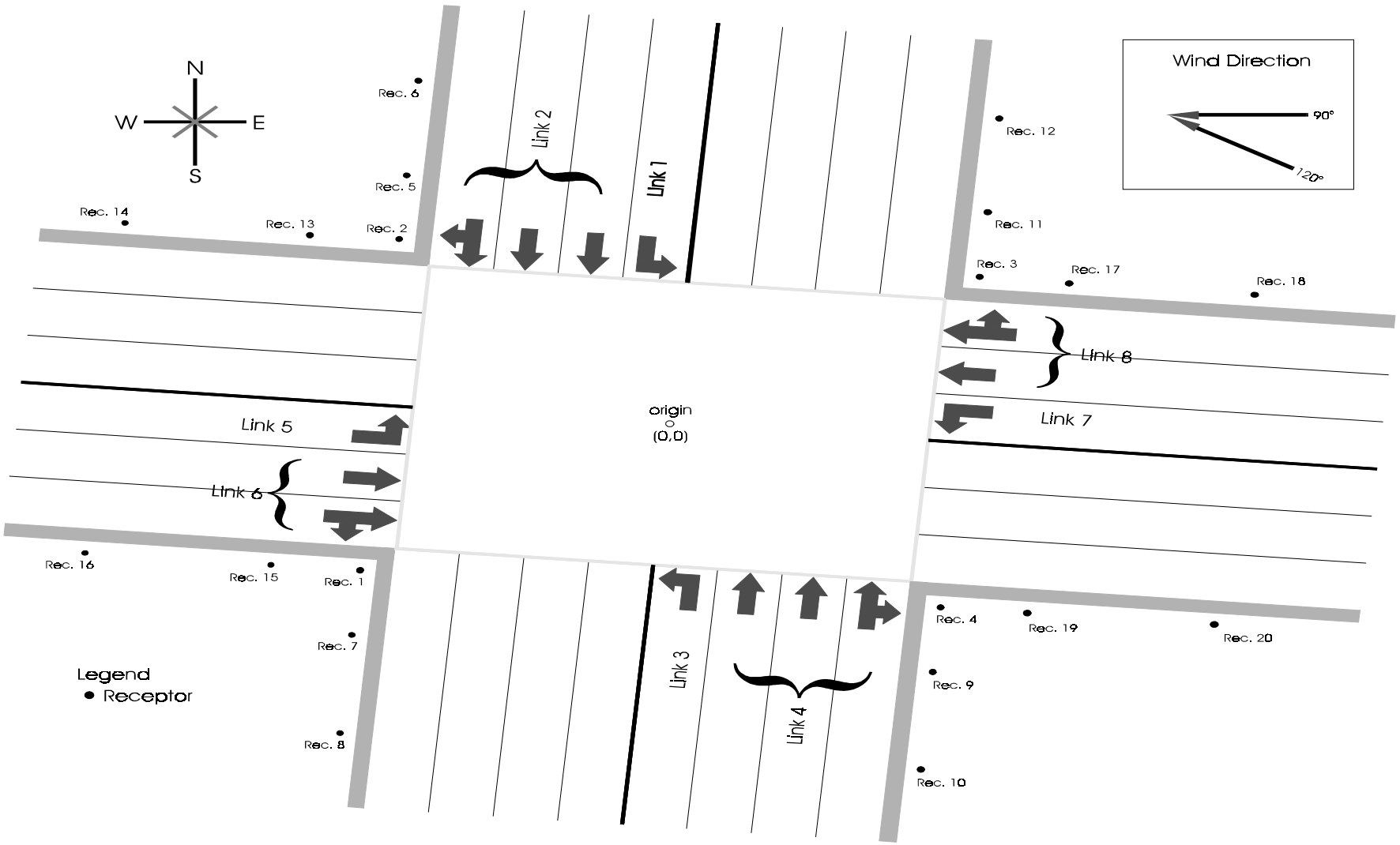

Figure 4.7 Intersection Geometry, No-Separate Right Turns

Table 4.14 Intersection Geometry: No Separate Right-Turn Lanes

Link	# of Lanes	Link Type	Link Width	Origin (x,y)	End (x,y)
1. EB LEFT	1	queue	12.0 ft	(-2.84, 36.39)	(81.18, 996.72)
2. EB THR&R.	3	queue	36.0ft	(-26.75, 38.48)	(57.27, 998.81)
3. WB LEFT	1	queue	12.0 ft	(2.84, -36.39)	(-81.18, -996.72)
4. WB THR&R	3	queue	36.0 ft	(20.77, -37.95)	(-63.24, -998.29)
5. NB LEFT	1	queue	12.0 ft	(-48.34, -1.79)	(-996.72, 81.18)
6. NB THR&R	2	queue	24.0 ft	(-49.39, -13.75)	(-997.76 ,69.22)
7. SB LEFT	1	queue	12.0 ft	(48.34, 1.79)	(996.72,-81.18)
8. SB THR&R	2	queue	24.0 ft	(49.39, 13.75)	(997.76, -69.22)
9. EB APPROACH	4	free-flow	67.6 ft	(63.25, 998.29)	(-23.91, 2.09)
10. EB DEPARTURE	4	free-flow	67.6 ft	(-23.91, 2.09)	(-111.07, -994.1)
11. WB APPROACH	4	free-flow	67.6 ft	(-63.25, -998.29)	(23.01, -2.09)
12. WB DEPARTURE	4	free-flow	67.6 ft	(23.01, -2.09)	(111.07, 994.10)
13. NB APPROACH	3	free-flow	55.6 ft	(-997.76, 69.07)	(-1.57, -17.93)
14. NB DEPARTURE	3	free-flow	55.6 ft	(-1.57, -17.93)	(994.63, -105.07)
15. SB APPROACH	3	free-flow	55.6 ft	(997.76, -69.07)	(1.57, 17.93)
16. SB DEPARTURE	3	free-flow	55.6 ft	(1.57, 17.93)	(-994.63, 105.07)

Table 4.15 Receptor Location: No Separate Right-Turn Lanes

Receptor	*x* coord. (ft)	*y* coord. (ft)	*z* coord. (ft)
1 (SE corner)	-61.57	-40.59	6.0
2 (SW corner)	-53.59	50.66	6.0
3 (NW corner)	61.57	40.59	6.0
4 (NE corner)	53.59	-50.66	6.0
5	-49.21	100.67	6.0
6	-15.57	485.20	6.0
7	-65.95	-90.60	6.0
8	-99.58	-475.13	6.0
9	49.21	-100.67	6.0
10	15.57	-485.20	6.0
11	65.95	90.59	6.0
12	99.59	475.13	6.0
13	-103.60	55.04	6.0
14	-467.21	86.85	6.0
15	-111.58	-36.21	6.0
16	-475.19	-4.40	6.0
17	113.57	36.04	6.0
18	490.13	3.09	6.0
19	105.59	-55.21	6.0
20	482.15	-88.15	6.0

The highest modeled [CO], 10.03 ppm occurred at receptor 5. The ending day and hour of this occurrence was (360, 13). The wind direction during this occurrence is also shown in Figure 4.7. Table 4.16 summarizes the contribution to this occurrence by each link.

Table 4.16 Eight-hour Avg. Contributions at Receptor 5

Link	Contribution (ppm)	% Contribution
1	0.35	4
2	6.62	58
3	0.03	0
4	0.43	1
5	0.10	3
6	0.27	5
7	0.08	1
8	0.43	5
9	0.68	9
10	0.15	2
11	0.15	2
12	0.27	3
13	0.07	1
14	0.15	2
15	0.12	2
16	0.13	2
Total	10.03	100

Comparing Table 4.16 with Table 4.13, dropping link 3 (EB right turn) accounts for a decrease in the highest maximum concentration to 10.03 ppm and a shift from a receptor 2 occurrence to a receptor 5 occurrence. In Table 4.13, the EB right turn (link 3) contributes the most (about 60%) to the total concentration while in Table 4.16, link 2 (merged EB right turn and through) contributed the most (about 58%) to the total concentration.

In the second part of this analysis, all left-turn movements were forced to share the left-most lane of the through link. This reduced the total number of links to twelve: four queue links and eight free-flow links. The signal phase was adjusted to reflect the change in the movement combination of each link. In addition, signal timing and traffic volume data were adjusted so that the intersection ASD was again held constant at 31.5 seconds. The details on the hourly traffic volume changes are provided in Appendix IV. Table 4.17 presents the signalization data. Intersection geometry and receptor locations are shown in Figure 4.8 and summarized in Table 4.18 and Table 4.19, respectively.

Table 4.17 Signalization Data

Phase	Green Time (Sec.)	Yellow plus Red Time (Sec.)
1. *EB* all movements	25.0	4.0
2. *WB* movements	25.0	4.0
3. *SB* movements	14.0	4.0
4. *NB* movements	16.0	4.0

Note: Cycle Length = 96 seconds

Table 4.18 Intersection Geometry: No Separate Left-Turn Lanes

Link	# of Lanes	Link Type	Link Width	Origin (x,y)	End (x,y)
EB LEFT/RIGHT/THRU.	3	queue	36.0 ft	(-15.8, 25.5)	(69.2, 997.8)
WB LEFT/RIGHT/THRU.	3	queue	36.0 ft	(15.8, -25.5)	(-69.2, -997.8)
NB LEFT/RIGHT/THRU.	2	queue	24.0 ft	(-37.4, -14.8)	(-997.8, 69.2)
SB LEFT/RIGHT/THRU.	2	queue	24.0 ft	(37.4, 14.8)	(997.8, -69.2)
EB APPROACH	3	free-flow	55.6 ft	(69.2, 997.8)	(-17.3, 1.6)
EB DEPARTURE	3	free-flow	55.6 ft	(-17.9 1.6)	(-105.6 -994.6)
WB APPROACH	3	free-flow	55.6 ft	(-69.2, -997.8)	(17.9, -1.6)
WB DEPARTURE	3	free-flow	55.6 ft	(17.9, -1.6)	(105.6, 994.6)
NB APPROACH	2	free-flow	43.6 ft	(-997.8, 69.2)	(-1.1, -11.9)
NB DEPARTURE	2	free-flow	43.6 ft	(-1.1, -11.9)	(995.2, -99.2)
SB APPROACH	2	free-flow	43.6 ft	(997.8, -69.2)	(1.1, 11.9)
SB DEPARTURE	2	free-flow	43.6 ft	(1.1, 11.9)	(-995.2, 99.2)

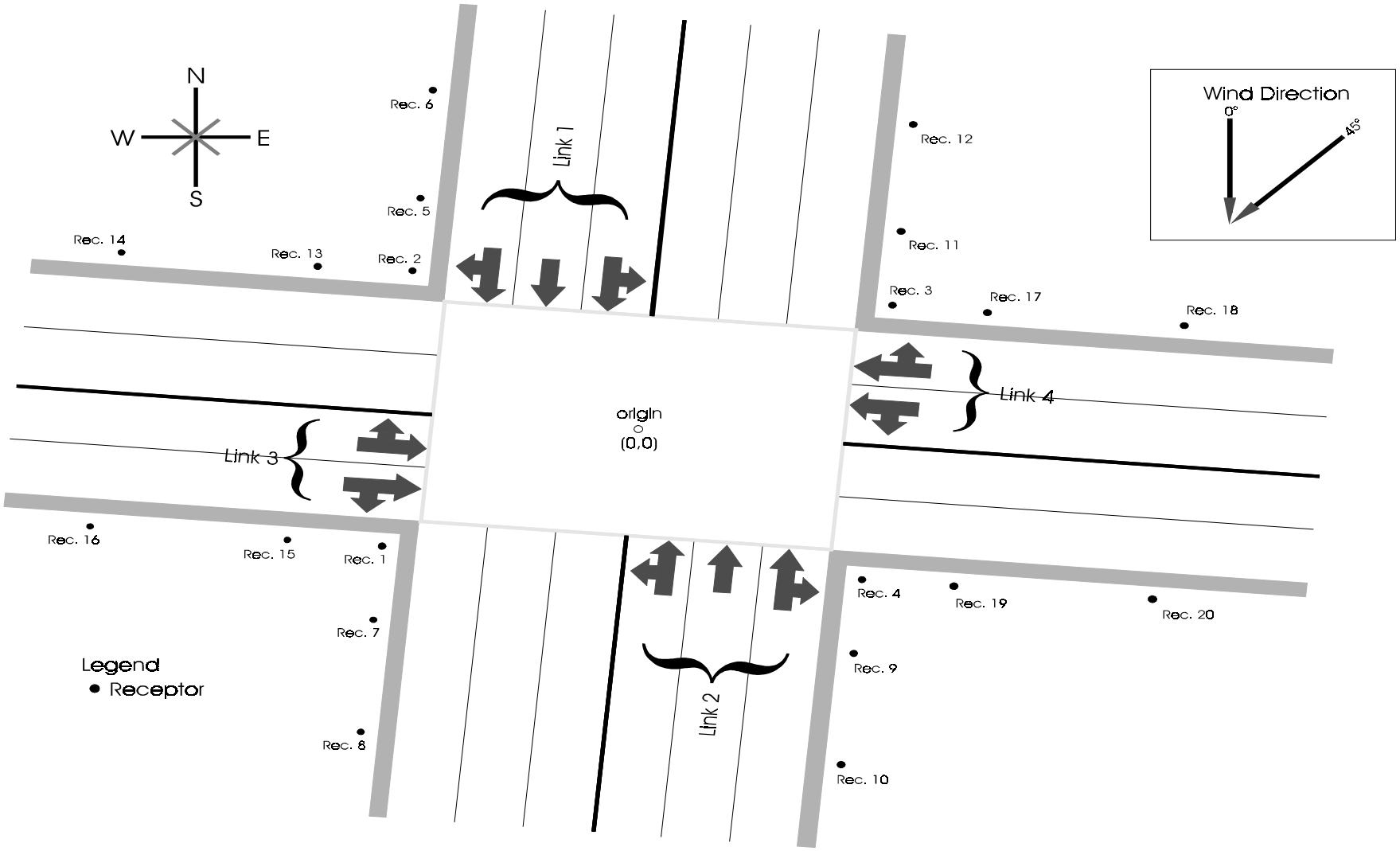

Figure 4.8 Intersection Geometry, No-Separate Right or Left Turns

Table 4.19 Receptor Location: No Separate Left-Turn Lanes

Receptor	*x* coord. (ft)	*y* coord. (ft)	*z* coord. (ft)
1 (SE corner)	-48.51	-29.68	6.0
2 (SW corner)	-42.68	37.66	6.0
3 (NW corner)	48.57	29.68	6.0
4 (NE corner)	42.68	-37.66	6.0
5	-38.30	87.67	6.0
6	-4.66	472.20	6.0
7	-52.94	-79.69	6.0
8	-86.58	-464.22	6.0
9	38.30	-87.67	6.0
10	4.66	-472.20	6.0
11	52.94	79.69	6.0
12	86.59	464.22	6.0
13	-92.69	42.04	6.0
14	-456.60	73.85	6.0
15	-98.58	-25.30	6.0
16	-462.19	6.50	6.0
17	100.57	25.13	6.0
18	477.13	-7.81	6.0
19	94.68	-42.20	6.0
20	471.24	-75.15	6.0

The highest modeled [CO], 14.55 ppm occurred at receptor 1. The ending day and hour of this occurrence was (354, 11) with wind direction shown in Figure 4.8. Table 4.20 presents the contribution to this occurrence by each link.

Table 4.20 Eight-hour Avg. Contributions at Receptor 1

Link	Contribution (ppm)	% Contribution
1	1.60	11
2	0.18	1
3	11.17	76
4	0.38	3
5	0.32	2
6	0.25	2
7	0.05	0
8	0.22	2
9	0.18	2
10	0.03	0
11	0.03	0
12	0.13	1
Total	14.55	100

The modeled [CO] with a constant ASD but different intersection geometry varies from 10.03 ppm (merge EB right turn with EB through turn) to 14.55 ppm (merge all left turns with through turns).

4.4 Preliminary Findings

Holding ASD constant at 31.5 seconds, the modeled [CO] for intersections with different meteorological data (Section 4.3.1), intersection orientation (Section 4.3.2), or intersection geometry are summarized in Table 4.21.

Table 4.21 Variation in Modeled [CO] when holding ASD Constant

Varying Factor	Range of [CO] (ppm)
Meteorological Data	4.18 ~ 8.67
Intersection Orientation	7.3 ~ 10.94
Intersection Geometry	10.03 ~ 14.55

As shown in Table 4.21, the intersections with constant ASD, but different meteorological data, intersection orientation, or intersection geometry result in a

substantial difference in modeled [CO] levels. These results imply that meteorological data, intersection orientation, and intersection geometry may also be major factors that contribute to modeled [CO].

5.0 THE DEVELOPMENT OF A NEW STATISTICAL MODEL: EXPLORATORY ANALYSIS

This study's major objective is to develop a new statistical model that incorporates not only the concept of ASD but also many other major factors known to contribute to the modeled [CO]. As shown in Section 4.3, intersections with a constant ASD, but varying meteorological data (Section 4.3.1), intersection orientation (Section 4.3.2), or geometry (Section 4.3.3) can produce different modeled [CO] levels. This implies that EPA's current LOS criterion for determining whether an intersection should be modeled for CO impacts, which is based only on ASD, is not appropriate. There is a need for a new methodological approach that better links the major contributing factors to the modeled [CO].

To better understand the relationships between the modeled [CO] and individual modeling factors, we begin by varying only the factor of interest and holding all the others constant. The factors to be examined include:

- ASD;

  Rationale: EPA's current LOS criterion depends on ASD

- intersection geometry;

  Rationale: As discussed in Section 4.3.3 intersection geometry has an important impact on the modeled [CO]

- total vehicle red time (TVRT);

  Rationale: TVRT is a new variable introduced to this study to incorporate the impacts of ASD, intersection geometry, and total traffic volume on the modeled [CO]

- free-flow and queue emissions factors;

Rationale: The uniform line source strength used in predicting [CO] (*q* in Equation 3.7) is directly related to free-flow and queue emissions factors

- intersection orientation;

  Rationale: As discussed in Section 4.3.2 and shown in Figure 4.5, modeled [CO] varies substantially with intersection orientation, even though the structural relationship is not clear at this point

- wind speed;

  Rationale: Wind speed determines the extent to which CO is initially diluted with ambient air at the point of release. Equation 3.7 exhibits an inverse relationship between wind speed and modeled [CO] concentration.

- atmospheric stability class and surface roughness.

  Rationale: The horizontal and vertical dispersion parameters σ_y and σ_z used in calculating [CO] (Equation 3.7) are dependent on stability class and surface roughness.

5.1 Relationship between Modeled [CO] and Individual Factors

5.1.1 The ASD

As noted in Section 2.2, the computation of ASD in HCS requires greater detail in terms of traffic data than that required to estimate the queue length used in CAL3QHCR. This is one important reason that ASD, rather than queue length, is selected as an independent variable for this study. A second reason is that the selection of ASD is more closely associated with the design parameters of interest to traffic engineers. A final reason to examine ASD is EPA's current policy of using intersection LOS as one of its

defining factors in determining whether an intersection should undergo detailed CO analysis by CAL3QHCR, and intersection LOS is solely dependent on ASD.

In the preliminary analysis, nineteen CAL3QHCR runs were executed, in which meteorological data, intersection geometry, emission factors, and signalization data were held constant, and traffic volumes were allowed to vary so that different ASD scenarios could be generated. The traffic volume of each approach was adjusted uniformly and allowed to range from a 16% decrease (with an ASD of 24.2 seconds, LOS C) to a 16% increase (with an ASD of 64.5 seconds, LOS F) from the traffic data as specified in Table 4.4. These ASD scenarios cover our study interest: LOS C, LOS D, and LOS E intersections. It is also important to note that the background [CO] is not included in this study.

As might be expected, the ASD changes with varying traffic volumes, ranging from 24.2 seconds to 64.5 seconds (Table 5.1). Also note that the signal timing has *not* been changed in these HCS runs to reflect changes in traffic volume. If the signal timing had been adjusted to reflect the changes in the traffic volume for each approach, the modeled [CO] would likely have been lower than those reported in Table 5.1, but LOS (i.e., ASD) would not have remained constant. The modeled maximum 8-hour average [CO] ranged from 11.67 ppm to 16.06 ppm. The ASD and predicted highest 8-hour [CO] for each traffic volume scenario are summarized in Table 5.1.

Note that all of the maximum concentrations occur at receptor 2 on the same ending day and hour, indicating that meteorological conditions are significant factors. In general, the predicted maximum concentration increases non-linearly as the ASD

increases. Figure 5.1 is the scatter plot of the ASD vs. the modeled highest maximum [CO].

Table 5.1 HCS and CAL3QHCR Outputs

Traffic Volume Scenario	ASD	[CO]	Receptor	Ending Day and Hour
16% Decrease	24.2	11.67	2	(354, 12)
15% Decrease	24.4	11.72	2	(354, 12)
14% Decrease	24.7	11.92	2	(354, 12)
12% Decrease	25.2	12.26	2	(354, 12)
10% Decrease	25.9	12.34	2	(354, 12)
8% Decrease	26.2	12.88	2	(354, 12)
6% Decrease	27.5	12.95	2	(354, 12)
4% Decrease	28.6	13.04	2	(354, 12)
2% Decrease	29.9	13.56	2	(354, 12)
0% (Basic vol.)	31.5	13.72	2	(354, 12)
2% Increase	33.5	14.06	2	(354, 12)
4% Increase	36.1	14.32	2	(354, 12)
6% Increase	39.2	14.81	2	(354, 12)
8% Increase	42.9	14.92	2	(354, 12)
10% Increase	47.2	15.24	2	(354, 12)
12% Increase	52.3	15.59	2	(354, 12)
14% Increase	58.1	15.69	2	(354, 12)
15% Increase	61.3	16.01	2	(354, 12)
16% Increase	64.5	16.06	2	(354, 12)

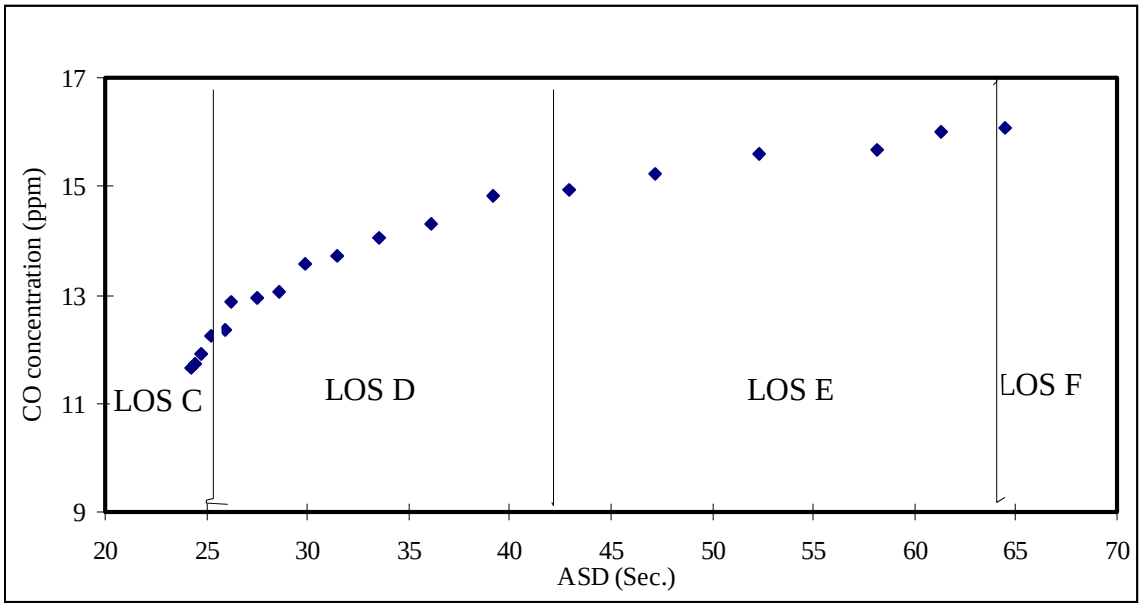

Figure 5.1 Scatter Plot of [CO] vs. ASD

Figure 5.1 indicates that ASD has an important impact on the modeled [CO]. However, ASD is a point estimate that lacks association to the physical configuration of, or the amount of traffic volume traveling through, an intersection (15). It is possible that a five-lane approach will produce dramatically different levels of modeled [CO] than a two-lane approach operating at the same ASD. This suggests the use of a new measurement that incorporates the impacts of not only the point estimate ASD but also the total traffic volume. This new measurement, total vehicle red time (TVRT), will be discussed in Section 5.2.3.

5.1.2 Intersection Geometry

As discussed in Section 4.3.3, the modeled CO varies with different intersection geometry. The intersection geometry depicted in Figure 4.6, Figure 4.7, and Figure 4.8 are referred to as intersection geometry I, intersection geometry II, and intersection geometry III, respectively. Using West LA (1981) meteorological data, traffic data as depicted in Table 4.4, and signalization data depicted in Table 4.5, the modeled [CO] with different intersection geometry are summarized in Table 5.2.

Table 5.2 Model [CO] with Different Intersection Geometry

Intersection Geometry	Modeled [CO] (ppm)
Geometry I	11.12
Geometry II	10.03
Geometry III	14.55

Modeled [CO] with different intersection geometry varies from 10.03 ppm to 14.55 ppm, indicating that intersection geometry has a pronounced effect on the modeled [CO]. Clearly, there will be many different types of intersection geometry in a typical

urban area. Hence, it will be very difficult, if not impossible, to develop a new statistical model for every possible type of intersection geometry. A new *quantitative* measurement, which reflects a geometric association, is required to incorporate the impact of intersection geometry into the new statistical model.

5.1.3 TVRT

There are two types of links that can be coded in CAL3QHCR: free-flow links and queue links. A recent study conducted by UC Davis (17) showed that queue links are by far the most dominant source of [CO] (about 80-85% of the total [CO] is attributable to queue links). Hereafter, the traffic link with the longest queue is defined as the critical link, since the highest modeled [CO] at intersections often occurs at the downwind direction of the link with the longest queue. As indicated in Equation 3.2, Equation 3.3, and Equation 3.5 in Section 3, the total line source strength of queue emission links is a function of total traffic volume and the ratio of signal red time to signal cycle length. Consequently, a new quantitative measurement, total vehicle red time (TVRT) of the critical link, is introduced. TVRT is defined as the product of the traffic volume on the critical link and the ratio of signal red time for the critical link to the signal cycle length:

$$TVRT = v(r / C) \tag{5.1}$$

where

$TVRT$ = Total vehicle red time (vehicles)
v = Hourly traffic volume on the critical link (vehicle)
r = Signal red time for the critical link (seconds)
C = Signal cycle length (seconds)

To examine the effect of TVRT on the modeled [CO], for each of the intersection geometry patterns discussed in Section 4.3.3, seven different TVRT scenarios were simulated. Each TVRT scenario and the corresponding modeled [CO] are summarized in Table 5.3. Figure 5.2 is the scatter plot of TVRT vs. the modeled [CO].

Table 5.3 Modeled [CO] with Varying TVRT

Intersection Geometry	ASD (sec/veh)	Traffic Volume (vehicle/hour)	r/C	TVRT (vehicle)	[CO] (ppm)
II	24.2	2153	0.326	702	10.03
II	25.2	2340	0.326	763	10.86
III	24.2	3154	0.260	820	11.67
II	26.2	2546	0.326	830	11.72
I	24.2	2577	0.326	840	11.92
III	25.2	3307	0.260	860	12.26
II	28.6	2699	0.326	880	12.34
I	25.2	2758	0.326	899	12.88
III	26.2	3530	0.260	918	12.95
II	31.5	2877	0.326	938	13.04
I	26.2	2936	0.326	957	13.56
III	28.6	3757	0.260	977	13.72
II	36.1	3058	0.326	997	14.06
III	31.5	3919	0.260	1019	14.55
II	42.9	3178	0.326	1036	14.81
I	28.6	3236	0.326	1055	14.92
III	36.1	4135	0.260	1075	15.24
I	31.5	3356	0.326	1094	15.59
I	36.1	3417	0.326	1114	15.69
III	42.9	4323	0.260	1124	16.01
I	42.9	3475	0.326	1133	16.06

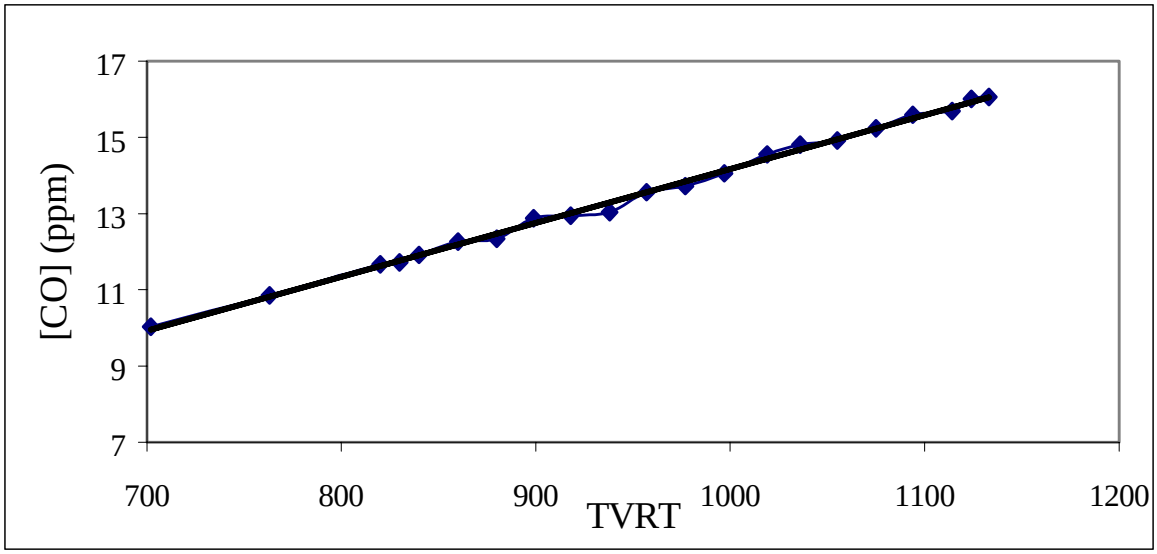

Figure 5.2 Modeled [CO] vs. TVRT

Figure 5.2 reveals a very strong, approximately linear relationship between TVRT and the modeled [CO]. The modeled [CO] increases as TVRT increases, regardless of ASD, intersection geometry, and traffic volume on the critical link. That is, TVRT subsumes the effects of ASD, intersection geometry, and traffic volume on the modeled [CO]. Thus, for this study TVRT will be used in developing the new statistical model by varying the factor from 700 vehicles to 1450 vehicles, which will cover most of the possible combinations of ASD, intersection geometry, and critical link traffic volumes.

5.1.4 Intersection Orientation

Intersection orientation is defined here as the relative angle between the dominant wind direction and the critical link of the intersection. As shown in Section 4.3.2 and Figure 4.5, the modeled [CO] varies substantially with intersection orientation. For this study, different intersection orientations will be generated by rotating the hypothetical intersection counter-clockwise, at ten-degree increments.

5.1.5 Queue/Free-Flow Emission Factors

The uniform line source strength (q) used in predicting [CO] (Equation 3.7) is directly related to queue and free-flow emission factors. As discussed in Section 4.1.3, the emission factors are dependent on the percent of cold starts and free-flow speeds. Using EMFAC7f, a mobile emission program based on California vehicle fleet characteristics (34), the emission factors for fleet year 1997 assuming varying percentages of cold start and free-flow speeds can be summarized as in Table 5.4.

Table 5.4 Emission Factors

	20% cold start	30% cold start	40% cold start	50% cold start
Idling	314.4 grams/hour	426.0 grams/hour	537.6 grams/hour	649.8 grams/hour
20 mph	17.5 grams/mile	23.1 grams/mile	28.7 grams/mile	34.3 grams/mile
25 mph	14.2 grams/mile	18.7 grams/mile	23.2 grams/mile	27.6 grams/mile
30 mph	11.9 grams/mile	15.7 grams/mile	19.4 grams/mile	23.1 grams/mile
35 mph	10.3 grams/mile	13.5 grams/mile	16.7 grams/mile	19.9 grams/mile

The effect of free-flow emission factors is examined using the hypothetical intersection depicted in Figure 4.1, the meteorological data of West Los Angeles and holding the queue emission factor constant at 423.0 grams/veh-hour and ASD constant at 31.5 seconds, while varying the free-flow emission factor from 10 grams/veh-mile to 30 grams/vehicle-mile. The modeled [CO] with different free-flow emission factors are summarized in Table 5.5 and Figure 5.3.

Table 5.5 Modeled [CO] with Different Free-Flow Emission Factors

Free-Flow Emission Factor (g/veh-mile)	10	15	20	25	30
Modeled [CO] (ppm)	6.68	7.11	7.59	8.26	8.74

Figure 5.3 is the scatter plot of the highest modeled [CO] vs. free-flow emission factor. The highest modeled [CO] increases as free-flow emission factor increases, and the relationship is expected to be very close to linear. The modeled [CO] with different free-flow emission factors varies from 6.68 ppm to 8.74 ppm, indicating that the free-flow emission factor has a substantial impact on modeled [CO] and should also be included in the new statistical model.

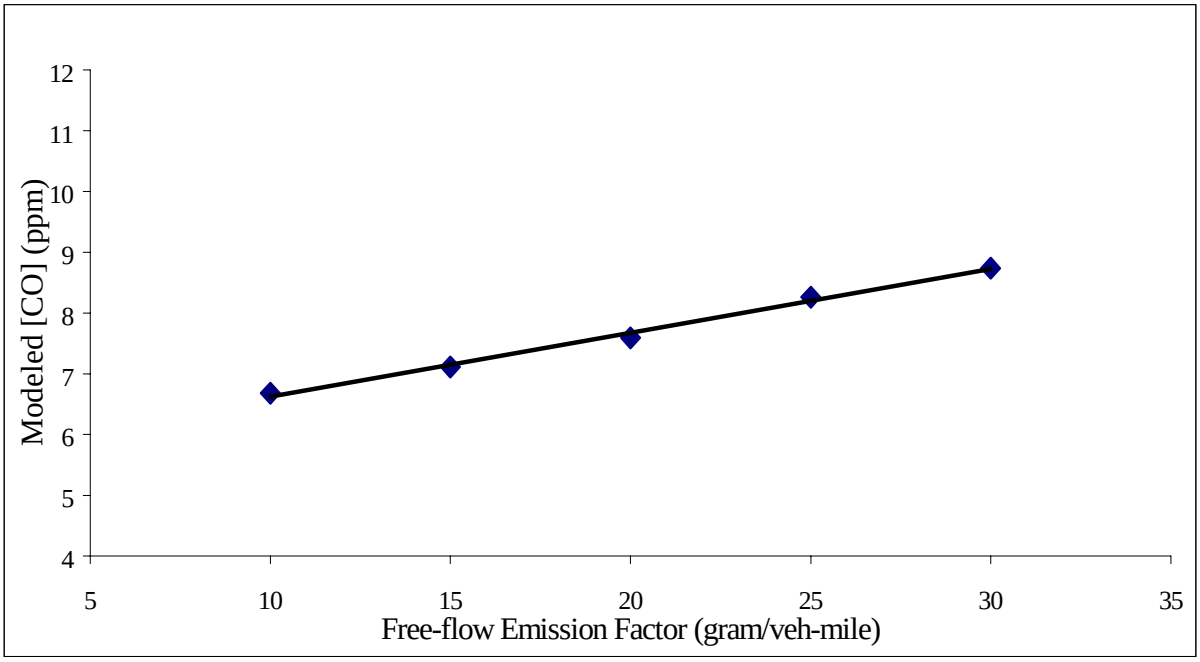

Figure 5.3 Modeled [CO] vs. Free-flow Emission Factors

The effect of the queue emission factor is examined using the hypothetical intersection depicted in Figure 4.1 and the meteorological data of West Los Angeles and holding the free-flow emission factor constant at 23.6 grams/veh-mile and ASD constant at 31.5 seconds, while varying the queue emission factor from 200 grams/veh-hour to 400 grams/vehicle-hour. The modeled [CO] with different queue emission factors are summarized in Table 5.6 and Figure 5.4.

Table 5.6 [CO] Level (ppm) with Different Queue Emission Factors (g/veh-hr)

Queue Emission Factor (gram/veh-hr)	300	350	400	450	500
Modeled [CO] (ppm)	5.9	6.68	7.55	8.35	9.13

Figure 5.4 is the scatter plot of the highest modeled [CO] vs. queue emission factors. The highest modeled [CO] increases as the queue emission factor increases. Again, the relationship is expected to be linear.

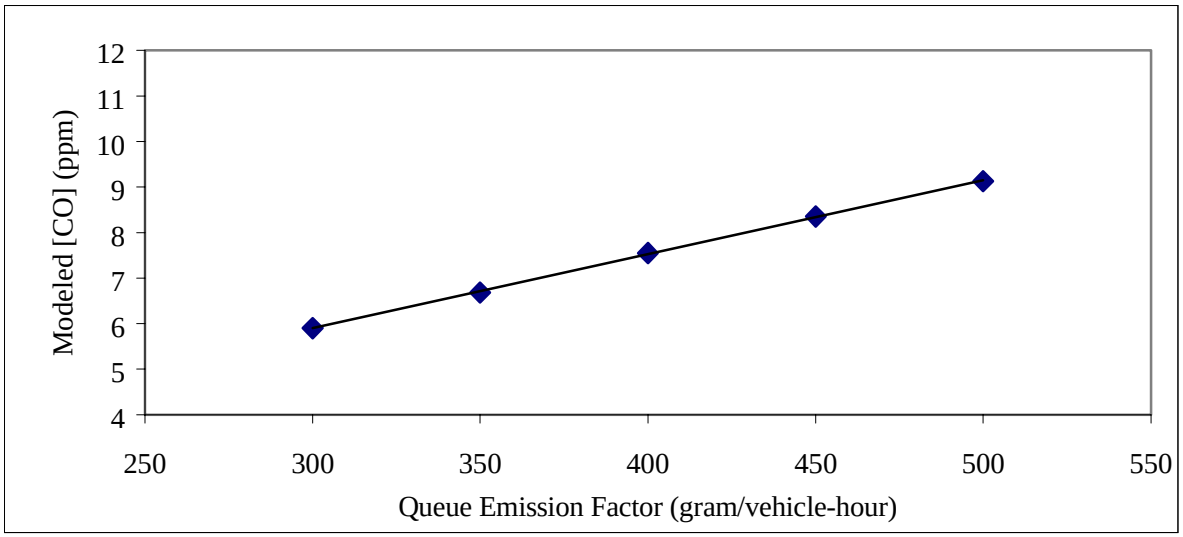

Figure 5.4 Modeled [CO] vs. Queue Emission Factor

As shown in Figure 5.3 and Figure 5.4, the relationships of modeled [CO] and the emission factors (queue and free-flow) are very close to linear. In developing the new statistical model in this study, the free-flow emission factors will take values of 10 grams/vehicle-mile, 15 grams/vehicle-mile, 20 grams/vehicle-mile, 25 grams/vehicle-mile, and 30 grams/vehicle-mile; and the queue emission factors will take values of 300 grams/vehicle-hour, 350 grams/vehicle-hour, 400 grams/vehicle-hour, 450 grams/vehicle-hour, and 500 grams/vehicle-hour. These values of emission factors cover the range of most of the values that emission factors will likely take in the future, based on different percent of cold starts, free-flow speeds, ambient temperature, and future year fleet characteristics.

5.1.6 Wind Speed

Wind speed determines the extent to which CO is initially diluted with ambient air at the point of release. The inverse relationship between wind speed and modeled [CO] is

shown in Equation 3.7. The preliminary study of the relationship between the highest modeled [CO] and wind speed is summarized in Table 5.7 and Figure 5.5.

Table 5.7 Modeled [CO] (ppm) with Different Wind Speeds (m/s)

Wind Speed	1.0	1.5	2.0	2.5	3.0
[CO]	6.68	4.13	3.23	2.69	2.21

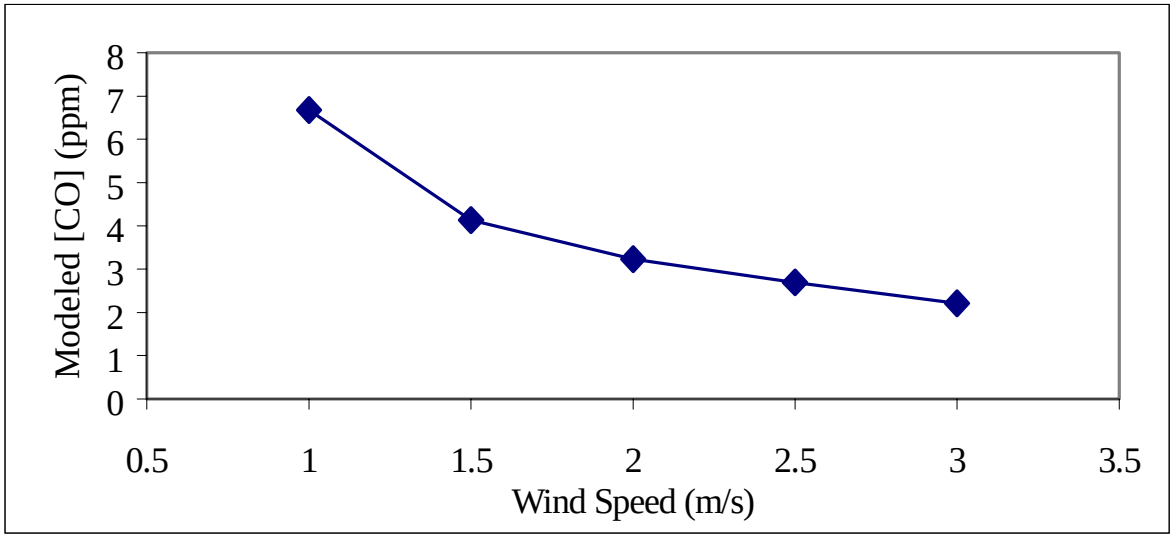

Figure 5.5 Modeled [CO] vs. Wind Speed

Figure 5.5 indicates that modeled [CO] decreases non-linearly as wind speed increases. It is generally believed that the highest [CO] is very unlikely to happen when the wind speed is greater than 3 m/s (17&18). Meanwhile, the dispersion algorithm used in CAL3QHCR has not been validated for wind speeds less than 1.0 m/s. Hence, in developing the statistical model, wind speed will take the following values: 1.0 m/s, 1.5 m/s, and 2.0 m/s, 2.5 m/s, and 3.0 m/s.

5.1.7 Surface Roughness

As discussed in Section 2.3, the horizontal and vertical dispersion parameters σ_y and σ_z are dependent on the surface roughness, because air movement over the surface generates mechanical turbulence. An increase in the amount of turbulence can "enhance

both the vertical and horizontal dispersion of pollutants released near ground level." (7&26) Typically, the mechanical turbulence increases as the surface roughness increases, and surface roughness depends on the type of the surface. The surface roughness lengths (Z_0) used in CALINE3, the dispersion algorithm in CAL3QHCR, for different land uses are summarized in Table 5.8.

Table 5.8 Surface Roughness for Different Land Uses

Type of Surface	**Surface Roughness Z_0 (cm)**
Grass	0.14 - 11.4
Wheat	22.0
Corn	74.0
Citrus orchard	198.0
Single family residential	108.0
Apartment residential	370.0
Office	175.0
Central business district	321.0
Park	127.0

(Source: reference 38)

For the purpose of protecting of general public health, potential CO hot-spot intersections in the central business district are of more interest than any other land use. Hence, only one surface roughness value, 321 centimeters for central business districts, will be applied in developing the new statistical model.

5.1.8 Stability Class

The ambient atmosphere is said to be *unstable* if the buoyancy forces enhance vertical motion of a parcel of air and it is said to be *stable* if the buoyancy forces oppose the vertical motion of a parcel of air (7&26). The horizontal and vertical dispersion parameters used in Equation 3.7 are dependent on the ambient stability class. Stability classes are based on the surface wind speed (speed at ten meters) and on ground radiation

balance (7). These classes have letter designations, from A (extremely unstable) to G (very stable).

In contrast to the theoretical premise, in the dispersion algorithm used in CAL3QHCR (CALINE3), the horizontal and vertical dispersion parameter σ_y and σ_z are insensitive to stability class when the wind direction is close to perpendicular to the traffic link (2). Also as discussed before, in this study the highest [CO] is more likely to occur when the wind direction is close to perpendicular to the critical link. Hence, atmospheric stability class will not be included in the new statistical model as an independent variable. One plausible explanation of CAL3QHCR's insensitivity to atmospheric stability class could be the receptor locations. As discussed in Section 4.1.2., a standard of 3 meters away from the traveled roadway is applied. And the receptors might be too close to the intersections to let atmospheric stability class have a significant impact on the modeled [CO].

5.1.9 Ambient Temperature

Ambient temperature is one of several meteorological input variables required by CAL3QHCR. Both free-flow and queue emission factors are a function of the ambient temperature. That is, ambient temperature affects the modeled [CO] indirectly through emission factors. Hence, ambient temperature will not be included into the new statistical model as an independent variable.

6.0 STATISTICAL MODELING

In this section, the statistical analysis of the relationship between the modeled [CO] (dependent variable) and the individual input factors identified in Section 5 (independent variables) is conducted. The discussion begins with the application of several statistical modeling techniques, which include traditional linear regression, linear regression with data transformations, and the generalized additive model (GAM) to these data. Finally, interactions among independent variables will be examined.

The values of the dependent variable used in developing the statistical models are [CO] predicted by CAL3QCHR. By doing so, we are assuming that CAL3QHCR is a "perfect" model for estimating [CO] at intersections. In addition, the proposed models are expected to slightly overestimate [CO] when compared to values computed using CAL3QHCR. This overestimating is designed by controlling the variability in wind direction, as will be discussed in Section 7.3.

Based on the discussion in Section 5, Table 6.1 summarizes the independent variables and the values that each independent variable will be assigned in developing a new integrated statistical model.

Table 6.1 Independent Variable and Assigned Values

Factor	**Assigned Values**
TVRT (vehicle)	700, 820, 970, 1150, and 1300
Intersection Orientation (degree)	0 ~ 360, at a 10 deg. increment
Free-flow Emission Factor (gram/veh-mile)	10, 15, 20, 25, and 30
Queue Emission Factor (gram/veh-hour)	200, 250, 300, 350, and 400
Wind Speed (m/s)	1.0, 1.5, 2.0, 2.5, and 3.0

Note that the proposed models are applicable to any geographical area, as long as the input variables take values from the ranges summarized in Table 61.

Table 6.1 indicates that in total, there will be $5 \times 36 \times 5 \times 5 \times 5 = 22{,}500$ CAL3QHCR simulations required to generate the input data for statistical modeling. The NAAQS for CO are 8-hour average and 1-hour average standards. The annual highest 8-hour averaged [CO] modeled by CAL3QHCR is selected as the dependent variable in developing the statistical models, since usually the 8-hour average [CO] is computed first and then converted to the 1-hour average [CO] using a "worst case" persistence factor (9). The annual highest 8-hour averaged [CO] modeled by CAL3QHCR, together with the five corresponding values of the independent variables from each simulation were assembled into a text file suitable for use by the statistics package, S-Plus. Because of the file's large size, the input data file is not attached to this document. However, it is available from the author upon request.

The discussion of the statistical modeling techniques begins with the application of standard linear regression (Section 6.1) because of its parametric functional form and simplicity in interpretation. Then, the discussion turns to data transformations for the dependent and independent variables (Section 6.2 and Section 6.3). These transformations are required to improve the model performance, since the dependency of modeled [CO] on the independent variables is not linear in some cases. Finally, the discussion of the application of an advanced regression technique, the generalized additive model, is presented (Section 6.6); this technique is very useful when it is theoretically difficult to know the appropriate data transformation form.

6.1 Traditional Linear Regression

The standard linear regression model may be stated as:

$$E([CO]) = \beta_0 + \Sigma_{i=1}^{n} X_i \beta_i \tag{6.1}$$

where

$[CO]$ = modeled CO concentration
$E([CO])$ = mean of the modeled CO concentration
β_0, β_i = estimated parameters
X_i = predictors
n = number of predictors

The parameters are usually estimated by least-squares and this model is very useful if the dependence of [CO] on the predictors is close to linear. For example, consider the relationships between the modeled [CO] and the emission factors (refer to Figure 5.3 and Figure 5.4).

The traditional linear regression model is given as:

$$\begin{aligned} E([CO)] = {} & 2.762 + 0.0039(TVRT) + 0.073(\,ffef\,) + 0.0135(qef\,) \\ & - 4.1177(ws) - 0.0015(deg) \end{aligned} \tag{6.2}$$

where

$E([CO])$ = mean of the modeled CO concentration (ppm)
$TVRT$ = total vehicle red time (vehicles)
$ffef$ = free - flow emission factor (grams/vehicle - mile)
qef = queue emission factor (grams/vehicle - hour)
ws = wind speed (m/s)
deg = intersection orientation (degrees)

The statistics of this linear regression model, hereafter referred to as MODEL1, are summarized in Table 6.2.

Table 6.2 Statistics of MODEL 1

Variable	Coefficient	Std. Error	t-value	Pr(t)
Intercept	2.7616	0.1737	15.9010	0.000
TVRT	0.0039	0.0001	25.8434	0.000
ffef	0.0730	0.0018	40.9342	0.000
qef	0.0135	0.0002	75.7509	0.000
ws	-4.1177	0.0357	-115.4628	0.000
deg	-0.0015	0.0001	-10.4844	0.000

Adjusted R-square: 0.881
Residual Sum of Squares (RSS): 1998.67
Degrees of Freedom (d.f.): 2910

Note that in Equation 6.2, all the estimated coefficients are significant at a significance level $\alpha = 0.05$. The *positive* coefficients (associated with *TVRT*, *ffef*, and *qef*) indicate the *increase* in the mean of the probability distribution of the modeled [CO] per unit increase in the independent variables. The *negative* coefficients (associated with *ws* and *deg*) indicate the *decrease* in the mean of the probability distribution of the modeled [CO] per unit increase in the independent variables. The signs of all the estimated coefficients are as expected except for the negative coefficient associated with *deg*.

For MODEL1, the diagnostic plots of residuals versus fitted values, responses versus the fitted values, and normal probabilities of residuals are given in Figure 6.1, Figure 6.2, and Figure 6.3, respectively. The plot of residuals versus fitted values reveals unexplained structure in the residuals. Figure 6.1 reveals a systemic pattern: error variances increase as the fitted values increase. The plot of responses against fitted values indicates how well the model represents the data. Figure 6.2 indicates that MODEL1 does a fairly good job in representing the data. The normal probability plot of residuals tests one of the model's assumptions: the model's errors are normally

distributed. Many ordered residuals at the two tails of Figure 6.3 do not cluster along the superimposed quantile-quantile line, indicating that MODEL1's errors are not normally distributed.

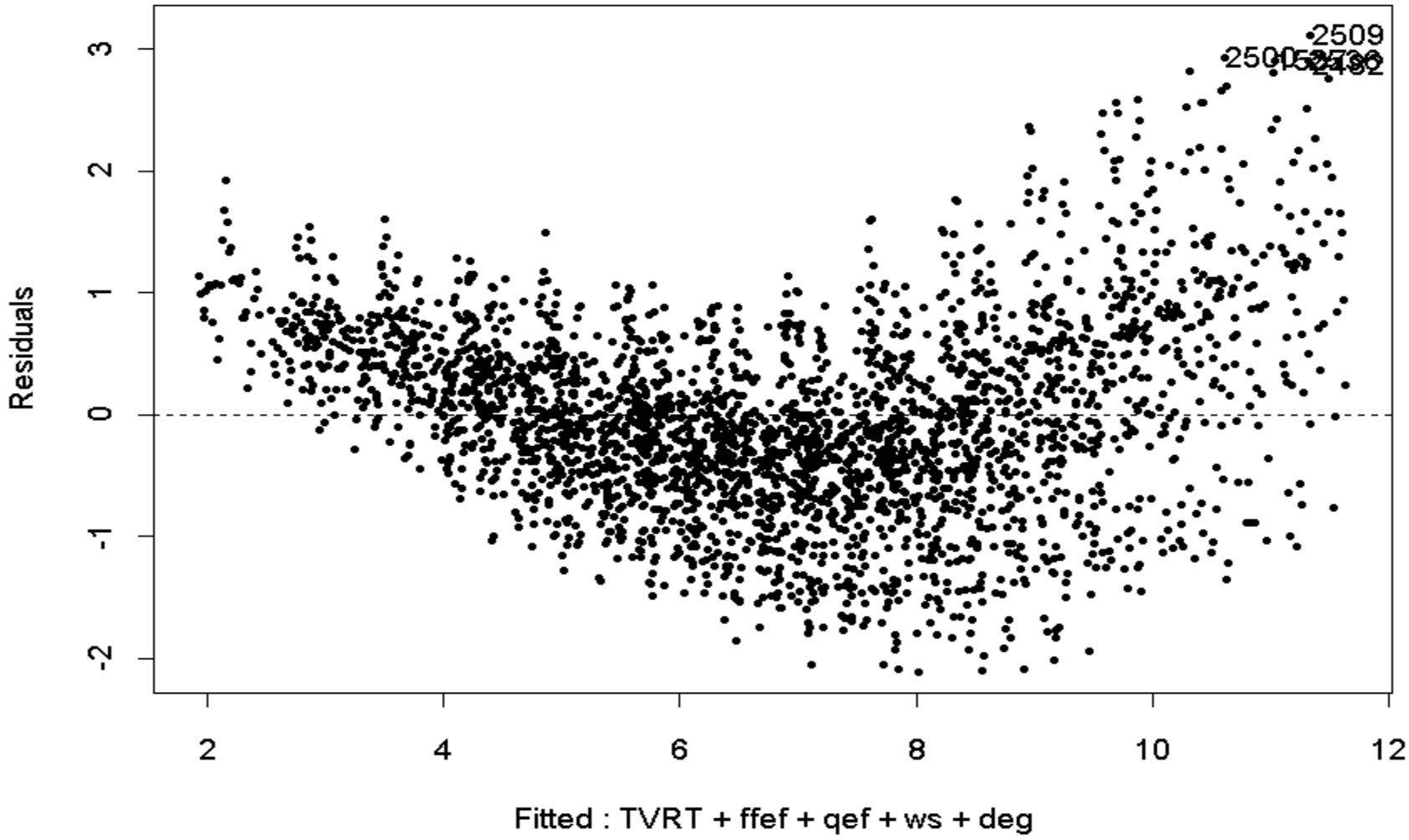

Figure 6.1 Plots of Residuals versus Fitted Values, MODEL1

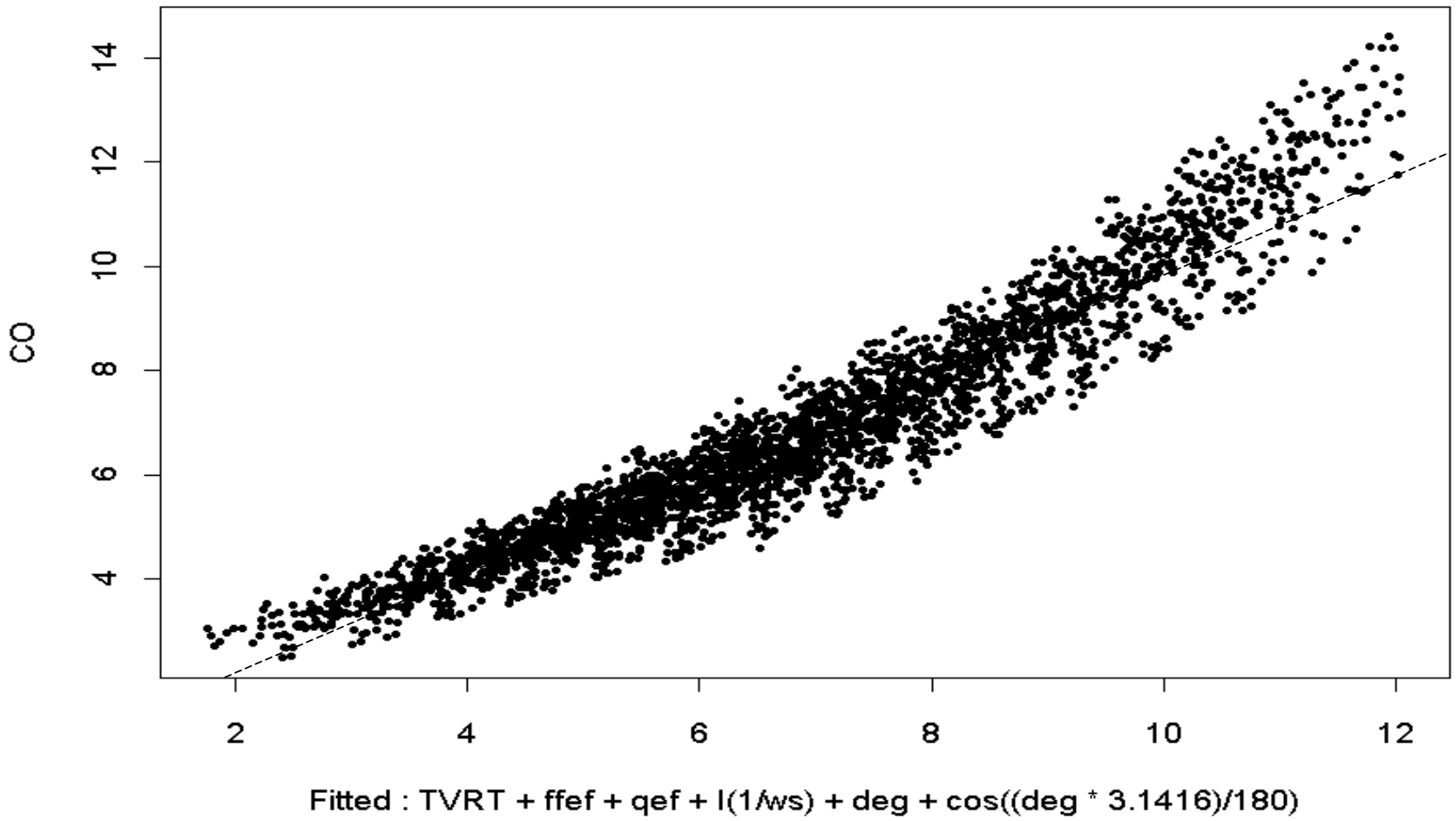

Figure 6.2 Plot of Response versus Fitted Values, MODEL1

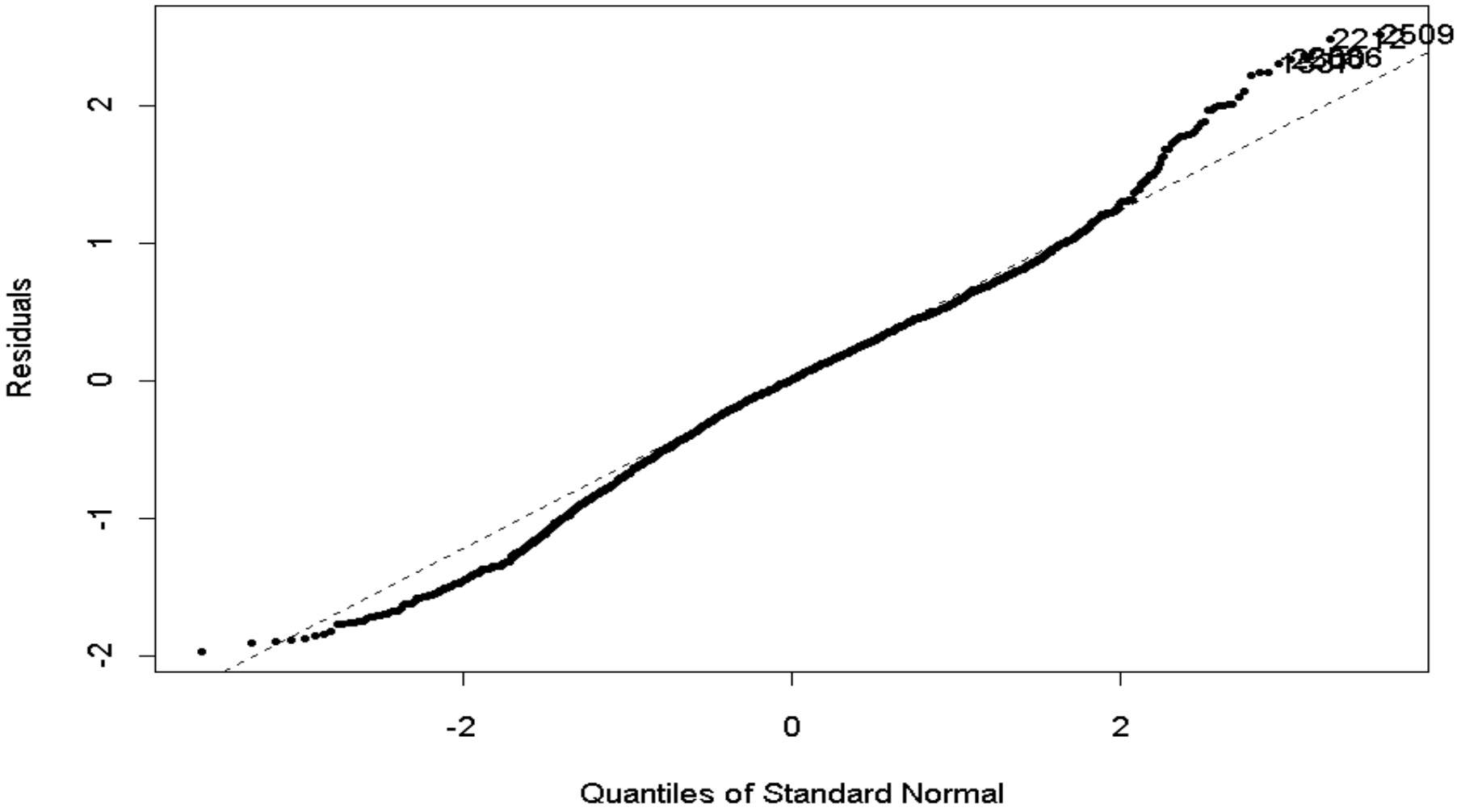

Figure 6.3 Normal Probability Plot of Residuals, MODEL1

6.2 Linear Regression with Data Transformation

In the traditional linear regression model (MODEL1), it is assumed that the relationship between modeled [CO] and individual factors is linear. However, the residual plots of MODEL1 (Figure 6.1 and Figure 6.2) reveal a strong systematic pattern retained in the data, indicating that the assumption of the linear dependence may not be valid. In addition, both Figure 4.5 and Figure 5.5 suggest a strong non-linear relationship between the modeled [CO] and intersection orientation (Figure 4.5) and wind speed (Figure 5.5). Under these circumstances, some parametrical data transformation techniques on these two predictors might be desirable to improve the model performance. The most popular data transformation choices are log, square root, inverse and other power transformations (13).

Figure 5.5 suggests an inverse transformation on *wind speed*, and this regression model is stated as:

$$E([CO)] = -9.34 + 0.004 * TVRT + 0.073 * \ ffef \ + 0.014 * qef + 8.2 * (1/ws) - 0.0015 * \deg \tag{6.3}$$

The summary statistics of this linear regression model, hereafter referred to as MODEL2, are given in Table 6.3.

Table 6.3 Statistics of MODEL2

Variable	Coefficient	Std. Error	t-value	Pr(t)
Intercept	-9.3381	0.1611	-57.9534	0.000
TVRT	0.0039	0.0001	27.7149	0.000
ffef	0.0730	0.0017	43.8985	0.000
qef	0.0135	0.0002	81.2364	0.000
1/ws	8.2013	0.0653	125.5751	0.000
deg	-0.0015	0.0001	-11.2436	0.000

Adjusted R-square: 0.896
RSS: 1563.96
d.f: 2910

Note that the negative intercept (-9.3381) indicates that when everything else equals zero, the modeled [CO] is –9.3381 ppm, which is counterintuitive. However, since the proposed model was formulated to apply to the input scenarios where each independent variable can only take values summarized in Table 6.1, and none of the ranges covers zero, the intercept does not have any intrinsic meaning of its own here.

For MODEL2, the diagnostic plots of residuals versus fitted values, responses versus the fitted values, and normal probabilities of residuals are given in Figure 6.4, Figure 6.5, and Figure 6.6, respectively.

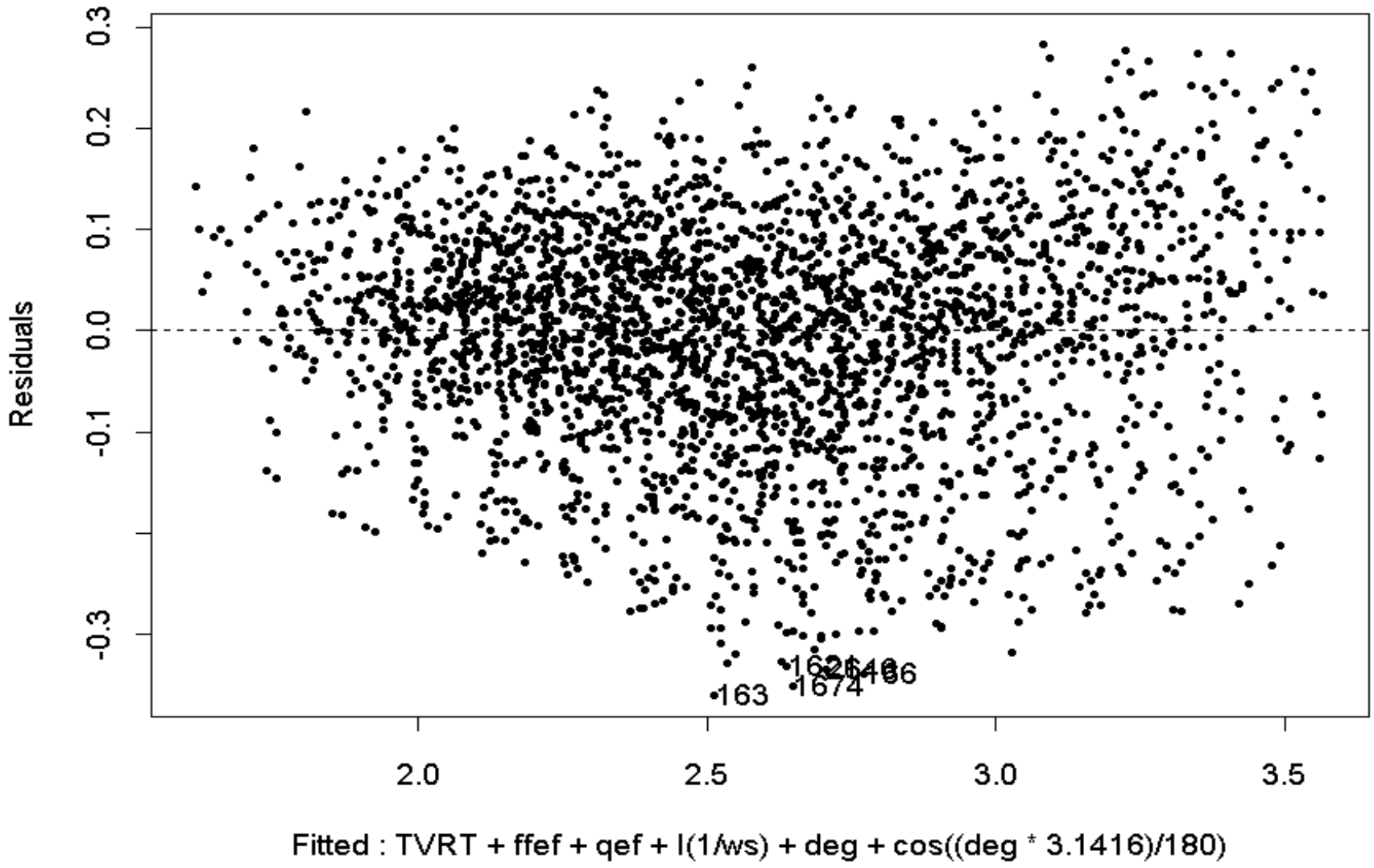

Figure 6.4 Plot of Residuals versus Fitted Values, MODEL2

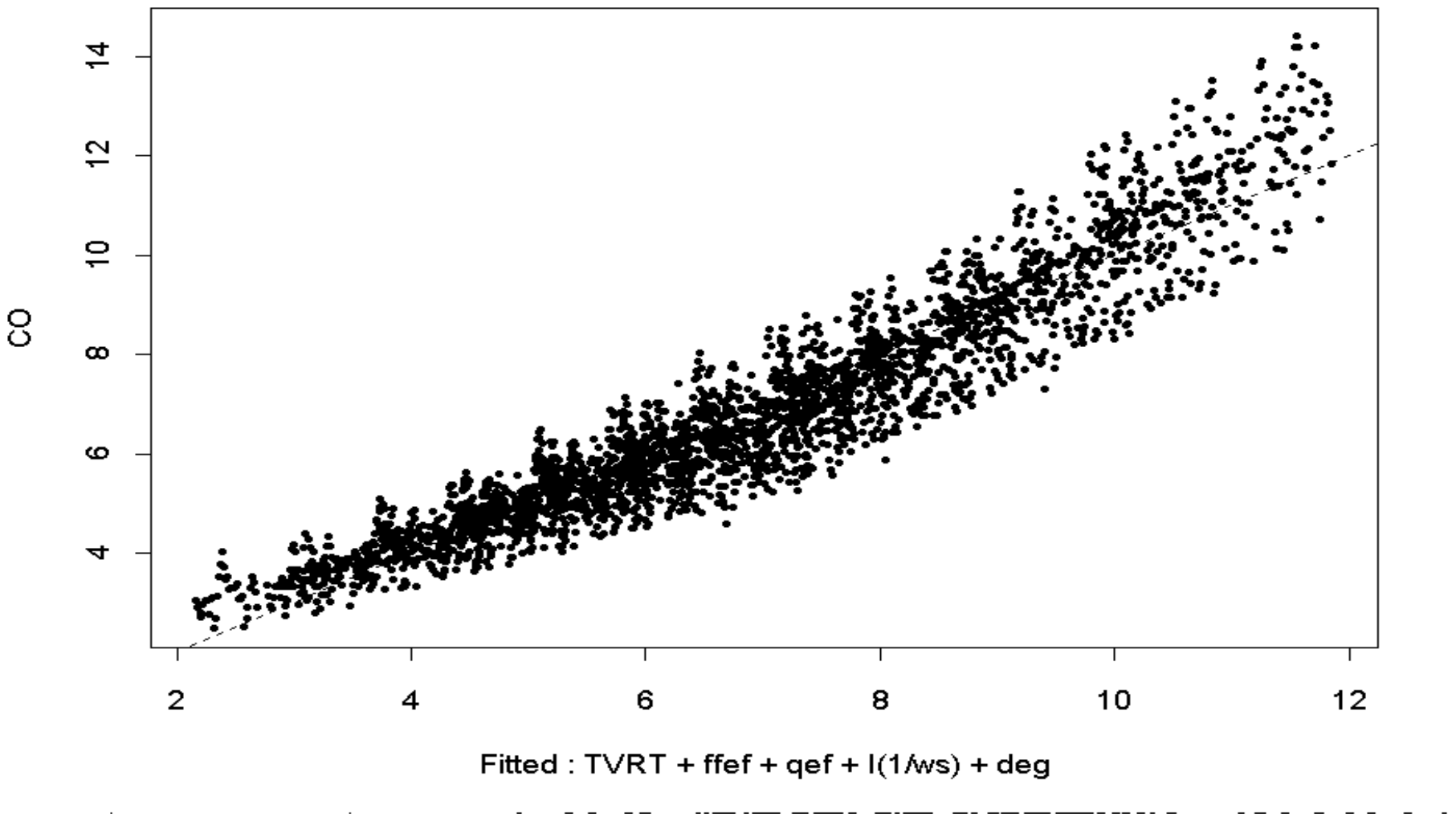

Figure 6.5 Plot of Responses versus Fitted Values, MODEL2

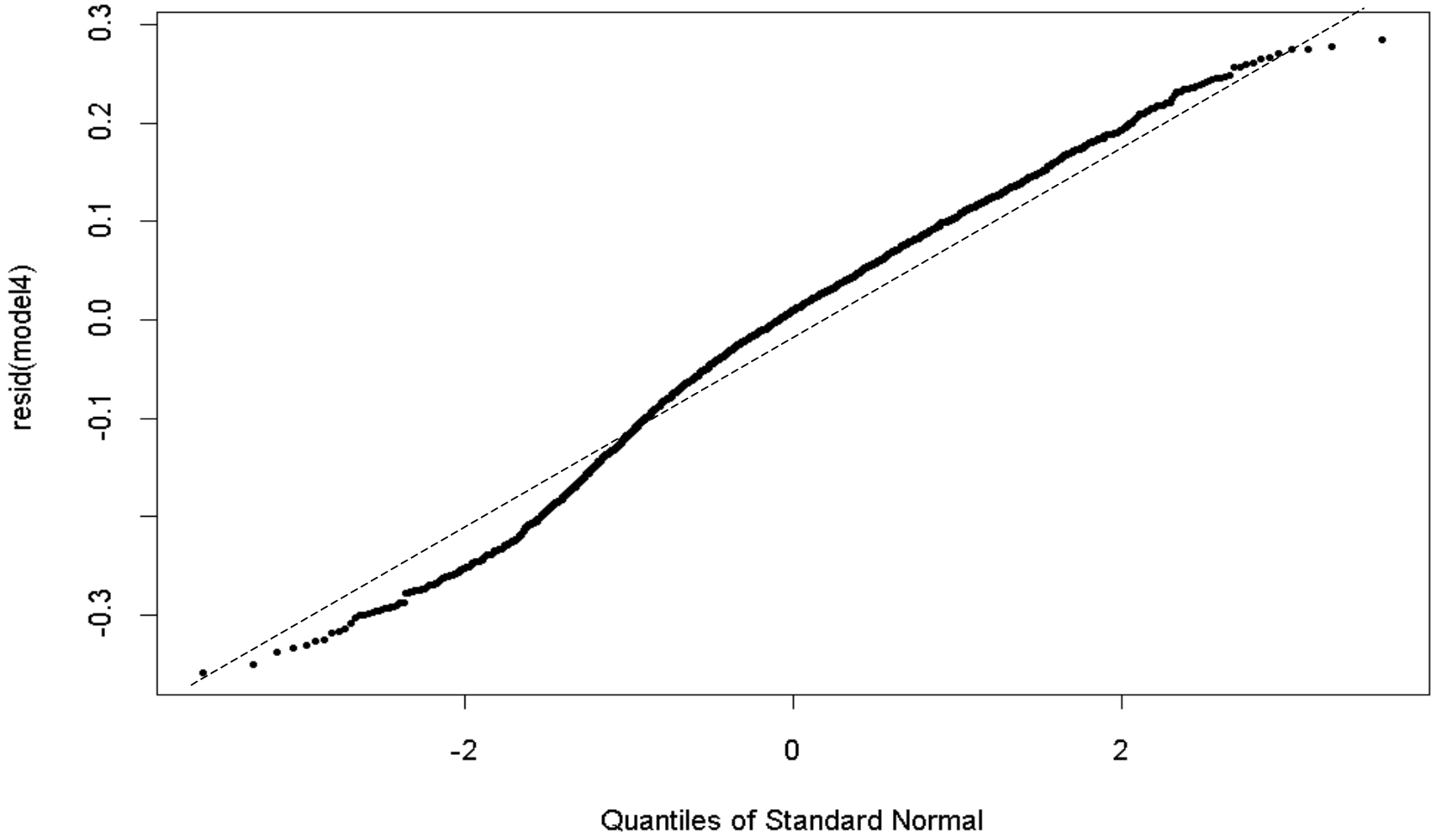

Figure 6.6 Normal Probability Plot of Residuals, MODEL2

The choice between MODEL1 and MODEL2 can be determined by comparing the model diagnostic plots and the adjusted R-square associated with these two models. MODEL2 has a slightly higher adjusted R-square (0.896) than MODEL1 does (0.881), indicating that MODEL2 explains slightly more variability than MODEL1. However, the diagnostic plots of MODEL2 (inverse transformation on *ws* and continued use of traditional linear regression on the remaining input variables) still reveal a systematic pattern remaining in the data.

6.3 Trigonometric Model

The small difference in the adjusted R-square between MODEL1 and MODEL2 and the systematic pattern revealed in the diagnostic plots of MODEL2 indicate that the data transformation on *wind speed* alone does not dramatically improve the model performance. The scatter plot of modeled [CO] vs. intersection orientation (Figure 4.5) exhibits a non-linear relationship, and the shape of the plot suggests that a trigonometric transformation, *cosine*, on *intersection orientation*, together with the inverse transformation on *wind speed*, might improve the model's performance, and this regression model is stated as:

$$E([CO)] = -9.37 + 0.004 * TVRT + 0.073 * ffef + 0.014 * qef + 8.2 * (1/ws) - 0.0013 * \deg - 0.4326 * \cos(\deg) \quad (6.4)$$

The statistics of this linear regression model, hereafter referred to as MODEL3, are summarized in Table 6.4.

Table 6.4 Statistics of MODEL3

Variable	Coefficient	Std. Error	t-value	Pr(t)
Intercept	-9.37	0.1462	-64.1063	0.000
TVRT	0.0039	0.0001	30.5367	0.000
ffef	0.0730	0.0015	43.3680	0.000
qef	0.0135	0.0002	89.5075	0.000
1/ws	8.2013	0.0593	138.3606	0.000
deg	-0.0013	0.0001	-10.6595	0.000
cos(deg)	-0.4326	0.0175	-20.9747	0.000

Adjusted R-square: 0.915
RSS: 1087.83
d.f.: 2909

From the physical point of view, including both *deg* and *cos(deg)* in the proposed model can incorporate the impacts of the relative angle between wind direction and the critical traffic link (i.e., intersection orientation) and the relative location of receptor to wind direction and the traffic link with the longest queue. For MODEL3, the diagnostic plots of residuals versus fitted values, responses versus fitted values, and normal probabilities of residuals are given in Figure 6.7, Figure 6.8, and Figure 6.9, respectively, and discussed in Section 6.5 when compared to those of MODEL4.

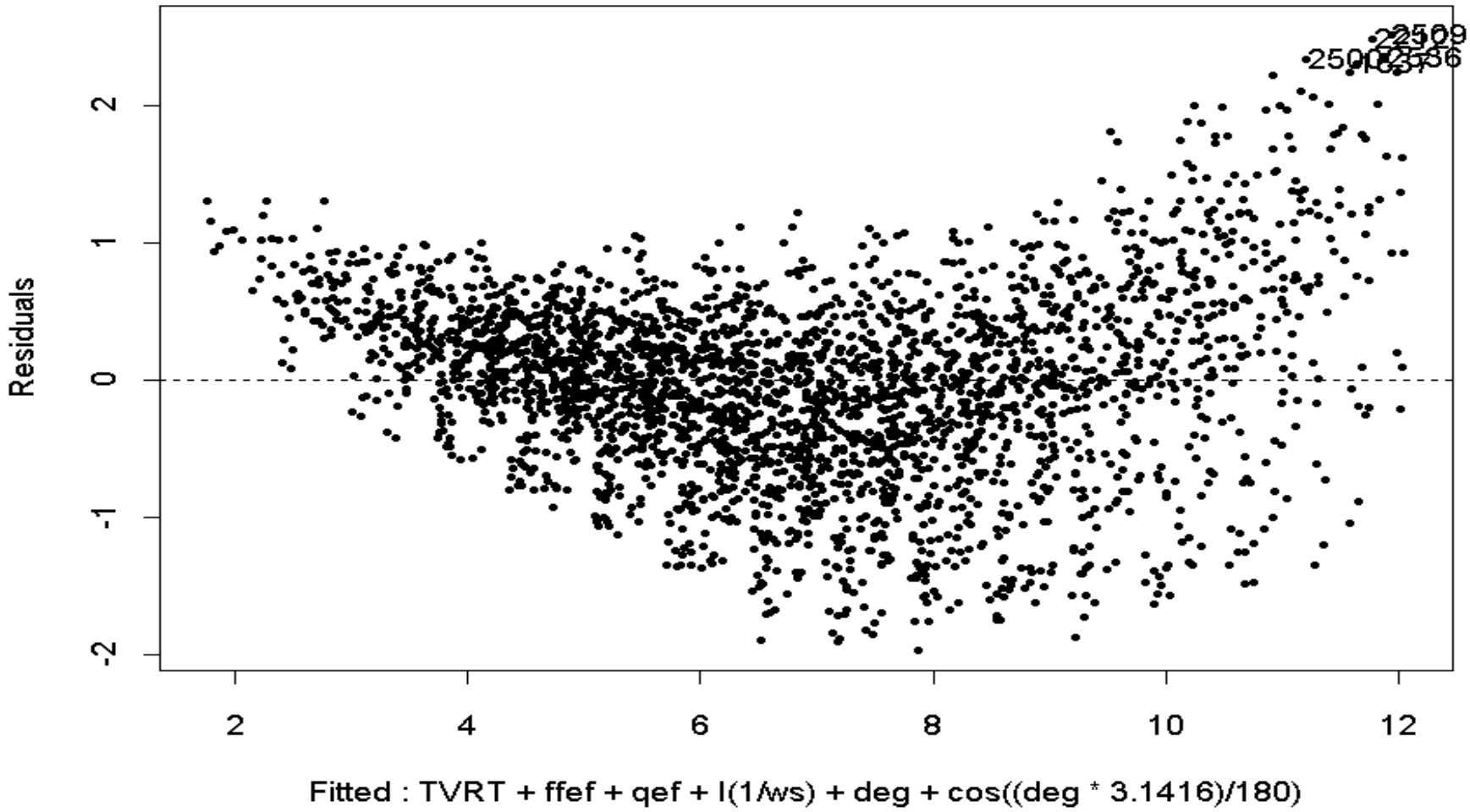

Figure 6.7 Plot of Residuals versus Fitted Values, MODEL3

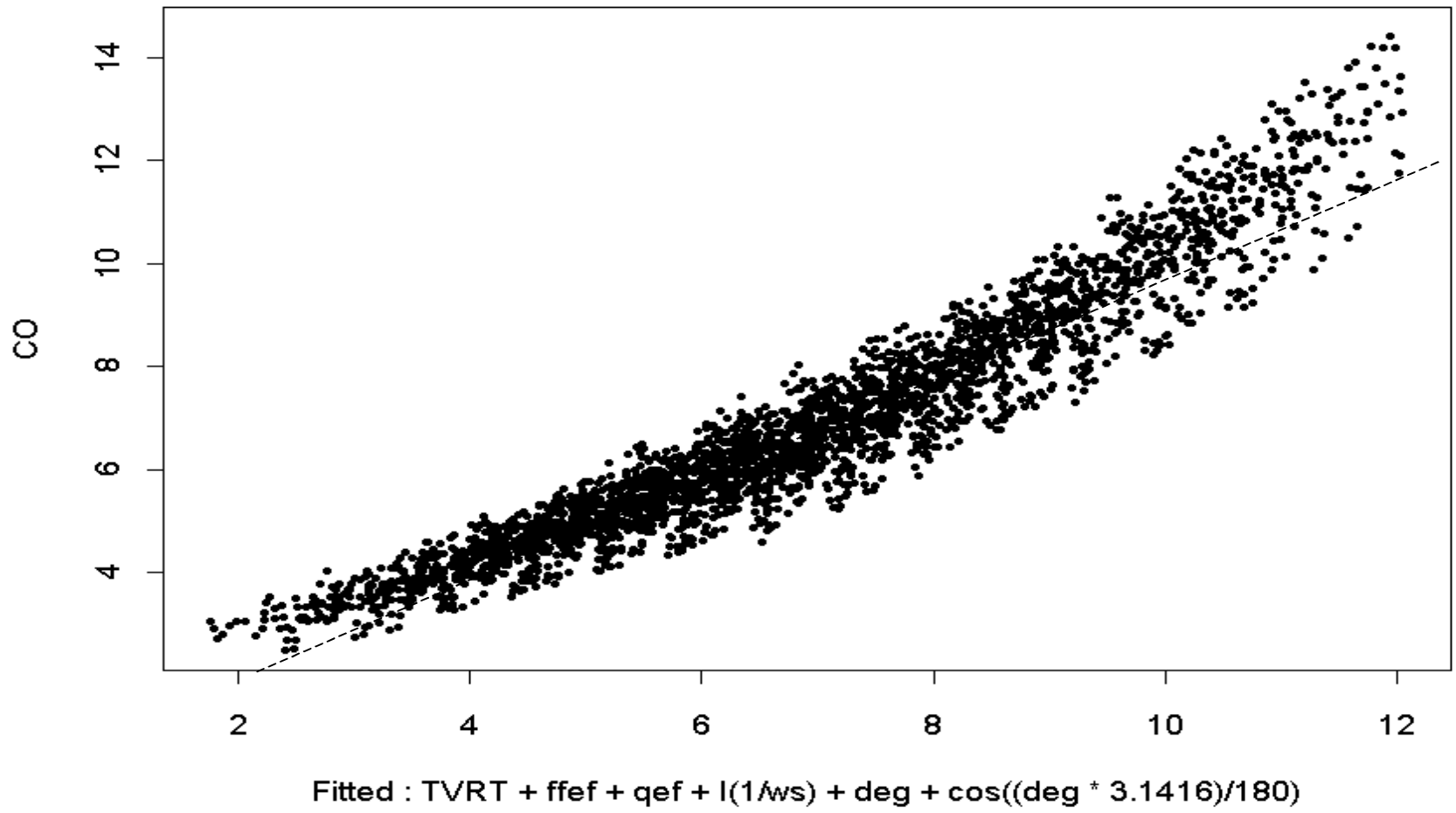

Figure 6.8 Pot of Responses versus Fitted Values, MODEL3

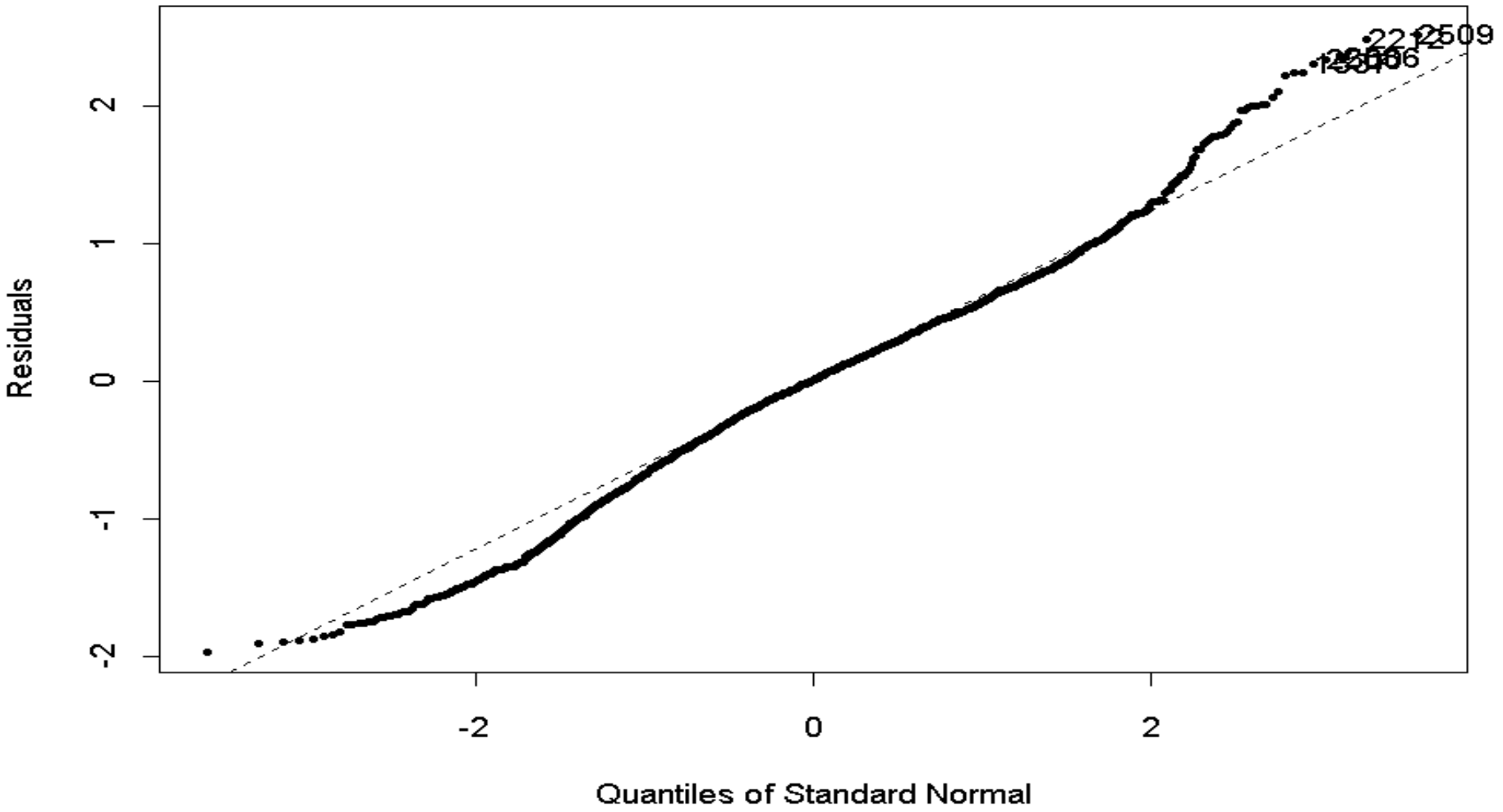

Figure 6.9 Normal Probability Plot of Residuals, MODEL3

6.4 Approximate F-test

The approximate F-Test is used in this study to determine the variability explained by adding factors in the statistical model. Hereafter, the model with the factor of interest as an independent variable is referred to as the *full* model, and the model without the factor of interest is referred to as the *reduced* model. Letting RSS (R) and RSS (F) be the residual sum of squares, df_R and df_F be the degrees of freedom for the reduced model and full model, respectively, and *n* be the sample size, the F-test for comparing models can be stated as (13&20),

$$F^* = \frac{((RSS(R) - RSS(F))/(df_R - df_F)}{RSS_F/(n - df_F)} \sim F_{df_R - df_F,\, n - df_F} \qquad (6.5)$$

Large values of F^* lead to the conclusion that including the factor improves the model performance statistically.

For the test of including *cosine(deg)*, the full model is MODEL2 and the reduced model is MODEL3.

$$\begin{aligned} n &= 2916 \\ df_F &= 6 \\ df_R &= 7 \\ RSS(F) &= 1563.96 \\ RSS(R) &= 1087.83 \end{aligned}$$

Using Equation 6.5, the F-statistic of the comparison between MODEL2 and MODEL3 is 898.35 on one and 2910 degrees of freedom. The F value for this test at 95% confidence, $F_{0.95,\,1,\,2910}$ is 3.84. The F-statistic (898.35) is greater than the F-value (3.84), indicating that including *cosine(deg)* improves the model performance statistically.

6.5 Model Diagnostics

Compared to the diagnostic plots of MODEL1 and MODEL2, Figure 6.7 reveals that there is less unexplained structure in the residuals in MODEL3; and Figure 6.8 reveals that MODEL3 does a better job in representing the data than MODEL1 and MODEL2. However, both Figure 6.7 and Figure 6.8 suggest that a systematic *quadratic* pattern has been retained in the data. It is possible that an appropriate transformation on the dependent variable, [CO], might enhance the model's performance. The normal probability plot of residuals tests one of the model's assumptions: the model's errors are normally distributed. As in Figure 6.3 and Figure 6.6, many ordered residuals at the two tails of Figure 6.9 do not cluster along the superimposed quantile-quantile line, indicating that MODEL3's errors are not normally distributed.

The quadratic pattern revealed in both Figure 6.7 and Figure 6.8 suggest that a square root transformation on the dependent variable can be used to improve the model fit. This regression model, hereafter referred to as MODEL4, is given as:

$$E(sqrt[CO)] = -0.4968 + 0.0007 * TVRT + 0.0141 * \ ffef \ + 0.0026 * qef \\ + 1.5421 * (1/ws) - 0.0002 * \deg - 0.0807 * \cos(\deg)) \qquad (6.6)$$

The statistics of MODEL4 are summarized in Table 6.5.

Table 6.5 Statistics of MODEL4

Variable	Coefficient	Std. Error	t-value	Pr(t)
Intercept	-0.4968	0.0246	-20.1965	0.000
TVRT	0.0007	$2.30*10^{-5}$	34.5366	0.000
ffef	0.0141	0.0003	55.4643	0.000
qef	0.0026	$2.56*10^{-5}$	101.6620	0.000
1/ws	1.5421	0.0100	154.824	0.000
deg	-0.0002	$1.61*10^{-5}$	-12.4195	0.000
cos(deg)	-0.0817	0.0029	-27.8441	0.000

Adjusted R-square: 0.932
RSS: 36.36
d.f.: 2909

MODEL4 has the same degrees of freedom as MODEL3, but a higher adjusted R-square (0.93) than MODEL3 does (0.915), indicating that the square root transformation on the dependent variable improves the model performance. As might be expected from a transformation on the dependent variable, the RSS is reduced from 1087.83 in MODEL3 to 36.36 in MODEL4.

For MODEL4, the diagnostic plots of residuals versus fitted values, responses versus the fitted values, and normal probabilities of residuals are given in Figure 6.10, Figure 6.11, and Figure 6.12, respectively.

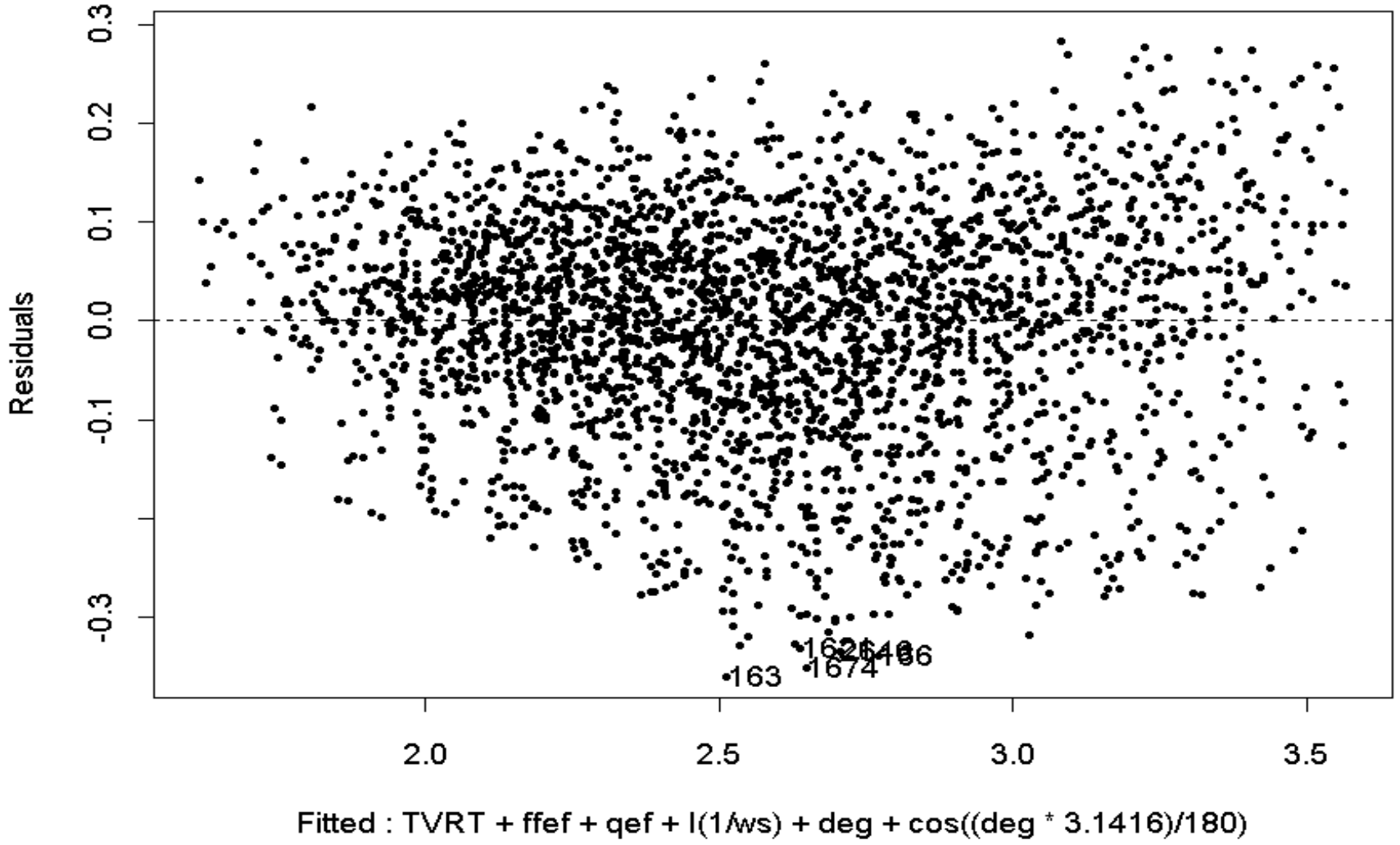

Figure 6.10 Plot of Residuals versus Fitted Values, MODEL4

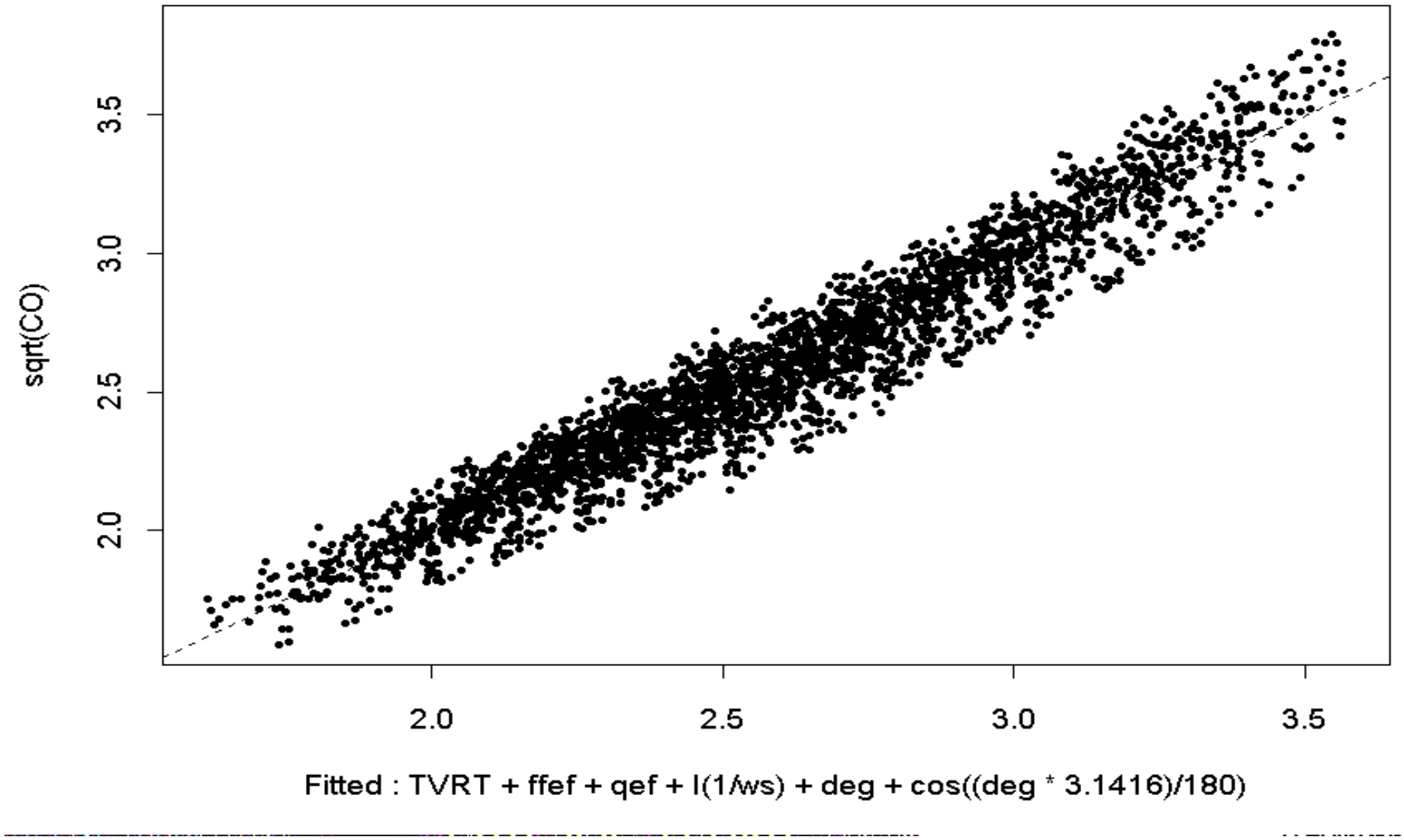

Figure 6.11 Plot of Responses versus Fitted Values, MODEL4

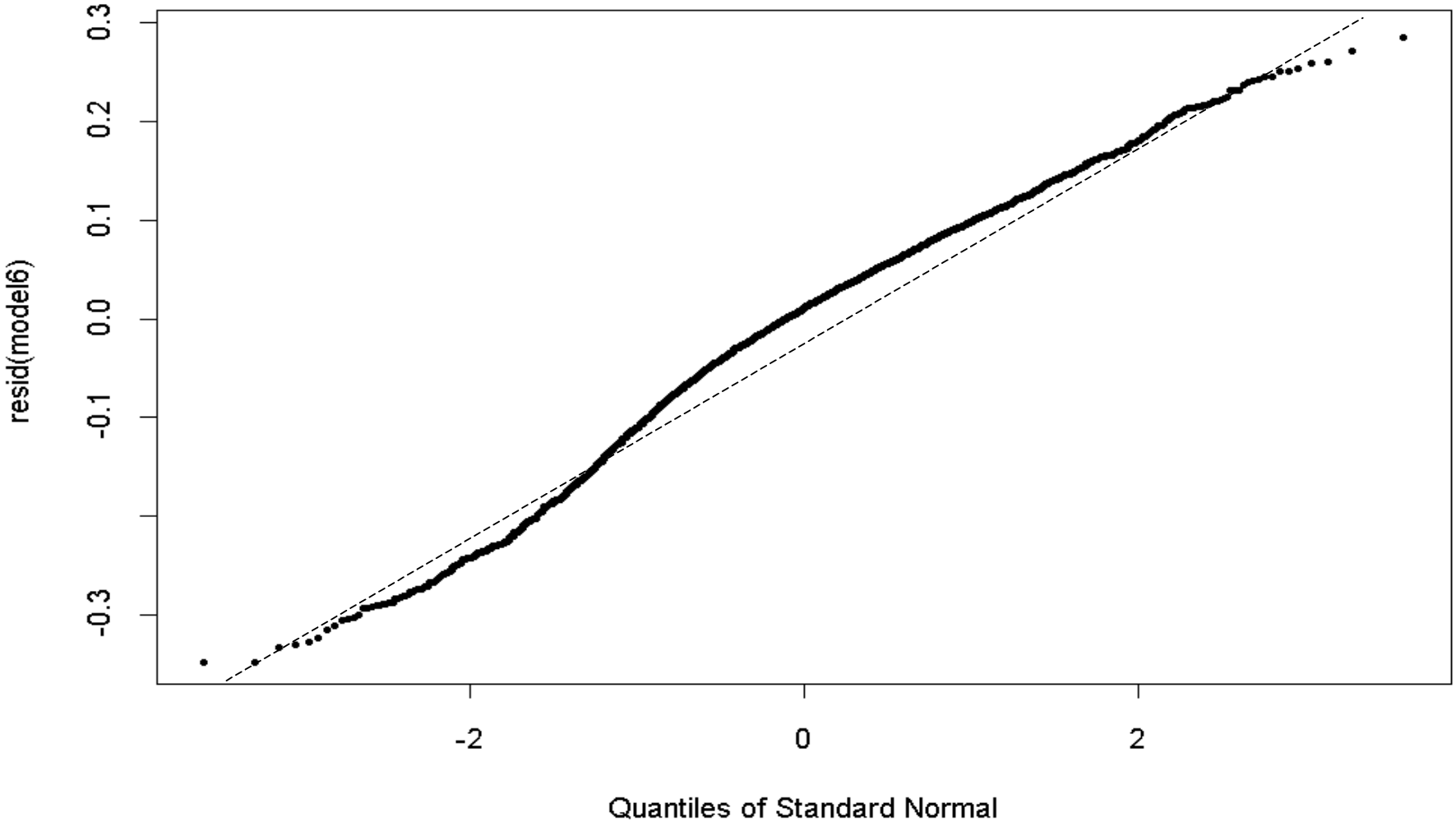

Figure 6.12 Normal Probability Plot of Residuals, MODEL4

Compared to Figure 6.7 and Figure 6.8, there is less systematic pattern in Figure 6.10 and Figure 6.11, indicating less unexplained structure in residuals in MODEL4 when compared to MODEL3. However, as in Figure 6.9, many of the ordered residuals are not clustered along the superimposed quantile-quantile line in Figure 6.12, indicating that MODEL4's errors are not normally distributed.

6.6 Generalized Additive Model

The statistical fitting techniques used in MODEL4 are summarized in Table 6.6.

Table 6.6 Fitting Techniques Used in MODEL4

Variable	Fitting Technique
[CO], dependent variable	square root of [CO]
TTVRT	traditional linear regression
Free-flow emission factor	traditional linear regression
Queue emission factor	traditional linear regression
Wind speed	Inverse transformation, linear regression
Intersection orientation	trigonometric transformation, linear regression

MODEL4 has a fairly high adjusted multiple R-square (0.93), indicating that this model can provide a concise and accurate description of the dependence of the modeled [CO] on the predictors. However, for the purpose of this study, the proposed new statistical model should predict [CO] as closely as possible to that predicted by CAL3QHCR. There would be little doubt about the appropriateness of the fitting techniques on the dependent variable, and the independent variables except for *intersection orientation*. Figure 4.5 indicates that theoretically there may not be an appropriate parametric data transformation function for the dependence of modeled [CO] on intersection orientation. Under this situation, an alternative modeling technique,

known as GAM, which uses smoothing, is useful to improve and/or evaluate the model performance.

The concept behind smoothing is to let the data show the appropriate (data transformation) functional form (13). A smoother does not presume a rigid form for the dependence of the dependent variable on the predictors (e.g., the smoothers are of a nonparametric nature, particularly in multidimensional space). The standard linear regression model (Equation 6.1) can then be generalized as:

$$E([CO]) = \beta_0 + \sum_{i=1}^{n} f_i(X_i) \tag{6.7}$$

where

E([CO]) = mean of the modeled CO concentration
β_0 = parameter
$f_i(X_i)$ = arbitrary unspecified functions
n = number of predictors

This model is known as the generalized additive model (GAM). Past uses of GAM include a study by Hastie and Tibshirani (1990) to predict ozone concentration in the Los Angeles basin (13). In this study, the dependent variable was the log of daily maximum 1-hour average ozone concentration. The predictors were 500 millibar pressure height, wind speed, humidity, temperature, inversion base height, pressure gradient, and visibility. Other recent examples include the application of GAM in psychology (5), generating probabilistic forecasting of aviation weather parameters (28), and analysis of ground-level ozone data (22).

6.6.1 Smoothers

A "smooth" in GAM is defined as an estimate of $f_i(X_i)$. Common ways to generate a smooth are: bin smoothers, running-mean and running-line smoothers, regression splines, cubic smoothing splines, and locally-weighted running-line (loess) smoothers. Each smoother requires a user-specified smoothing parameter, which governs the fundamental trade-off between bias and variance (8&13). The most common method for the selection of the smoothing parameter is a cross-validation procedure, which minimizes the cross-validation sum of squares (8&13):

$$\boldsymbol{CV}(\lambda) = \frac{\boldsymbol{1}}{\boldsymbol{n}} \sum_{\boldsymbol{i=1}}^{\boldsymbol{n}} [\boldsymbol{y_i} - \hat{\boldsymbol{f}}_{\lambda}^{-\boldsymbol{i}}(\boldsymbol{x_i})]^2 \qquad (6.11)$$

where

$CV(\lambda)$ = cross - validation sum of squares for smoother parameter λ

n = number of points in the smoothing of x_i

y_i = observed value at x_i

$\hat{f}^{-i}(x_i)$ = the fit at x_i, computed by leaving out the ith data point

CV(λ) is computed for a number of λ's, and the λ minimizing CV(λ) is selected.

Recommendations on the choice of smoother are rarely available because few systematic comparisons have been made thus far in the literature (13). The selection of a smoother is generally considered a matter of taste, and the most commonly used smoothers are *splines* and *loess smoothers*. It is generally believed that *loess* is more powerful for fitting two- or higher-dimensional surfaces while the theoretical and numerical behavior of *smoothing spline* is cleaner for fitting one-dimensional curves (13). In this study, both *loess* and *smoothing spline* will be explored and compared.

6.6.2 LOESS

LOESS obtains a smoothed curve by fitting successive linear regression functions in local neighborhoods. It obtains the smoothed *Y* value at a given *x* by fitting a linear regression to the data in the neighborhood of the *x* value and then using this regression line to obtain the smoothed value at *x* (20).

The first step in the loess procedure is to identify the *k* nearest neighbors of the target point, x_0 and these neighbors are denoted by $N(x_0)$. The distance of the furthest near-neighbor from x_0 is computed as:

$$\Delta(x_0) = \max_{N(x_0)} | x_0 - x_i | \tag{6.8}$$

The linear regression is weighted to give cases further from the target x_0 smaller weights. Hence, the second step is to assign weights w_i to each point in $N(x_0)$ using the tri-cube weight function

$$W\left(\frac{| x_0 - x_i |}{\Delta(x_0)}\right)$$

where

$$W(u) = \begin{cases} (1-u^3)^3, \text{ for } 0 \le u < 1; \\ 0 \qquad \text{otherwise} \end{cases} \tag{6.9}$$

Finally, the fitted value at x_0, $s(x_0)$ is computed from the weighted least-squares fit of *Y* to *x* confined to $N(x_0)$ using the weights , w_I, as computed in Equation 6.9 (13).

The regression model with loess smoothing on *intersection orientation* and continued use of linear regression on other input variables is given as:

$$\begin{aligned} E(sqrt([CO])) = {} & -0.5422 + 7.32 * 10^{-4} * TVRT + 0.014 * ffef + 0.0026 * qef \\ & + 1.542 * (1/ws) - 1.6038 * lo(\text{deg}) \end{aligned} \tag{6.10}$$

where *lo(deg)* denotes the loess smoothing on intersection orientation.

The statistics of this model, hereafter referred to as MODEL5, are summarized in Table 6.7.

Table 6.7 Statistics of MODEL5

Variable	Coefficient	d.f.	Std. Error	t-value	Pr(t)
Intercept	-0.5422	1	0.130	-87.798	0.000
TVRT	$7.3*10^{-4}$	1	0.034	46.142	0.000
ffef	0.0140	1	0.001	74.008	0.000
qef	$2.6*10^{-3}$	1	10^{-4}	136.956	0.000
1/ws	1.542	1	0.039	211.706	0.000
LOESS(deg.)	-1.604	2.3	0.034	5.008	0.000

The Adjusted R-square: 0.982
RSS: 15.17
d.f.: 2907.68

The loess smoothing on *intersection orientation* (deg) is also given in Figure 6.13. Using the figure, the value of the non-parametric term, *lo(deg)* in Equation 6.10, can be approximately inferred by reading from the curve.

For MODEL5, the diagnostic plots of residuals versus fitted values, responses versus the fitted value, and normal probabilities plot of residuals are given in Figure 6.14, Figure 6.15, and Figure 6.16, respectively.

Compared to Figure 6.10 and Figure 6.11, there is slightly less systematic pattern in Figure 6.14 and Figure 6.15, indicating less unexplained structure in residuals in MODEL5 when compared to MODEL4. However, as in Figure 6.12, many ordered residuals are not clustered along the superimposed quantile-quantile line in Figure 6.16, indicating that MODEL5's errors are not normally distributed either.

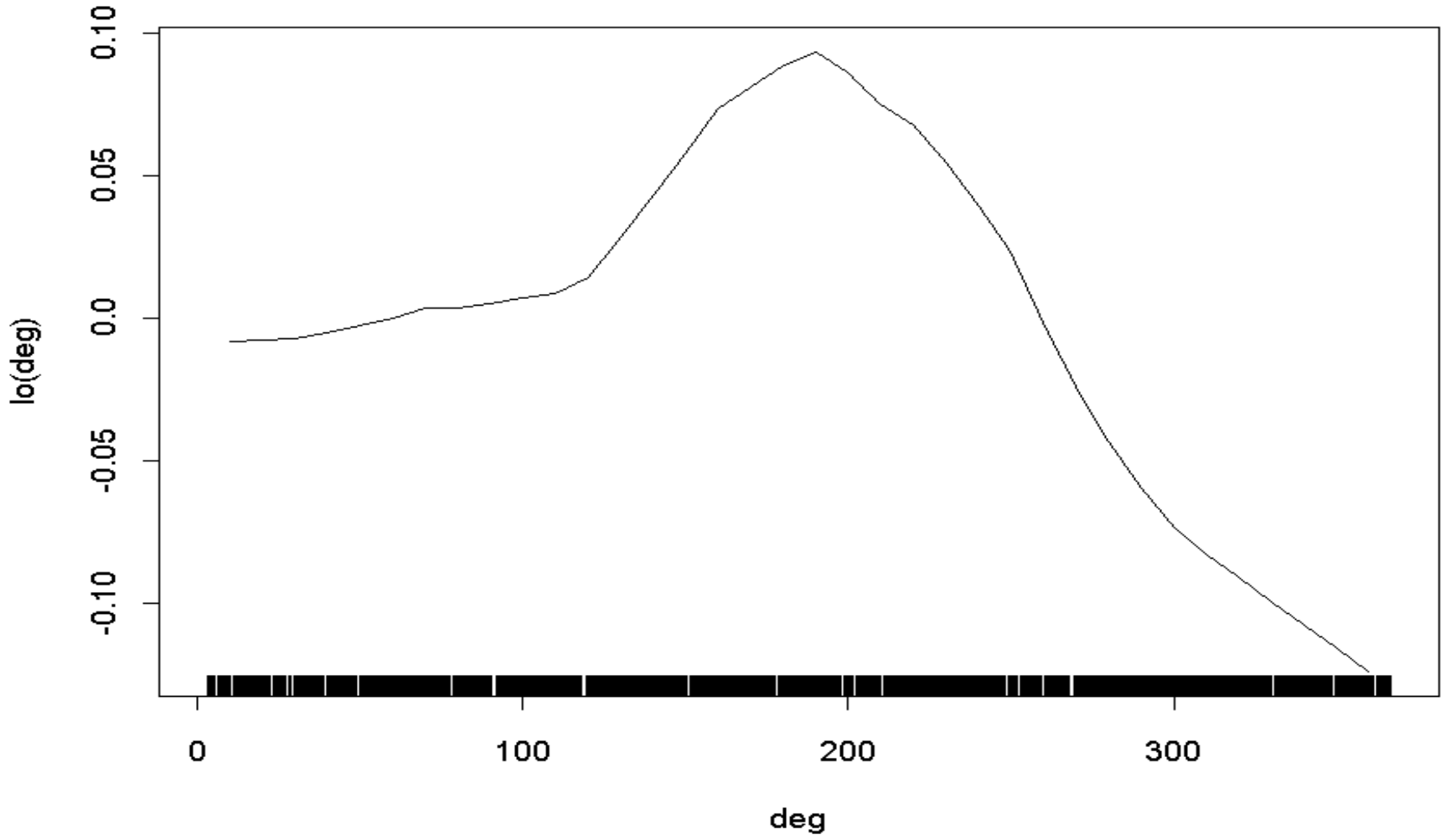

Figure 6.13 Loess Smoothing on Intersection Orientation, MODEL5

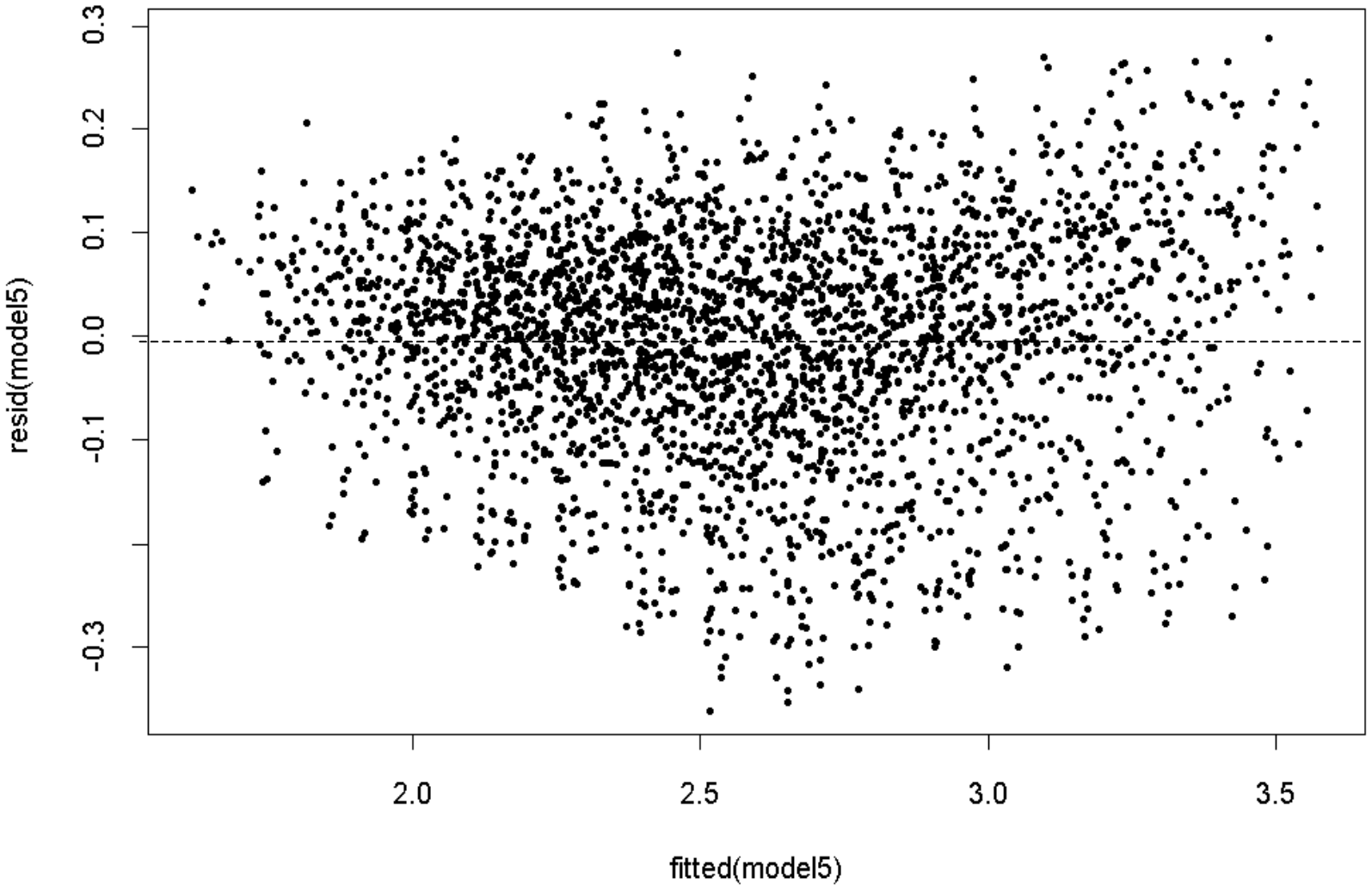

Figure 6.14 Residual Plot versus Fitted Values, MODEL5

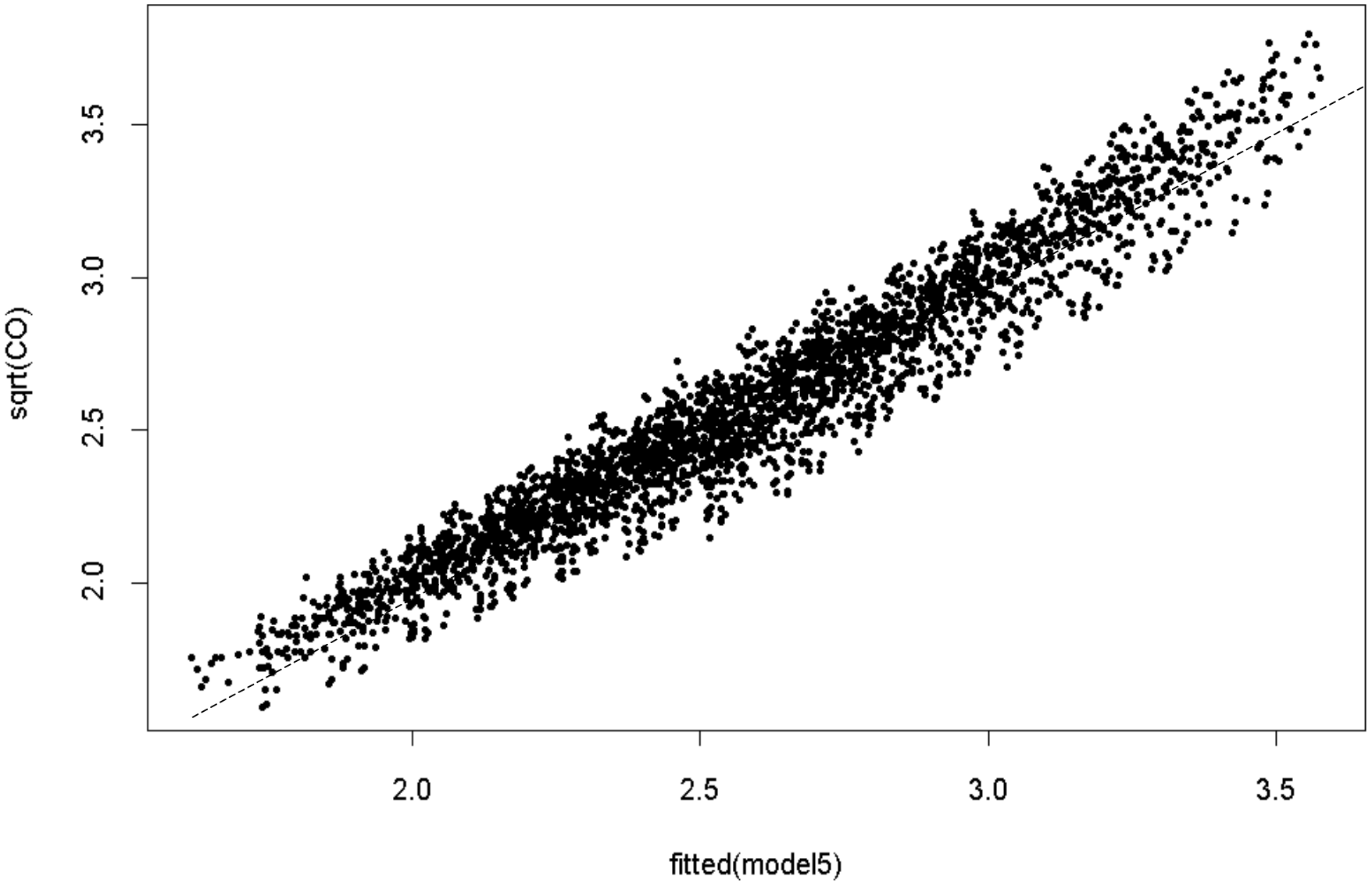

Figure 6.15 Plot of Residuals versus Fitted Values, MODEL5

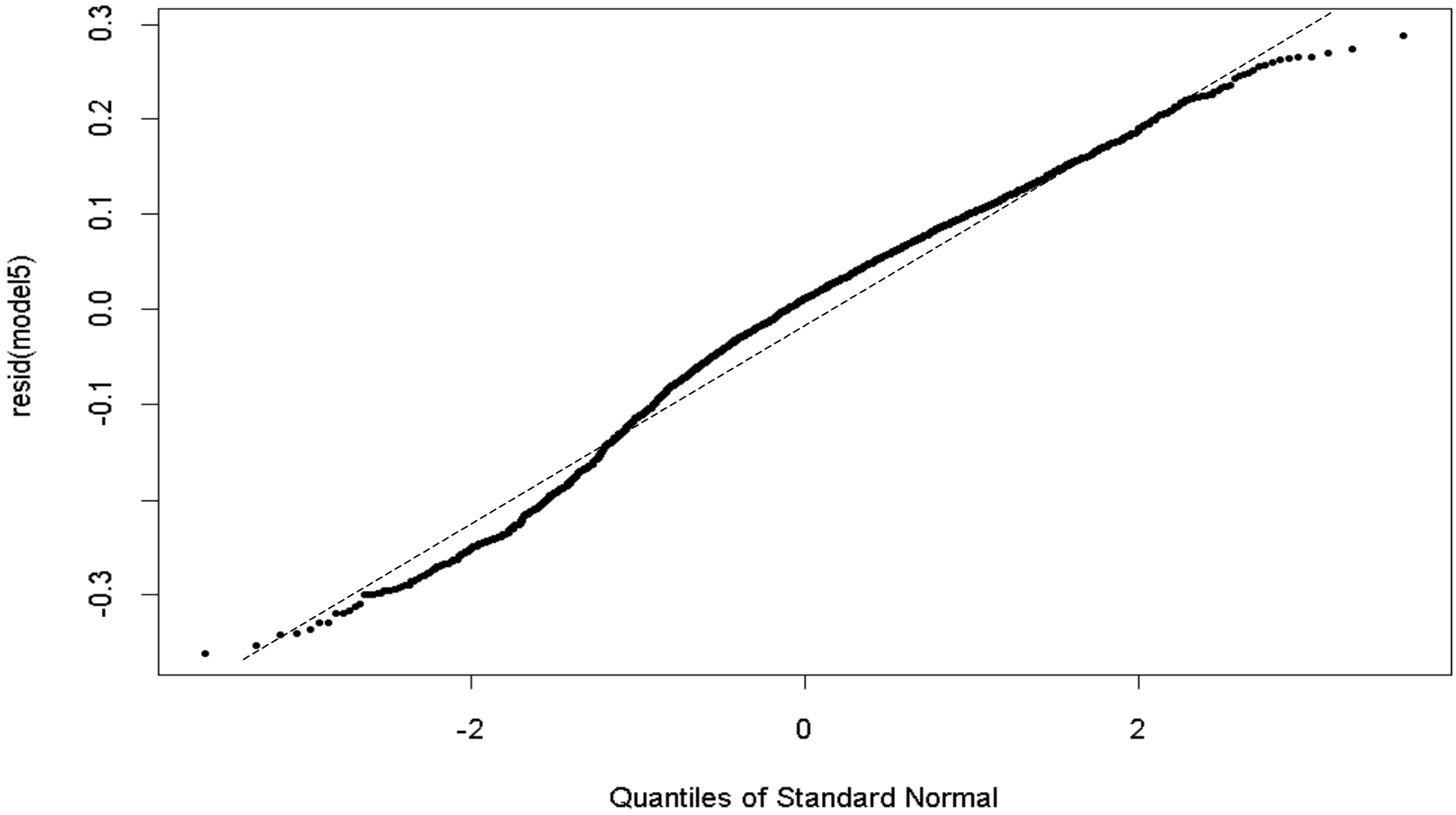

Figure 6.16 Normal Probability Plot of Residuals

6.6.3 Smoothing Splines

Smoothing splines minimize the penalized residual sum of squares (PRSS) rather than the weighted sum of squares as in loess. The PRSS is defined as (13):

$$\boldsymbol{PRSS} = \sum_{\boldsymbol{i=1}}^{\boldsymbol{n}} [\boldsymbol{y_i} - \boldsymbol{f}(\boldsymbol{x_i})]^2 + \lambda \int_{\boldsymbol{a}}^{\boldsymbol{b}} [\boldsymbol{f}''(\boldsymbol{t})]^2 \boldsymbol{dt} \qquad (6.11)$$

where

$PRSS$ = penalized residual sum of squares
n = number of observations
y_i = observed value of response variable
$f(x_i)$ = fitted value of response variable
λ = smoothing parameter
$f''(t)$ = second-order derivative

The first term measures the distance between the response data and its corresponding smoothing value (i.e. smoother's closeness to the data) while the second term penalizes curvature in the fitted function (13). That is, larger values of the smoothing parameter, λ, produce smoother curves while smaller values of λ produce more undulations in the curves.

The model with smoothing spline on *intersection orientation* and continued use of linear regression on the remaining input variables is given as:

$$\begin{aligned} E(sqrt([CO])) = {} & -0.489 + 7.320 * 10^{-4} * TVRT + 0.014 * ffef + 2.6 * 10^{-3} * qef \\ & + 1.547 * (1/ws) - 2.860 * 10^{-4} * s(deg) \end{aligned} \qquad (6.12)$$

where *s(deg)* denotes the spline smoothing on intersection orientation.

The statistics of this model, hereafter referred to as MODEL6, are summarized in Table 6.8

Table 6.8 Statistics of MODEL6

Variable	Coefficient	d.f.	Std. Error	t-value	Pr(t)
Intercept	-0.489	1	0.0223	-21.938	0.000
TVRT	$7.00E10^{-4}$	1	0.0100	30.089	0.000
ffef	0.014	1	0.0003	49.057	0.000
qef	$2.60E10^{-3}$	1	0.0000	89.919	0.000
1/ws	1.547	1	0.0113	136.939	0.000
s(deg.)	$-2.80E10^{-3}$	3	0.0000	-12.688	0.000

Adjusted R-square: 0.988
RSS: 12.9276
d.f.: 2907.002

The spline smooth on *intersection orientation* (deg) is also given in Figure 6.17. Again, the value of the non-parametric term, *s(deg)* in Equation 6.12, can be approximately inferred by reading from the curve presented.

For MODEL6, the diagnostic plots of residuals versus fitted values, responses versus the fitted values, and normal probabilities plot of residuals are given in Figure 6.18, Figure 6.19, and Figure 6.20, respectively. There is no appreciable difference in the diagnostic plots of MODEL6 compared to those of MODEL5.

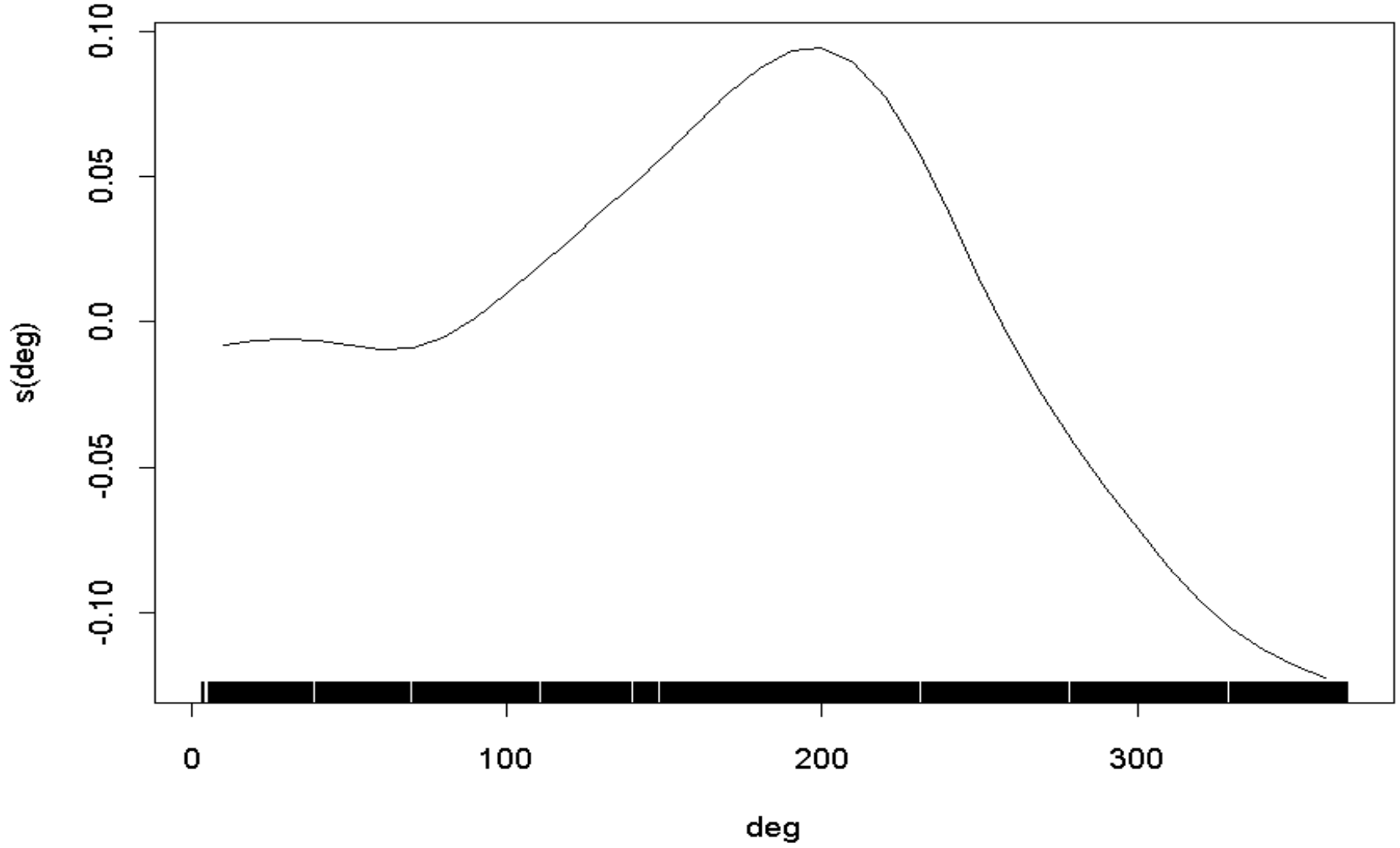

Figure 6.17 Spline Smoothing on Intersection Orientation, MODEL6

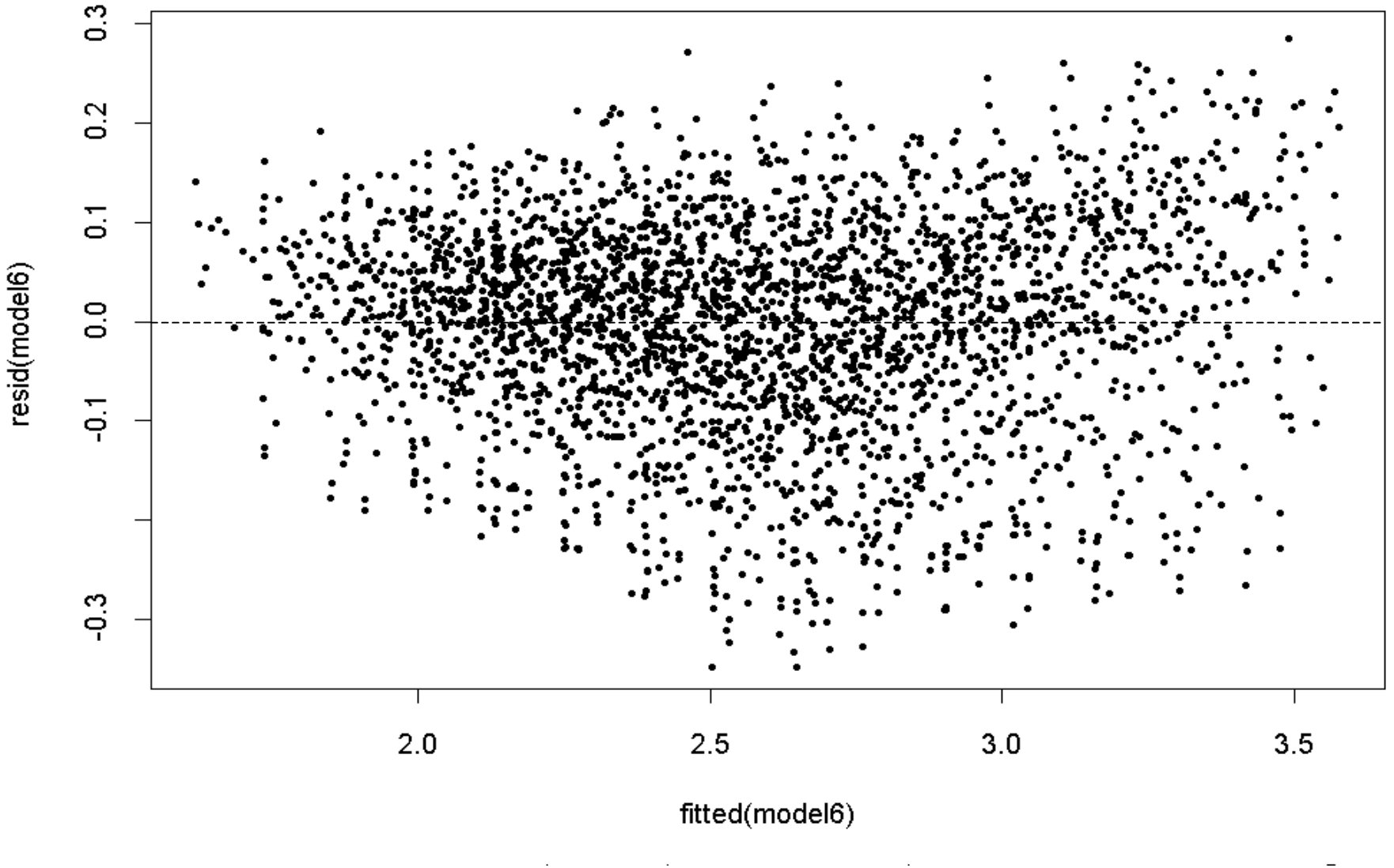

Figure 6.18 Residuals Plot versus Fitted Values, MODEL6

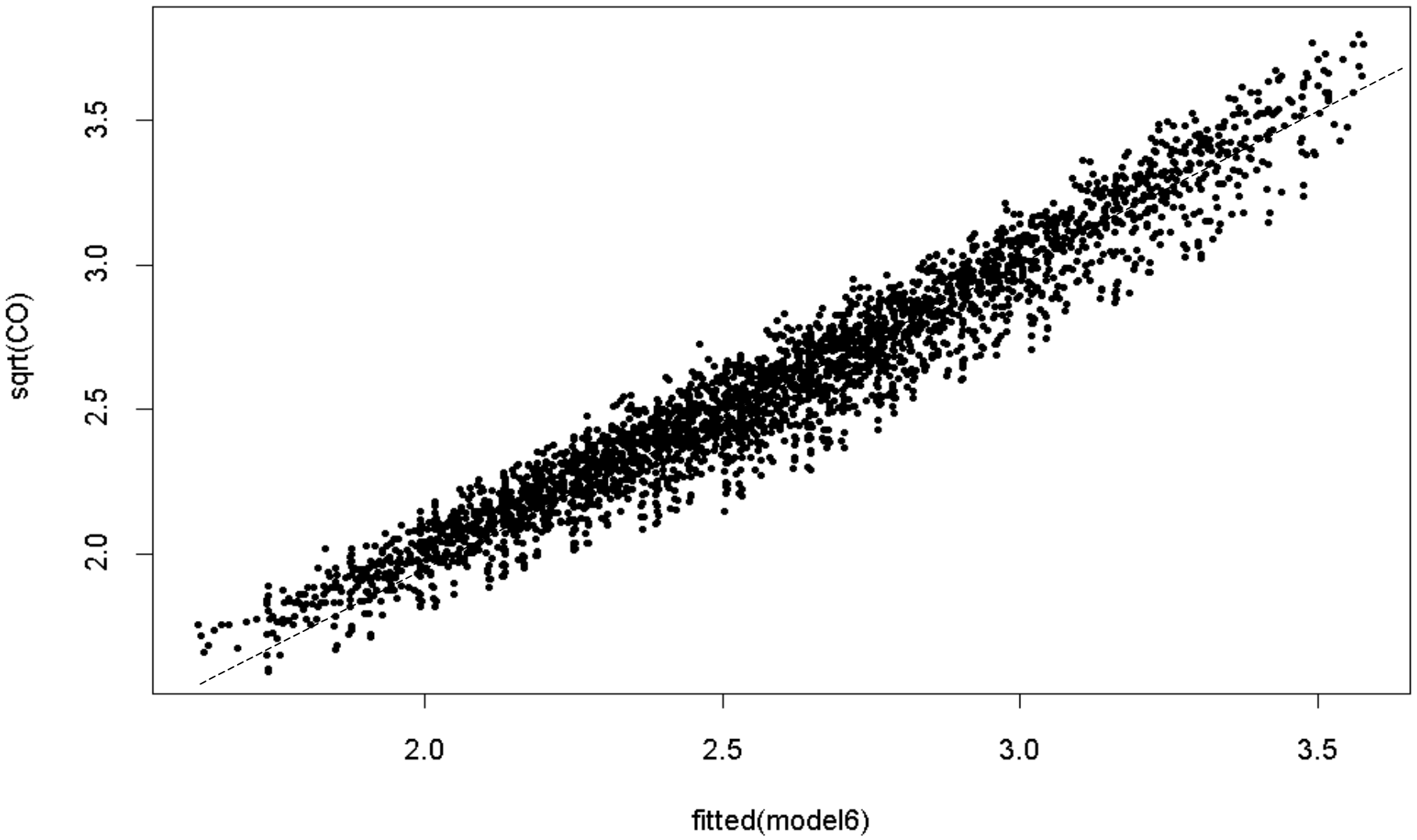

Figure 6.19 Plot of Response versus Fitted Values, MODEL6

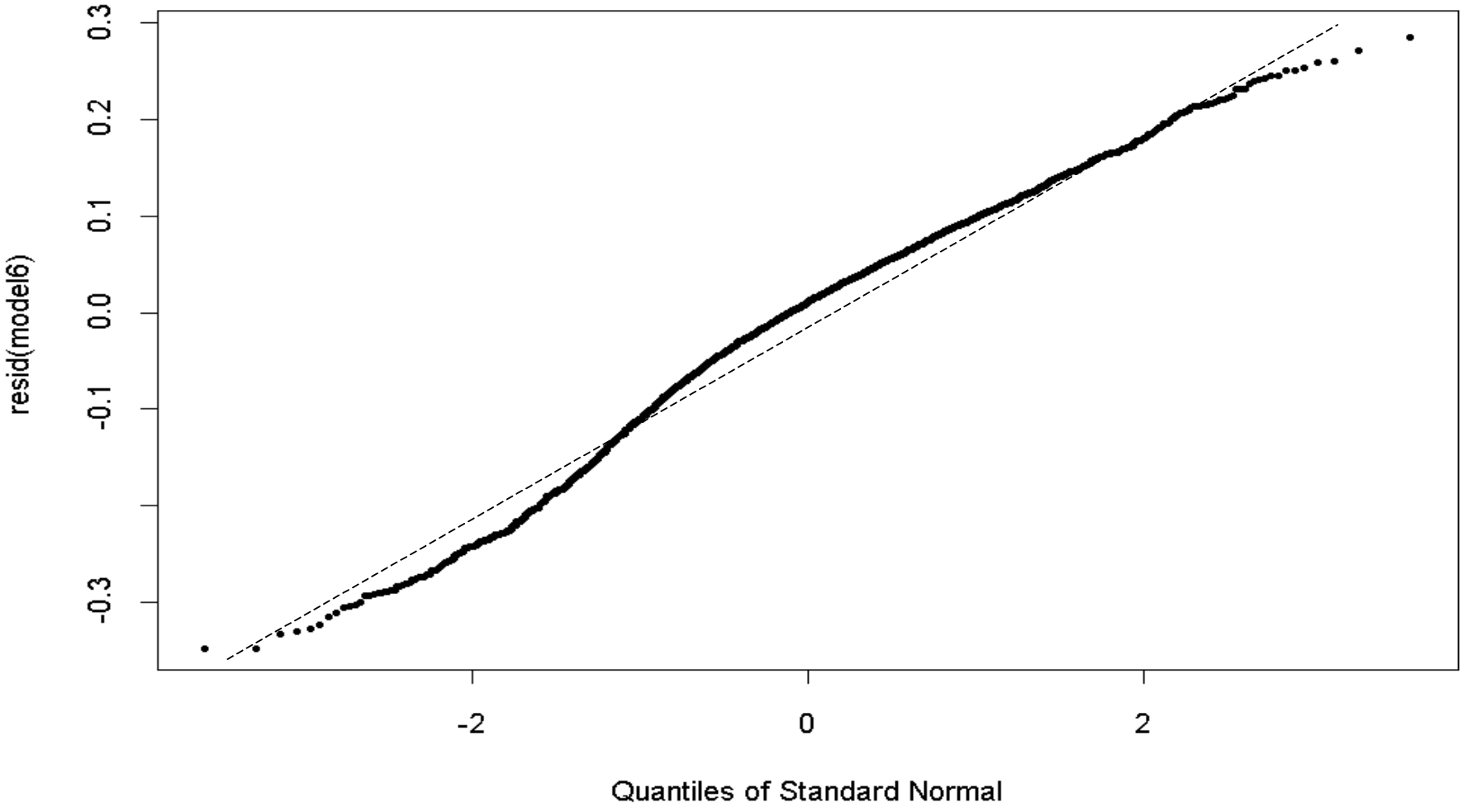

Figure 6.20 Normal Probability Plot of Residuals, MODEL6

The choice between MODEL5 and MODEL6 is best determined by looking at the RSS or adjusted R-square associated with each model, since there is no appreciable difference in model diagnostic plots between these two models. Compared to MODEL5, MODEL6 has a slightly lower RSS (12.93 versus 15.16) and higher adjusted R-square (0.988 versus 0.982), indicating that MODEL6 provides a slightly better model fit to the data than MODEL5.

It is important to note that the performance of the GAM (e.g. MODEL6) is not uniformly better than the standard linear models (e.g. MODEL4). When the dependence of [CO] on the predictors is close to linear (e.g. the dependency of modeled [CO] on TVRT and emission factors) or a suitable parametric data transformation function is available (e.g. the dependency of modeled [CO] on wind speed), the standard linear model is very useful because of its simplicity in interpretation and computational cleanness (13). However, the dependency on *intersection orientation* (refer to Figure 4.5) exhibits a relationship far from linear and when none of the common parametric data transformation functions are effective, then GAM is useful.

As can be seen in Section 6.6.2 and 6.6.3, the use of smoothers (loess in MODEL5 and smoothing spline in MODEL6) improves the model's performance in terms of the adjusted R-squared over the standard linear regression model (e.g. MODEL3). It is also important to note that both MODEL5 and MODEL6 are of a semi-parametric nature: non-parametric fitting on *intersection orientation*, while parametric fitting on the other independent variables (i.e. TVRT, wind speed, free-flow emission factor, and queue emission factor).

6.7 Interactions between Independent Variables

All the statistical models developed so far (MODEL1 through MODEL6) lack interactions between independent variables. If an interaction between two variables is observed, an interaction term can be introduced into GAM as:

$$E([CO]) = \beta_0 + \sum_{i=1}^{m} \beta_i X_i + \sum_{i'=1}^{n} f_{i'}(X_{i'}) + \sum \beta_{ij} X_i X_j + \sum f_{i'j'}(X_{i'}, X_{j'}) + \sum_{i=1}^{m} \sum_{i'=1}^{n} f_{i'}(X_{i'}) X_i \quad (6.13)$$

where

X_i = parametric predictors
X_j = nonparametric predictors
β_0 = estimated parameter
m = number of parametric predictors
n = number of nonparametric predictors

and the last three terms are the parametric, non-parametric, and semi-parametric interaction terms, respectively. For this study, the number of non-parametric predictors, *n*, is one (i.e., intersection orientation); and the number of parametric predictors, *m*, is four (i.e., TVRT, Wind Speed, Queue Emission Factor, and Free-flow Emission Factor). Hence, there is no non-parametric interaction term in our study. Taking MODEL6 for example, Equation 6.13 can be stated as:

$$E([CO]) = \beta_0 + \sum_{i=1}^{4} \beta_i X_i + s(\deg) + \sum \beta_{ij} X_i X_j + \sum_{i=1}^{4} s(\deg)(X_i) \quad (6.14)$$

where *s(deg)* is the non-parametric term. The last two terms are the parametric and semi-parametric interaction terms, respectively.

Similarly, three-, four-, and five-way interactions among independent variables can be introduced into MODEL6, which we will refer to as MODEL7. In total, there are

31 terms in MODEL7 and the estimated functional form is too long to be included in the main body of this document. The residual sum of squares (RSS) and degrees of freedom of MODEL7 are 9.458 and 2881.02, respectively. The detailed statistics of this model (e.g., estimated coefficients and their associated t-statistics) have been provided in Appendix V.

The F-statistic for the comparison between MODEL7 (full model with up to five-way interactions) and MODEL6 (reduced model without any interaction between independent variables) is 0.494 on 26 and 2881 degrees of freedom. The F value for this test at 95% confidence, $F_{0.95,\ 1,\ \infty}$ is 1.52. The F-statistic (0.494) is less than the critical F-value (1.52), indicating that MODEL7 is not statistically better than MODEL6 and there are no significant interaction effects among the independent variables.

7.0 THE CHOICE OF A MODEL

In this section, a summary of all the models developed in Section 6 is given along with a discussion of the recommended model. As noted in Section 2.2, one of the study objectives is to develop a new statistical model as a screening tool to replace EPA's current LOS D criterion for identifying intersections that should undergo the detailed CO analysis. Another study objective is to develop a new statistical model that directly connects the air quality analysis to the intersection design level and thus, can be used by traffic engineers during the design process. For these objectives, we would like the [CO] predicted by the proposed statistical models to be slightly higher (conservancy) than, but close to (accuracy) those predicted by CAL3QHCR. The aspects of conservancy and accuracy of the proposed models will be covered in the following discussion on the recommended model.

7.1 Model Summary

In total, seven models have been presented in Section 6 describing the dependence of modeled [CO] on prominent factors. The dependent variable, statistical fitting techniques on the independent variables, residual sums of squares, and the adjusted R-square of each model are summarized in Table 7.1.

Table 7.1 Model Summary

Variable	MODEL1	MODEL2	MODEL3	MODEL4	MODEL5	MODEL6	MODEL7
Intercept	✓	✓	✓	✓	✓	✓	✓
TVRT	✓	✓	✓	✓	✓	✓	✓
Ffef	✓	✓	✓	✓	✓	✓	✓
Qef	✓	✓	✓	✓	✓	✓	✓
Ws	✓						
Deg	✓	✓	✓	✓			
1/ws		✓	✓	✓	✓	✓	✓
Cos(deg)			✓	✓			
Loess(deg)					✓		
S(deg)						✓	✓
Interactions							✓
Y	✓	✓	✓				
$\sqrt{Y}$				✓	✓	✓	✓
Adj. R^2	0.881	0.896	0.915	0.932	0.982	0.988	0.991
RSS	1998.67	1563.96	1087.83	36.36	15.17	12.93	9.46
d.f.	2910.00	2910.00	2909.00	2909.00	2907.68	2907.00	2881.02

"✓" denotes that the variable is included in the model.

7.2 Model Selection

As indicated in Table 7.1 and discussed in Section 6.5, the use of square root of the modeled [CO] as the dependent variable in MODEL4, MODEL5, and MODEL6 improves the model performance dramatically. The same statistical fitting technique, linear regression, is applied to TVRT, free-flow emission factor, queue emission factor, and wind speed for MODEL4, MODEL5, and MODEL6. The only difference among these three models lies in the fitting technique on *intersection orientation*: trigonometric transformation (cosine) in MODEL4, non-parametric fitting (LOESS) in MODEL5 and non-parametric fitting (Smoothing Spline) in MODEL6. It is straightforward to use MODEL4, since it is simply a linear regression model and has a parametric functional form. To use MODEL4 as a forecasting tool, the analyst needs only to plug in values of predictors into MODEL4 (Equation 6.6) and compute the modeled [CO] level.

The use of MODEL5 and MODEL6 is less straightforward, because of their semi-parametric nature. That is, there is no parametric functional form for the non-parametric term, *loess(deg)* in MODEL5 and *s(deg)* in MODEL6. In general, to use MODEL5 and MODEL6 for prediction, the analyst first needs to obtain the original data used to develop these models and then use any statistical package which has the GAM functions (e.g. S-Plus) to compute the new concentration level. This process is clearly less straightforward than that of using MODEL4.

An alternative, but slightly less accurate approach is to obtain an approximate value of the non-parametric term: *loess (deg)* in MODEL5 and *S (deg)* in MODEL6, by reading values directly from Figure 6.13 or Figure 6.17. Once the values of the non-

parametric term have been identified, prediction using MODEL5 and MODEL6 is as easy as using MODEL4.

Intuitively, there is little reason to expect an appreciable difference in performance between MODEL5 and MODEL6, since both apply non-parametric smoothing in which the fitting model follows trends in the original data. This small difference in performance is also shown by the small difference in the adjusted R-square between these two models (0.988 - 0.982 = 0.006). Recommendations on the choice between *loess* and *smoothing spline* are rarely available (13). Because of the nature of our study, fitting one-dimensional curves, the theoretical and numerical behavior of *smoothing spline* (MODEL6) is computationally preferred over *loess* (MODEL5). In addition, the slightly higher adjusted R-square suggests the choice of MODEL6.

In summary, MODEL6 is the recommended model for use both as a screening tool to replace EPA's current LOS D criterion and use as a prediction tool for traffic engineers to approximate [CO] at the intersection design level. Especially, the approximation of the non-parametric term in MDOEL6, *S(deg),* by reading directly from Figure 6.17 makes the application of MODEL6 as simple as the application of MODEL4. However, MODEL4 can be used for the areas where the non-parametric charts (e.g. Figure 6.13 and Figure 6.17) are not available or can be used by traffic engineers at the intersection design level because of its computational simplicity.

7.3 Model Validation

As discussed in Section 1.2, one of the study objectives is to develop a new statistical model to replace EPA's current LOS D criterion for identifying those intersections that should undergo detailed CO analysis (i.e. running CAL3QHCR). In

addition, the new statistical model should be simple enough to be used by traffic engineers to approximate [CO] levels during the intersection design process. Ideally, any potential CO exceedance could be mitigated in the design process as opposed to much later in the conformity process. For these study objectives, the validation of the proposed statistical model will be conducted comparing the [CO] levels predicted by the proposed models and those predicted by CAL3QHCR, using the same inputs.

Based on the real field meteorological situations of the California cities of Sacramento, San Jose, Redlands, West Los Angeles, and San Diego, several model validation scenarios were developed. These scenarios are summarized in Table 7.2. Two ASD scenarios, 25.9 seconds/vehicle and 39.2 seconds/vehicle, were generated by adjusting the traffic volume on each link uniformly 10% down and 6% up from the traffic volumes depicted in Table 4.4, respectively. Two free-flow emission factor scenarios, 21.3 grams/vehicle-mile and 17.7 grams/vehicle-mile, and two queue emission factor scenarios, 391.2 grams/vehicle-hour and 324.0 grams/vehicle-hour were generated by assuming a 30% cold start and a 20 mph free-flow speed for fleet years 1998 and 2000. Intersection orientation (deg) and 8-hour average wind speed and wind direction data when the highest [CO] occurred in the CAL3QHCR modeling were used as inputs to the proposed models (MODEL4 and MODEL6). Note that 1 m/s is used when the 8-hour averaged *wind speed* is less than 1.0 m/s, since CAL3QHCR has not been validated for the conditions where wind speed is less than 1.0 m/s.

Table 7.2 Model Validation Scenarios

Scenario	Location	ASD	ffef	qef	ws	deg
1	Sacramento	25.9	21.3	391.2	1.415	320
2	Sacramento	25.9	17.7	324.0	1.415	320
3	Sacramento	39.2	21.3	391.2	1.415	320
4	Sacramento	39.2	17.7	324.0	1.286	119
5	WLA	25.9	21.3	391.2	1.000	198
6	WLA	25.9	17.7	324.0	1.000	198
7	WLA	39.2	21.3	391.2	1.000	198
8	WLA	39.2	17.7	324.0	1.000	198
9	Redlands	25.9	21.3	391.2	1.354	154
10	Redlands	25.9	17.7	324.0	1.354	154
11	Redlands	39.2	21.3	391.2	1.354	154
12	Redlands	39.2	17.7	324.0	1.354	154
13	San Jose	25.9	21.3	391.2	1.430	205
14	San Jose	25.9	17.7	324.0	1.430	205
15	San Jose	39.2	21.3	391.2	1.430	205
16	San Jose	39.2	17.7	324.0	1.430	205
17	San Diego	25.9	21.3	391.2	1.100	154
18	San Diego	25.9	17.7	324.0	1.100	154
19	San Diego	39.2	21.3	391.2	1.100	149
20	San Diego	39.2	17.7	324.0	1.100	149

As summarized in Table 7.2, 20 input scenarios (five locations * two ASD * two emission factors = 20) are generated. For each input scenario, the [CO] levels predicted by MODEL4 and MODEL6 will be compared to those directly predicted by CAL3QHCR. These comparisons are summarized in Table 7.3 and Figure 7.1.

Table 7.3 Model Validation Results – [CO] (ppm)

Scenario	CAL3QHCR	MODEL4 (%)[1]	MODEL6 (%)
1	4.73	5.31 (12%)	5.30 (12%)
2	3.95	4.26 (8%)	4.24 (7%)
3	5.25	5.95 (13%)	5.97 (14%)
4	4.37	4.77 (9%)	4.63 (6%)
5	9.47	9.18 (-3%)	9.21 (-3%)
6	7.77	7.78 (0.1%)	7.89 (2%)
7	9.33	8.12 (-13%)	8.41 (-10%)
8	9.42	8.50 (-9%)	8.64 (-8%)
9	6.74	6.84 (1%)	6.76 (0.3%)
10	5.55	5.71 (3%)	5.63 (1%)
11	7.44	7.51 (1%)	7.47 (0.4%)
12	6.13	6.34 (3%)	6.24 (2%)
13	6.29	6.47 (3%)	6.49 (3%)
14	5.17	5.38 (4%)	5.37 (4%)
15	6.92	7.13 (3%)	7.23 (4%)
16	5.76	5.95 (3%)	6.09 (6%)
17	7.96	8.29 (4%)	8.18 (3%)
18	6.54	7.05 (8%)	6.95 (6%)
19	8.80	9.85 (12%)	9.73 (10%)
20	7.27	8.46 (16%)	8.35 (15%)

[1] "%" denotes the percentage of difference in predicted [CO] levels between the proposed models and CAL3QHCR.

For the purpose of this study, the [CO] modeled by CAL3QHCR can be treated as the "true" values. We are interested in the deviations of the [CO] levels modeled by each proposed model (i.e., MODEL4 and MODEL6) from the true values (the [CO] levels modeled by CAL3QHCR). This deviation is measured by the percentages of difference in predicted [CO] levels between the proposed models and CAL3QHCR, which are provided in Table 7.3 and summarized Figure 7.2. Positive percentage deviations denote that the proposed model overestimates the [CO] level, while negative percentage deviations denote that the proposed model underestimates the [CO] level.

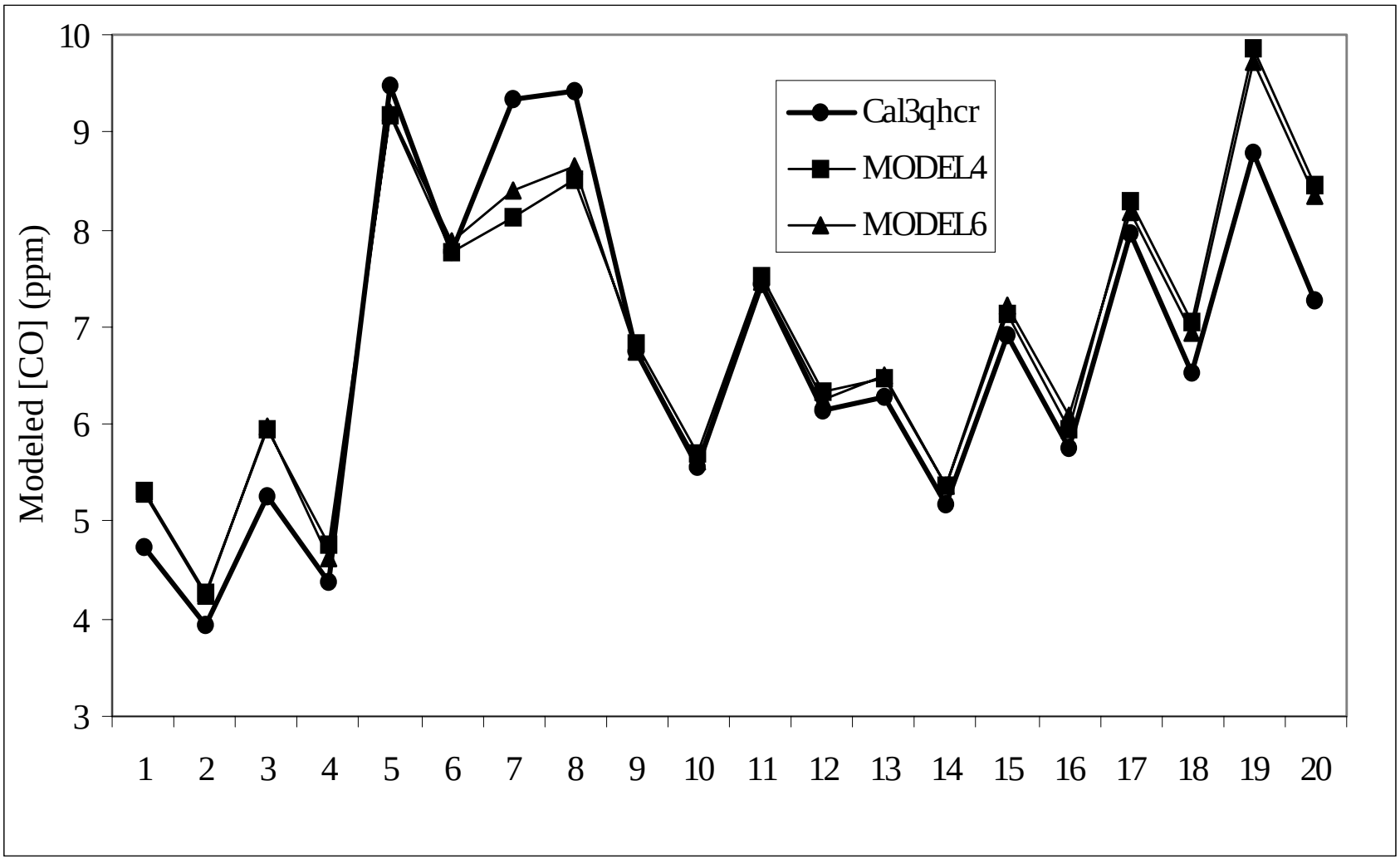

Figure 7.1 Model Comparison

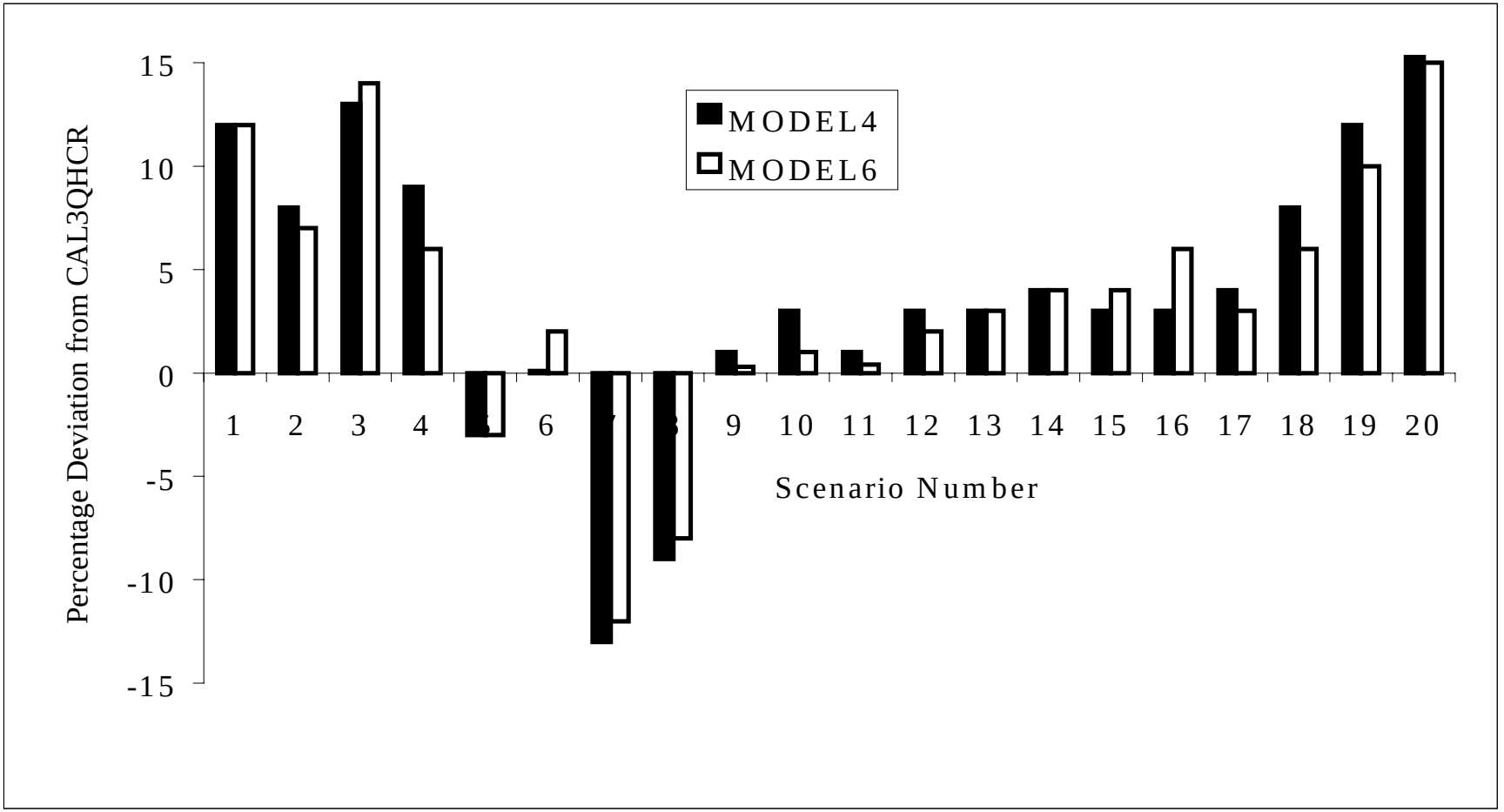

Figure 7.2 Model Performance

The proposed models are expected to slightly overestimate [CO] when compared to values computed using CAL3QHCR. This overestimating is designed by controlling the variability in wind direction: it was assumed that wind comes from the same direction during the 8-hour averaged period. By assuming zero variability in wind direction, the proposed models would tend to overestimate [CO] levels when compared to those predicted by CAL3QHCR, in which field collected meteorological data are used and the variability of wind direction is usually greater than zero.

The amount of overestimation of the proposed models for a certain location depends on the variability of field wind direction data in the study area: the greater the variability in measured wind direction, the more likely the proposed model will overestimate [CO] levels. However, as shown in Figure 7.1 and Figure 7.2, these new models are not uniformly overestimating for all the input scenarios; they underestimate [CO] levels for three of the West Los Angeles input scenarios (data points 5, 7, and 8). One plausible explanation of the underestimating of scenario 5, 7 and 8 in Figure 7.1 and Figure 7.2 could be that the modeling error due to unobserved factors makes the proposed models underestimate [CO], which counters the overestimating effect from the assumption of zero variability in wind direction. For example, because of the sea-breeze effects, West LA has very little variability in wind direction (17). The lower variability in wind direction results in less overestimation of [CO] than other areas. This overestimation is apparently not large enough to counter the underestimating effects that arise from the unobserved factors not included in the model. Thus, the proposed model, MODEL6, might not be conservative enough for areas that have very small variability in

wind direction (e.g., West LA). The variability of wind direction can be obtained from the local meteorological condition plot such as Figure 4.3 and Figure 4.4.

7.4 Model Application

To use the proposed model as a screening tool, the analyst needs to:

1. Gather the local worst case meteorological data including 8-hour averaged wind direction and wind speed (*ws*) from air quality perspective (e.g. early morning of winter months when atmosphere has a stable wind direction and low wind speed) from local air district;
2. Determine intersection orientation (*deg*) based on intersection geometry and wind direction;
3. Gather the traffic and signalization data and compute the intersection *TVRT* transportation agency (e.g. Caltrans);
4. Determine the projection/design year and obtain emission factors (*ffef* and *qef*) using the EMFAC or MOBILE series models; and
5. Compute [CO] level using the recommended model, MODEL6 (the semi-parametric model with smoothing spline on intersection orientation) by plugging in *ws*, *deg*, *TVRT*, *ffef*, and *qef* obtained in Step 1 through Step 4.

If the [CO] level predicted by MODEL6 plus an appropriate local background concentration is less than 8.00ppm, the intersection is exempted from running CAL3QHCR. As shown in, [CO] levels modeled by MODEL6 deviate from those modeled by CAL3QHCR within (+ 1.0ppm, - 1.0ppm). In other words, if the [CO] predicted by MODEL6 is 8.00ppm, and the worst scenario is that MODEL6 underestimates by 0.92ppm. That is, the actual [CO] level predicted by CAL3QHCR

would be 8.00 + 1.00 = 9.0ppm, which still does not exceed 9.00ppm, the NAAQS for 8-hour averaged [CO].

Again, the proposed models are spatially transferable to any states other than California, as long as every model input variable (i.e., TVRT, intersection orientation, wind speed, free-flow emission factor, and queue emission factor) takes value that are in the range summarized in Table 6.1.

The recommended procedures for the application of the proposed models are summarized in Figure 7.3.

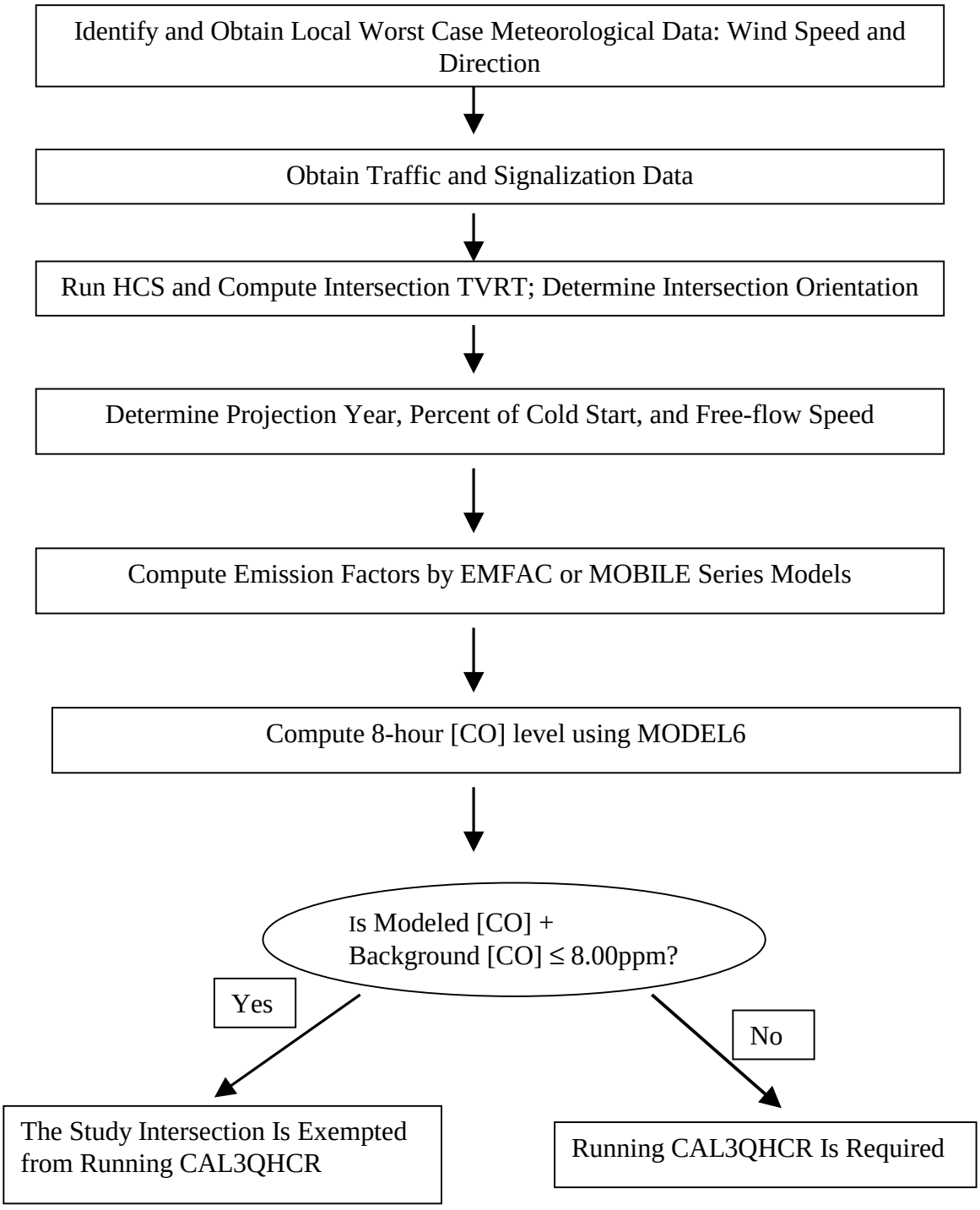

Figure 7.3 Application of the Proposed Models

7.5 Study Limitations

As discussed in Section 7.1, MODEL6 is a good pre-screening tool to running CAL3QHCR. It can be used to replace EPA's current intersection LOS criterion for determining whether an intersection should be considered for modeling CO impacts.

In addition, as shown in Table 7.3, most of the [CO] values predicted by MODEL6 deviate from those modeled by CAL3QHCR within [+ 1.0 ppm, - 1.0ppm], indicating that MODEL6 is accurate enough to give an approximate idea of the [CO] levels at the intersection design level (Step 1, Figure 2.1) so that any potential exceedance can be mitigated in the design process.

However, MODEL6 may result in an overestimation for intersections with semi-actuated and actuated signal operations because the analyses in this study are based on a hypothetical pre-timed intersection. The [CO] levels at intersections with semi-actuated or actuated signal operations will generally be lower than that modeled for an identical pre-timed intersection, since there is usually less traffic delay at the intersections with semi-actuated or actuated signal operation. Hence, for the intersections with semi-actuated or actuated signal operation, the proposed model would overestimate [CO] levels and provides a conservative estimates. In addition, a hypothetical typical urban traffic pattern (Table 4.4 and Figure 4.2) was used in developing the statistical models. It is possible that the proposed models are a function of the traffic pattern assumed. Different traffic patterns more likely will generate different queue patterns at intersections, therefore, has a significant on the determination of intersection orientation (the relative angle between the wind direction and the traffic link with the longest queue). Future study should address this issue.

Other limitations come from CAL3QHCR rather than this study itself. The dependent variable, modeled [CO] level, used in this study is the output of the computer program CAL3QHCR rather than actual measured field [CO]. Thus, we are assuming that CAL3QHCR is a "perfect" model for estimating [CO] at intersections. However, a recent study shows that under certain situations, CAL3QHCR tends to overestimate [CO] (2). In addition, the dispersion module used in CAL3QHCR - CALINE3 has not been validated for so called "street canyon" effects or for situations in which the wind speed is less than 1 m/s. Unfortunately, the proposed model does not overcome these limitations.

8.0 CONCLUSIONS

EPA's guideline for modeling CO impacts from roadway intersections uses intersection ASD/LOS as one of its major defining factors in identifying those intersections that require detailed CO analysis. However, this study identified other major factors, beyond ASD, that contribute to the modeled [CO] at roadway intersections. These factors include *intersection orientation*, which incorporates the impacts of the relative angle between predominant wind direction and the critical traffic link; *total vehicle red time* (TVRT), which incorporates the impacts of intersection ASD, traffic volume, and intersection geometry; *wind speed*, which incorporates the dilution impacts of CO with ambient air at the point of release; and free flow and queue *emission factors*, which incorporate the impact of the strength of the uniform line source used in CAL3QHCR.

Based on these major modeling factors, a new statistical framework was proposed in this study for determining whether an intersection should be modeled for CO emission impact with CAL3QHCR and for estimating [CO] levels at intersection design level. Both the traditional linear regression technique and a more advanced regression technique, the generalized additive model, were applied in developing the new statistical framework. The proposed statistical framework is based on not only the intersection LOS (as EPA's current criterion) but also other major modeling factors as identified in this study. These factors are intersection orientation, intersection geometry, wind speed, and emission factors. Most of the [CO] levels predicted by the proposed statistical model are slightly higher than but very close to those predicted by CAL3QHCR so that the new statistical model can be used to replace EPA's current LOS criterion to determine those

intersections that require detailed CO analysis. The study intersection is exempted from detailed CO analysis (by running CAL3QHCR) if the [CO] level predicted by the proposed model plus an appropriate local background concentration is less than 8.00ppm. Note that the NAAQS for 8-hour average [CO] is 9.00ppm. The 1.00ppm difference is designed to account for possible errors in the proposed model. In addition, the proposed model is much simpler to use than CAL3QHCR so that traffic engineers can use it at the intersection design level to approximate [CO] (step 1 in Figure 2.1). Ideally, any potential exceedance could be mitigated in the design level.

This study contributes to air quality-transportation research by identifying the major modeling factors that contribute to the modeled [CO], developing an improved framework for determining whether an intersection should be modeled for CO emission impact (Step 3 in Figure 2.1), and providing a simple method to approximate the [CO] level so that traffic engineers can avoid wasted effort and money in the iteration of Step 1 and Step 2 in Figure 2.1.

However, the proposed statistical model may result in an overestimation for intersections with semi-actuated and actuated signal operations because the analyses in this study are based on a hypothetical pre-timed intersection. A recent study conducted by UC Davis (17&18) suggests a 15 ~ 20 % reduction in the model [CO] for an actuated intersection when compared to a pre-timed intersection. Future studies should incorporate the impact of signal type (i.e. pre-timed, semi-actuated, and actuated) into the statistical model quantitatively or qualitatively.

Other limitations come from CAL3QHCR rather than this study itself. The dependent variable, modeled [CO] level, used in developing the proposed statistical

model is the output of the computer program CAL3QHCR rather than actual measured field [CO]. The study methodology presented in this study can be applied to a future study to explore the statistical relationship between the real field collected [CO] (rather than the modeled [CO]) and the major factors.

References:

1. Barth, Matthew, Feng An, Joseph Norbeck, and Marc Ross (1996). "Modal Emission Modeling: A physical Approach." *Transportation Research Record* Vol. 1520: 81
2. Benson, Paul (1979), *CALINE3 - A Versatile Dispersion Model For Predicting Air Pollutant Levels Near Highway and Arterial Streets*, Office of Transportation Laboratory, California Department of Transportation, 1979.
3. Benson, Paul (1989) *CALINE4 - A Dispersion Model For Predicting Air Pollution Concentrations Near Roadways* Division of New Technology and Research, 1989.
4. Bishop, A. Gary and Donald H. Stedman (1990). "On-Road Carbon Monoxide Emission Measurement Comparisons for the 1988-1989 Colorado Oxy-Fuel Program." *Environmental Science Technology*. Vol. 24, 843-847
5. Brown, C. Hendricks (1993). "Analyzing Preventive trials with Generalized Additive Models." *American Journal of Community Psychology*. Vol. 21, No. 5: 635
6. Bullin, J. A. and J. J. Korpics (1986), *User's Guide to the TEXIN3 Model-a Model for Predicting Carbon Monoxide Concentrations Near Intersections*. Texas Transportation Institute Research Report 283-3F, Texas A&M University, College Station, TX.
7. Carroll, J.J., D.P.Y. Chang, and O.G. Raabe. "Lecture Notes of Atmospheric Science and Civil Engineering - 149." Fall, 1996.
8. Chambers, M. John and Trevor J. Hastie (1992), *Statistical Models In S-Plus*, Wadsworth & Brooks/Cole Advanced Books & Software Pacific Grove, California
9. Cooper, C. David, Linda C. Malone and Pwu-Sheng Liu (1992). "Identifying "Worst Case" Persistence Factors for Carbon Monoxide Modeling Near Intersections in Orlando, Florida" *Journal of Air Waste Management Association.* Vol. 42, No. 11: 1461-1465
10. Eckhoff, Peter A. and Thomas N. Braverman (1995), *ADDENDUM TO THE USER'S GUIDE TO CAL3QHC VERSION 2.0 (CAL3QHCR USER'S GUID*. Research Triangle Park, North Carolina 27711: Office of Air Quality Planning and Standards, Technical Support Division, September, 1995.
11. Frazier, James and John Henneman (1996). "Project-Level Air Quality Assessment Actions: Interrelating Conformity with National Environmental Policy Act Process." *Transportation Research Record* Vol. 1520: 3
12. Hartnett, Laureen and Matthew Lawlor (1996). "Role of Off-Model Tools in Network-Based Regional Confirmity Analysis." *Transportation Research Record* Vol. 1520: 19
13. Hastie, T.J. and R.J. Tibshirani (1990), *Generalized Additive Models*. CHAPMAN AND HALL.
14. Hilbe, M. Joseph (1993), "Generalized Additive Models Software." *The American Statistician*. Vol. 47, No. 1: 59
15. Holmén, Britt and Debbie Niemeier (1997). "A Missing Link in Automobile Emission Factors: Driver Variability." Submitted to: *Journal of the Air & Waste Management Association*
16. Kear, Tom, Anthony Held, Daniel P.Y. Chang, and John J. Carroll (1996). "During Worst Case Meteorology Are Buoyancy Effects Important?" Presented at: *The*

Transportation Research Board, Transportation & Air Quality Committee (A 1 F03) 1996 Summer Conference

17. Meng, Yu and Debbie Niemeier (1997), *Modeling Carbon Monoxide Concentrations at Level-of-Service D Intersections*. Final Report. UCD-ITS-RR-98-7. Institute of Transportation Studies, Univ. of California at Davis, Davis CA 95616.
18. Meng, Yu and Debbie Niemeier (1998), "Project Level Carbon Monoxide Hot-spot Analysis for Level of Service D Intersections", Presented at Transportation Research Board (TRB) 77th Annual Conference, January 10 to 15, 1998, Washington D.C.
19. Moseholm, Lars, Jeff Silva, and Tomothy Larson (1996), "Forecasting Carbon Monoxide Concentrations Near A Sheltered Intersection Using Video Traffic Surveillance and Neural Networks." *Transportation Research Part D: Transport and Environment*. Vol 1D, No. 1, September 1996
20. Neter, John et al (1996), *Applied Linear Statistical Models (4th Edition)*, IRWIN
21. Nelli, J.P., A. D. Messina, and J. A. Bullin (1989). "Analysis and modeling of air quality street intersections." *Journal of Air Pollution Control Association.* Vol. 33: 760
22. Niu, X. Feng (1996), "Nonlinear Additive Models for Environmental Time Series, With Applications to Ground-Level Ozone Data Analysis." *Journal of American Statistical Association*. Vol. 91, No. 435: 1310
23. Petersen, W.B. (1980), *User's Guide for HIGHWAY-2, A Highway Air Pollution Model*. EPA-600/8-80-018, PB 80-227556, US Environmental Protection Agency Environmental Science Research Triangle Park, NC.
24. Griffin, R. (1980), *Air Quality Impact of Signaling Decisions, Program MICR0 User's Guide,* CDOH-DTP-R-80-13, FHWA-CO-RD-80-12, Colorado Department of Highway, Denver, CO.
25. Griffin, R. (1983), *MICR02-an Air Quality Intersection Model, Final Report,*
26. Seinfeld, John (1986), *Atmospheric Chemistry and Physics of Air Pollution*. A Wiley Interscience Publication, JOHN WILEY & SONS.
27. Schreffler, Eric, Theresa Costa, and Carl Moyer (1996). "Evaluating Travel and Air Quality Cost-Effectiveness of Transportation Demand Management Projects." *Transportation Research Record* Vol. 1520: 11
28. Sculley, D. Robert (1989), "Vehicle Emission Rate Analysis for Carbon Monoxide Hot Spot Modeling." *Journal of Air Pollution Control association.* Vol. 39: 1334-1343.
29. Vislocky, L. Robert and J. M. Fritsch (1995), "Generalized Additive Models vs. Regression in Generating Probabilistic MOS Forecasting of Aviation Weather Parameters." *Weather and Forecasting*. Vol. 10, No. 4: 669
30. Zamurs, John (1990), "Intersection Carbon Monoxide Modeling." *Journal of Air Waste Management Association.* Vol. 40, No. 5: 760-771
31. Zamurs, John and Robert Conway (1991), "Comparison of Intersection Air Quality Model's Ability To Simulate Carbon Monoxide Concentrations in an Urban Area." *Transportation Research Record*. No. 1312: 23-32. Transportation Research Board, National Research Council, Washington, D.C.
32. American Society of Civil Engineers (1992), *Transportation Planning Requirements of the Federal Clean Air Act Amendments*. New York, New York.

33. CALTRANS (1989), *Caline4 - A Dispersion Model For Predicting Air Pollution Concentrations Near Roadways*. Division of New Technology And Research, Sacramento, California.
34. California Air Resource Board (CARB) (1996), *Methodology for Estimating Emissions from On-Road Motor Vehicles (Vol. I ~ Vol. VI)*. Technical Support Division, Sacramento, California.
35. Transportation Research Board (1994), *Highway Capacity Manual, Third Edition.* Washington, D.C.: National Research Council, 1994.
36. U.S. Department of Transportation/Federal highway Administration (1994), Air Quality Programs and Provisions of the Intermodal Surface Transportation Efficiency Act of 1991: a summary. Washington, D.C.
37. U.S. Environmental Protection Agency (1978). *Carbon Monoxide Hot Spot Guidelines, Volume V: Users Manual for the Intersection-Midblock Model (IMM).* EPA-450/3-78-037, Research Triangle Park, NC.
38. U.S. Environmental Protection Agency (1992), *Guideline For Modeling CO From Roadway Intersections*. Research Triangle Park, North Carolina 27711: Office of Air Quality Planning and Standards, Technical Support Division, November, 1992.
39. U.S. Environmental Protection Agency (1992), *Evaluation of CO Intersection Modeling Techniques Using a New York City Database, EPA-454/R-92-004,* Office of Air Quality Planning and Standards, Research Triangle Park, NC.
40. U.S. Environmental Protection Agency (1995), *User's Guide to CAL3QHC Version 2.0: A Modeling Methodology for Predicting Pollutant Concentration Near Roadway Intersections*. Research Triangle Park, NC 27711, 1995.
41. U.S. Government Printing Office (1970), *Clean Air Act.* Washington, D.C.; No. 95-11.

Appendix - I: CAL3QHCR Control File

```
 'FOUR WAY HYPOTHETICAL INTERSECTION '  60. 321.  0. 0.  20 0.3048 1
 1 1 81  12  31 81
  52158 81  91919 81
 1 0 'U'
'REC   1   (SE   CORNER)   '    -73.526131  -39.542236  6.0
'REC   2   (SW   CORNER)   '    -65.542664  51.709183  6.0
'REC   3   (NW   CORNER)   '    61.571808  40.588078  6.0
'REC   4   (NE   CORNER)   '    53.588295  -50.663342  6.0
'REC   5   (1ST   WB-EB)   '    -61.167351  101.718216  6.0
'REC   6   (2nd   WB-EB)   '    -27.525066  486.249329  6.0
'REC   7   (3rd   WB-EB)   '    -77.90136  -89.551208  6.0
'REC   8   (4th   WB-EB)   '    -111.54348  -474.082367  6.0
'REC   9   (5th   WB-EB)   '    49.213085  -100.672302  6.0
'REC   10   (6th   WB-EB)   '    15.57099  -485.20343  6.0
'REC   11   (7th   WB-EB)   '    65.947037  90.597061  6.0
'REC   12   (8th   WB-EB)   '    99.589394  475.128174  6.0
'REC   13   (1ST   SB-NB)   '    -115.551636  56.084404  6.0
'REC   14   (2ND   SB-NB)   '    -479.162689  87.896286  6.0
'REC   15   (3RD   SB-NB)   '    -123.535118  -35.166985  6.0
'REC   16   (4TH   SB-NB)   '    -487.146149  -3.355051  6.0
'REC   17   (5TH   SB-NB)   '    113.573166  36.038528  6.0
'REC   18   (6TH   SB-NB)   '    490.134735  3.093571  6.0
'REC   19   (7TH   SB-NB)   '    105.589676  -55.212856  6.0
'REC   20   (8TH   SB-NB)   '    482.151245  -88.157852  6.0
2 'C'
1 1 1 1 1 1 1
'MAIN ST. AND THIRD     INTERSECTION'       17
1 2
'EB   LEFTTURN   '   'AG'   -2.839542  36.385944  81.179054  996.71759  0.   12.0   1
2 2
'EB   THROUGH   '   'AG'   -26.748236  38.477684  57.270355  998.809326  0.   36.0   3
3 2
'EB   RIGHTTURN   '   'AG'   -50.656906  40.569424  33.361504  1000.901062  0.   12.0   1
4 2
'WB   LEFTTURN   '   'AG'   2.839547  -36.385944  -81.178909  -996.71759  0.   12.0   1
5 2
'WB   THROUGHT&RIGHT   '   'AG'   20.771053  -37.954758  -63.247513  -998.286438  0.
36.0   3
6 2
'NB   LEFTTURN   '   'AG'   -60.294617  -0.747807  -996.71759  81.178833  0.   12.0   1
7 2
'NB   THROUGH&RIGHT   '   'AG'   -61.340488  -12.702146  -997.763489  69.224449  0.   24.0
2
8 2
'SB   LEFTTURN   '   'AG'   48.340282  1.793671  996.71759  -81.179222  0.   12.0   1
9 2
'SB   THROUGH&RIGHT   '   'AG'   49.386158  13.748  997.763489  -69.224838  0.   24.0   2
10 1
'EB APPROACH '  'AG'  57.24   998.81   -29.89    2.61  0.  79.6
11 1
'EB DEPARTURE ' 'AG'  -29.89     2.61  -117.07 -993.58  0.  79.6
12 1
'WB APPROACH '  'AG'  -63.25  -998.29    23.01   -2.09  0.  67.6
13 1
'WB DEPARTURE ' 'AG'   23.01    -2.09   111.06  994.1   0.  67.6
14 1
'NB APPROACH '  'AG' -997.76    69.07    -1.57  -17.93  0.  55.6
15 1
'NB DEPARTURE ' 'AG'   -1.57   -17.93   994.63 -105.07  0.  55.6
16 1
'SB APPROACH '  'AG'  997.76   -69.07     1.57   17.93  0.  55.6
17 1
'SB DEPARTURE ' 'AG'    1.57    17.93  -994.63  105.07  0.  55.6
1       0      0
1       92      85      1     12      426     0       0      0
2       92      62      1     290     426     0       0      0
3       92      62      1     74      426     0       0      0
4       92      85      1     12      426     0       0      0
5       92      62      1     280     426     0       0      0
6       92      76      1     36      426     0       0      0
7       92      65      1     160     426     0       0      0
8       92      80      1     24      426     0       0      0
```

```
9       92      69      1     136     426     0       0       0
10      376     23
11      344     23
12      292     23
13      272     23
14      196     23
15      202     23
16      160     23
17      206     23
2       0       0
1       92      85      1     6       426     0       0       0
2       92      62      1     145     426     0       0       0
3       92      62      1     37      426     0       0       0
4       92      85      1     6       426     0       0       0
5       92      62      1     140     426     0       0       0
6       92      76      1     18      426     0       0       0
7       92      65      1     80      426     0       0       0
8       92      80      1     12      426     0       0       0
9       92      69      1     68      426     0       0       0
10      188     23
11      172     23
12      146     23
13      136     23
14      98      23
15      101     23
16      80      23
17      103     23
3       0       0
1       92      85      1     6       426     0       0       0
2       92      62      1     145     426     0       0       0
3       92      62      1     37      426     0       0       0
4       92      85      1     6       426     0       0       0
5       92      62      1     140     426     0       0       0
6       92      76      1     18      426     0       0       0
7       92      65      1     80      426     0       0       0
8       92      80      1     12      426     0       0       0
9       92      69      1     68      426     0       0       0
10      188     23
11      172     23
12      146     23
13      136     23
14      98      23
15      101     23
16      80      23
17      103     23
4       0       0
1       92      85      1     6       426     0       0       0
2       92      62      1     145     426     0       0       0
3       92      62      1     37      426     0       0       0
4       92      85      1     6       426     0       0       0
5       92      62      1     140     426     0       0       0
6       92      76      1     18      426     0       0       0
7       92      65      1     80      426     0       0       0
8       92      80      1     12      426     0       0       0
9       92      69      1     68      426     0       0       0
10      188     23
11      172     23
12      146     23
13      136     23
14      98      23
15      101     23
16      80      23
17      103     23
5       0       0
1       92      85      1     12      426     0       0       0
2       92      62      1     290     426     0       0       0
3       92      62      1     74      426     0       0       0
4       92      85      1     12      426     0       0       0
5       92      62      1     280     426     0       0       0
6       92      76      1     36      426     0       0       0
7       92      65      1     160     426     0       0       0
8       92      80      1     24      426     0       0       0
9       92      69      1     136     426     0       0       0
10      376     23
11      344     23
12      292     23
```

```
13      272     23
14      196     23
15      202     23
16      160     23
17      206     23
6       0       0
1       92      85      1       30      426     0       0       0
2       92      62      1       725     426     0       0       0
3       92      62      1       185     426     0       0       0
4       92      85      1       30      426     0       0       0
5       92      62      1       700     426     0       0       0
6       92      76      1       90      426     0       0       0
7       92      65      1       400     426     0       0       0
8       92      80      1       60      426     0       0       0
9       92      69      1       340     426     0       0       0
10      940     23
11      860     23
12      730     23
13      680     23
14      490     23
15      505     23
16      400     23
17      515     23
7       0       0
1       92      85      1       45      426     0       0       0
2       92      62      1       1088    426     0       0       0
3       92      62      1       278     426     0       0       0
4       92      85      1       45      426     0       0       0
5       92      62      1       1050    426     0       0       0
6       92      76      1       135     426     0       0       0
7       92      65      1       600     426     0       0       0
8       92      80      1       90      426     0       0       0
9       92      69      1       510     426     0       0       0
10      1410    23
11      1290    23
12      1095    23
13      1020    23
14      735     23
15      758     23
16      600     23
17      773     23
8       0       0
1       92      85      1       60      426     0       0       0
2       92      62      1       1450    426     0       0       0
3       92      62      1       370     426     0       0       0
4       92      85      1       60      426     0       0       0
5       92      62      1       1400    426     0       0       0
6       92      76      1       180     426     0       0       0
7       92      65      1       800     426     0       0       0
8       92      80      1       120     426     0       0       0
9       92      69      1       680     426     0       0       0
10      1880    23
11      1720    23
12      1460    23
13      1360    23
14      980     23
15      1010    23
16      800     23
17      1030    23
9       0       0
1       92      85      1       60      426     0       0       0
2       92      62      1       1450    426     0       0       0
3       92      62      1       370     426     0       0       0
4       92      85      1       60      426     0       0       0
5       92      62      1       1400    426     0       0       0
6       92      76      1       180     426     0       0       0
7       92      65      1       800     426     0       0       0
8       92      80      1       120     426     0       0       0
9       92      69      1       680     426     0       0       0
10      1880    23
11      1720    23
12      1460    23
13      1360    23
14      980     23
15      1010    23
16      800     23
```

```
17      1030    23
10      0       0
1       92      85      1       60      426     0       0       0
2       92      62      1       1450    426     0       0       0
3       92      62      1       370     426     0       0       0
4       92      85      1       60      426     0       0       0
5       92      62      1       1400    426     0       0       0
6       92      76      1       180     426     0       0       0
7       92      65      1       800     426     0       0       0
8       92      80      1       120     426     0       0       0
9       92      69      1       680     426     0       0       0
10      1880    23
11      1720    23
12      1460    23
13      1360    23
14      980     23
15      1010    23
16      800     23
17      1030    23
11      0       0
1       92      85      1       45      426     0       0       0
2       92      62      1       1088    426     0       0       0
3       92      62      1       278     426     0       0       0
4       92      85      1       45      426     0       0       0
5       92      62      1       1050    426     0       0       0
6       92      76      1       135     426     0       0       0
7       92      65      1       600     426     0       0       0
8       92      80      1       90      426     0       0       0
9       92      69      1       510     426     0       0       0
10      1410    23
11      1290    23
12      1095    23
13      1020    23
14      735     23
15      758     23
16      600     23
17      773     23
12      0       0
1       92      85      1       45      426     0       0       0
2       92      62      1       1088    426     0       0       0
3       92      62      1       278     426     0       0       0
4       92      85      1       45      426     0       0       0
5       92      62      1       1050    426     0       0       0
6       92      76      1       135     426     0       0       0
7       92      65      1       600     426     0       0       0
8       92      80      1       90      426     0       0       0
9       92      69      1       510     426     0       0       0
10      1410    23
11      1290    23
12      1095    23
13      1020    23
14      735     23
15      758     23
16      600     23
17      773     23
13      0       0
1       92      85      1       45      426     0       0       0
2       92      62      1       1088    426     0       0       0
3       92      62      1       278     426     0       0       0
4       92      85      1       45      426     0       0       0
5       92      62      1       1050    426     0       0       0
6       92      76      1       135     426     0       0       0
7       92      65      1       600     426     0       0       0
8       92      80      1       90      426     0       0       0
9       92      69      1       510     426     0       0       0
10      1410    23
11      1290    23
12      1095    23
13      1020    23
14      735     23
15      758     23
16      600     23
17      773     23
14      0       0
1       92      85      1       45      426     0       0       0
2       92      62      1       1088    426     0       0       0
```

```
3       92      62      1     278     426     0       0       0
4       92      85      1     45      426     0       0       0
5       92      62      1     1050    426     0       0       0
6       92      76      1     135     426     0       0       0
7       92      65      1     600     426     0       0       0
8       92      80      1     90      426     0       0       0
9       92      69      1     510     426     0       0       0
10      1410    23
11      1290    23
12      1095    23
13      1020    23
14      735     23
15      758     23
16      600     23
17      773     23
15      0       0
1       92      85      1     45      426     0       0       0
2       92      62      1     1088    426     0       0       0
3       92      62      1     278     426     0       0       0
4       92      85      1     45      426     0       0       0
5       92      62      1     1050    426     0       0       0
6       92      76      1     135     426     0       0       0
7       92      65      1     600     426     0       0       0
8       92      80      1     90      426     0       0       0
9       92      69      1     510     426     0       0       0
10      1410    23
11      1290    23
12      1095    23
13      1020    23
14      735     23
15      758     23
16      600     23
17      773     23
16      0       0
1       92      85      1     45      426     0       0       0
2       92      62      1     1088    426     0       0       0
3       92      62      1     278     426     0       0       0
4       92      85      1     45      426     0       0       0
5       92      62      1     1050    426     0       0       0
6       92      76      1     135     426     0       0       0
7       92      65      1     600     426     0       0       0
8       92      80      1     90      426     0       0       0
9       92      69      1     510     426     0       0       0
10      1410    23
11      1290    23
12      1095    23
13      1020    23
14      735     23
15      758     23
16      600     23
17      773     23
17      0       0
1       92      85      1     60      426     0       0       0
2       92      62      1     1450    426     0       0       0
3       92      62      1     370     426     0       0       0
4       92      85      1     60      426     0       0       0
5       92      62      1     1400    426     0       0       0
6       92      76      1     180     426     0       0       0
7       92      65      1     800     426     0       0       0
8       92      80      1     120     426     0       0       0
9       92      69      1     680     426     0       0       0
10      1880    23
11      1720    23
12      1460    23
13      1360    23
14      980     23
15      1010    23
16      800     23
17      1030    23
18      0       0
1       92      85      1     60      426     0       0       0
2       92      62      1     1450    426     0       0       0
3       92      62      1     370     426     0       0       0
4       92      85      1     60      426     0       0       0
5       92      62      1     1400    426     0       0       0
6       92      76      1     180     426     0       0       0
```

```
7       92      65      1     800     426     0       0       0
8       92      80      1     120     426     0       0       0
9       92      69      1     680     426     0       0       0
10      1880    23
11      1720    23
12      1460    23
13      1360    23
14      980     23
15      1010    23
16      800     23
17      1030    23
19      0       0
1       92      85      1     60      426     0       0       0
2       92      62      1     1450    426     0       0       0
3       92      62      1     370     426     0       0       0
4       92      85      1     60      426     0       0       0
5       92      62      1     1400    426     0       0       0
6       92      76      1     180     426     0       0       0
7       92      65      1     800     426     0       0       0
8       92      80      1     120     426     0       0       0
9       92      69      1     680     426     0       0       0
10      1880    23
11      1720    23
12      1460    23
13      1360    23
14      980     23
15      1010    23
16      800     23
17      1030    23
20      0       0
1       92      85      1     36      426     0       0       0
2       92      62      1     870     426     0       0       0
3       92      62      1     222     426     0       0       0
4       92      85      1     36      426     0       0       0
5       92      62      1     840     426     0       0       0
6       92      76      1     108     426     0       0       0
7       92      65      1     480     426     0       0       0
8       92      80      1     72      426     0       0       0
9       92      69      1     408     426     0       0       0
10      1128    23
11      1032    23
12      876     23
13      816     23
14      588     23
15      606     23
16      480     23
17      618     23
21      0       0
1       92      85      1     24      426     0       0       0
2       92      62      1     580     426     0       0       0
3       92      62      1     148     426     0       0       0
4       92      85      1     24      426     0       0       0
5       92      62      1     560     426     0       0       0
6       92      76      1     72      426     0       0       0
7       92      65      1     320     426     0       0       0
8       92      80      1     48      426     0       0       0
9       92      69      1     272     426     0       0       0
10      752     23
11      688     23
12      584     23
13      544     23
14      392     23
15      404     23
16      320     23
17      412     23
22      0       0
1       92      85      1     24      426     0       0       0
2       92      62      1     580     426     0       0       0
3       92      62      1     148     426     0       0       0
4       92      85      1     24      426     0       0       0
5       92      62      1     560     426     0       0       0
6       92      76      1     72      426     0       0       0
7       92      65      1     320     426     0       0       0
8       92      80      1     48      426     0       0       0
9       92      69      1     272     426     0       0       0
10      752     23
```

```
11      688     23
12      584     23
13      544     23
14      392     23
15      404     23
16      320     23
17      412     23
23      0       0
1       92       85      1       24      426     0       0       0
2       92       62      1       580     426     0       0       0
3       92       62      1       148     426     0       0       0
4       92       85      1       24      426     0       0       0
5       92       62      1       560     426     0       0       0
6       92       76      1       72      426     0       0       0
7       92       65      1       320     426     0       0       0
8       92       80      1       48      426     0       0       0
9       92       69      1       272     426     0       0       0
10      752     23
11      688     23
12      584     23
13      544     23
14      392     23
15      404     23
16      320     23
17      412     23
24      0       0
1       92       85      1       12      426     0       0       0
2       92       62      1       190     426     0       0       0
3       92       62      1       74      426     0       0       0
4       92       85      1       12      426     0       0       0
5       92       62      1       280     426     0       0       0
6       92       76      1       36      426     0       0       0
7       92       65      1       160     426     0       0       0
8       92       80      1       24      426     0       0       0
9       92       69      1       136     426     0       0       0
10      376     23
11      344     23
12      292     23
13      272     23
14      196     23
15      202     23
16      160     23
17      206     23
```

Appendix II: C Programming for Calculating the x, y Coordinates of Intersection

Rotations

```
#include <iostream.h>
#include <fstream.h>
#include <iomanip.h>
#include <string.h>
#include <math.h>

void main( )
{
  char filename[20];
  ifstream infile;
  ofstream outfile;
   float r,beta,A;
   float x1,y1;
   float k;
   char choice;
   float ag1;
    const float pi=3.1415926;


    cout<<"enter k value"<<endl;
    cin>>k;
    cout<<"k="<<k<<endl;
    cout<<"enter the name of the output file "<<endl;
    cin>>filename;

    outfile.open(filename);

      infile.open("a.inp");

     char a[6];
     char b[5];
     char c[10];
     char d[20];
     char e[10];
     char x[10];
     char y[10];
     char f[10];

  while (infile)
   {
      infile>>a
            >>b
              >>c
            >>d
            >>e
            >>x
            >>y
            >>f;

//       cout<<x[0]<<x[1]<<x[2]<<x[3]<<x[4]<<x[5]<<endl;

       if (x[3]=='.')
          {
          x1=(x[1]-48)*10+(x[2]-48)+(x[4]-48)*0.1;
          }
         else
```

```
          x1=(x[1]-48)*100+(x[2]-48)*10+(x[3]-48)+(x[5]-48)*0.1;

       if (x[0]=='-')
           x1=x1*(-1);


//        getch( );

       if (y[3]=='.')
          {
          y1=(y[1]-48)*10+(y[2]-48)+(y[4]-48)*0.1;
          }
       else
          y1=(y[1]-48)*100+(y[2]-48)*10+(y[3]-48)+(y[5]-48)*0.1;

       if (y[0]=='-')
       y1=y1*(-1);


       outfile<<a<<"   ";
       outfile<<b<<"   ";
         outfile<<c<<"   ";
       outfile<<d<<"   " ;
       outfile<<e<< "    ";
      //extracted out x and y , do some transformations
               if (x1>0)
                  beta=atan(y1/x1);
               else
            beta=pi+atan(y1/x1);
    //       cout<<beta<<endl;
            r=sqrt((x1*x1)+(y1*y1));
      //     cout<<r<<endl;

                  A=beta+(k/180)*pi;

         x1= r*(cos(A));
        // cout<<x1<<endl;
        // getch( );
         y1= r*(sin(A));
         //cout<<y1<<endl;
        // getch( );

      outfile<<x1<<"  ";
      outfile<<y1<<"  " ;
      outfile<<f<<"   ";
      outfile<<endl;

   }
   infile.close( );
   outfile.close {};
}
```

Appendix III: CAL3QHCR Output File for Rotating the Intersection 265 Degrees

```
CAL3QHCR (Dated: 95221)

JOB: EXAMPLE - TWO WAY INTERSECTION (EX-1)                      RUN: MAIN ST. AND THIRD
INTERSECTION

       ===================
       General Information
       ===================

         Run start date:  1/ 1/81    Julian:   1
               end date: 12/31/81    Julian: 365

         A Tier 2 approach was used for input data preparation.

         The MODE flag has been set to C for calculating CO averages.

         Ambient background concentrations are excluded from the averages below.


       Site & Meteorological Constants
       -------------------------------
         VS =    .0 CM/S       VD =    .0 CM/S       Z0 = 500. CM     ATIM =  60.

           Met. Sfc. Sta. Id & Yr = 52158    81
           Upper Air Sta. Id & Yr = 91919    81

         Urban mixing heights were processed.

         In 1981, Julian day 1 is a Thursday.

         The patterns from the input file
         have been assigned as follows:

           Pattern # 1 is assigned to Monday.
           Pattern # 1 is assigned to Tuesday.
           Pattern # 1 is assigned to Wednesday.
           Pattern # 1 is assigned to Thursday.
           Pattern # 1 is assigned to Friday.
           Pattern # 1 is assigned to Saturday.
           Pattern # 1 is assigned to Sunday.

       Link Data Constants - (Variable data in *.LNK file)
```

LINK DESCRIPTION	*	LINK COORDINATES (FT)				*	LENGTH	BRG	TYPE	H	W	NLANES
	*	X1	Y1	X2	Y2	*	(FT)	(DEG)		(FT)	(FT)	
1. EB LEFTTURN	*	-2.8	36.4	81.2	996.7	*	964.	5.	AG	.0	12.0	1
2. EB THROUGH	*	-26.7	38.5	57.3	998.8	*	964.	5.	AG	.0	36.0	3
3. EB RIGHTTURN	*	-50.7	40.6	33.4	000.9	*	964.	5.	AG	.0	12.0	1
4. WB LEFTTURN	*	2.8	-36.4	-81.2	-996.7	*	964.	185.	AG	.0	12.0	1
5. WB THROUGHT&RIGHT	*	20.8	-38.0	-63.2	-998.3	*	964.	185.	AG	.0	36.0	3
6. NB LEFTTURN	*	-60.3	-.7	-996.7	81.2	*	940.	275.	AG	.0	12.0	1
7. NB THROUGH&RIGHT	*	-61.3	-12.7	-997.8	69.2	*	940.	275.	AG	.0	24.0	2
8. SB LEFTTURN	*	48.3	1.8	996.7	-81.2	*	952.	95.	AG	.0	12.0	1
9. SB THROUGH&RIGHT	*	49.4	13.7	997.8	-69.2	*	952.	95.	AG	.0	24.0	2

```
       Receptor Data
       -------------

                                   *           COORDINATES (FT)
```

RECEPTOR	*	X	Y	Z
1. REC 1 (SE CORN	*	-73.5	-39.5	6.0
2. REC 2 (SW CORN	*	-65.5	51.7	6.0
3. REC 3 (NW CORN	*	61.6	40.6	6.0
4. REC 4 (NE CORN	*	53.6	-50.7	6.0
5. REC 5 (1ST WB-	*	-61.2	101.7	6.0
6. REC 6 (2nd WB-	*	-27.5	486.2	6.0
7. REC 7 (3rd WB-	*	-77.9	-89.6	6.0
8. REC 8 (4th WB-	*	-111.5	-474.1	6.0
9. REC 9 (5th WB-	*	49.2	-100.7	6.0
10. REC 10 (6th WB	*	15.6	-485.2	6.0
11. REC 11 (7th WB	*	65.9	90.6	6.0
12. REC 12 (8th WB	*	99.6	475.1	6.0
13. REC 13 (1ST SB	*	-115.6	56.1	6.0
14. REC 14 (2ND SB	*	-479.2	87.9	6.0
15. REC 15 (3RD SB	*	-123.5	-35.2	6.0
16. REC 16 (4TH SB	*	-487.1	-3.4	6.0
17. REC 17 (5TH SB	*	113.6	36.0	6.0
18. REC 18 (6TH SB	*	490.1	3.1	6.0
19. REC 19 (7TH SB	*	105.6	-55.2	6.0
20. REC 20 (8TH SB	*	482.2	-88.2	6.0

Model Results

Remarks : In search of the wind direction corresponding

==========
Output Section
==========

NOTES PERTAINING TO THE REPORT

1. THE HIGHEST AVERAGE IN EACH OF THE FIRST TWO COLUMNS OF EACH TABLE BELOW ARE SUFFIXED BY AN ASTERISK (*).
FOR PM OUTPUT, THERE IS ONLY ONE COLUMN AND ASTERISK FOR THE ANNUAL AVERAGE/PERIOD OF CONCERN TABLE.

2. THE NUMBERS IN PARENTHESES ARE THE JULIAN DAY AND ENDING HOUR FOR THE PRECEDING AVERAGE.

3. THE NUMBER OF CALM HOURS USED IN PRODUCING EACH AVERAGE ARE PREFIXED BY A C.

PRIMARY AVERAGES.

MAXIMUM 8-HOUR RUNNING NONOVERLAPPING AVERAGE CONCENTRATIONS
IN PARTS PER MILLION (ppm),
EXCLUDING AMBIENT BACKGROUND CONCENTRATIONS.

Receptor Number	Highest Conc	Highest Ending Day Hr	Highest Calm	Second highest Conc	Second highest Ending Day Hr	Second highest Calm
1	4.18	(354,12)	C 2	4.06	(323,13)	C 1
2	10.94*	(362,14)	C 0	9.61*	(364,13)	C 1
3	5.78	(157,12)	C 2	5.50	(230,13)	C 2
4	6.30	(318,24)	C 1	5.93	(62, 1)	C 2
5	6.74	(55,13)	C 0	6.66	(272,13)	C 0
6	2.33	(230,14)	C 2	2.17	(157,12)	C 2
7	2.90	(354,11)	C 2	2.58	(288,11)	C 2
8	.70	(354,11)	C 2	.41	(8, 9)	C 1
9	5.82	(290,24)	C 2	5.79	(40,12)	C 1
10	.88	(354,11)	C 2	.73	(353, 9)	C 2
11	3.65	(338,22)	C 2	3.30	(324,21)	C 1
12	1.75	(345,19)	C 4	1.73	(265,21)	C 2
13	3.68	(362,14)	C 0	3.27	(364,13)	C 1
14	1.10	(362,13)	C 0	.86	(27,14)	C 1
15	4.92	(354,11)	C 2	4.43	(42,11)	C 1
16	.97	(317,10)	C 2	.85	(362,13)	C 0
17	5.91	(149,15)	C 0	5.80	(299,23)	C 2
18	.70	(318,24)	C 1	.70	(6,23)	C 1
19	2.97	(6,24)	C 1	2.87	(40,12)	C 1

20 .63 (270,11) C 2 .55 (72,10) C 2

FIVE HIGHEST 1-HOUR END-TO-END AVERAGE CONCENTRATIONS IN PARTS PER MILLION
EXCLUDING AMBIENT BACKGROUND CONCENTRATIONS.

Rcptr	Highest Ending			Second Highest Ending			Third Highest Ending			Fourth Highest Ending			Fifth Highest Ending		
	Conc	Day	Hr Calm	Conc	Day	Hr Calm	Conc	Day	Hr Calm	Conc	Day	Hr Calm	Conc	Day	Hr Calm
1	8.80	(32,	8) C0	8.70	(1,	9) C0	7.60	(354,	9) C0	7.50	(304,	19) C0	6.80	(320,	7) C0
2	17.50*	(362,	9) C0	16.80*	(362,	10) C0	16.60	(364,	9) C0	16.30	(363,	19) C0	16.20	(362,	8) C0
3	8.00	(49,	18) C0	8.00	(111,	19) C0	8.00	(126,	19) C0	8.00	(288,	19) C0	8.00	(364,	19) C0
4	7.50	(61,	19) C0	7.50	(70,	8) C0	7.50	(79,	8) C0	7.50	(129,	8) C0	7.50	(138,	19) C0
5	10.00	(10,	9) C0	9.90	(6,	9) C0	9.90	(7,	8) C0	9.90	(14,	10) C0	9.90	(16,	18) C0
6	7.30	(249,	10) C0	7.20	(32,	19) C0	7.20	(236,	19) C0	7.20	(268,	19) C0	7.20	(336,	8) C0
7	5.30	(32,	8) C0	5.20	(1,	9) C0	4.70	(304,	19) C0	4.60	(354,	9) C0	4.30	(30,	9) C0
8	2.70	(32,	8) C0	2.40	(1,	9) C0	2.00	(354,	9) C0	1.60	(304,	19) C0	1.60	(354,	8) C0
9	8.80	(52,	9) C0	8.80	(322,	9) C0	8.80	(327,	8) C 0	8.70	(18,	8) C0	8.70	(22,	8) C0
10	3.50	(304,	19) C0	3.30	(354,	9) C0	3.00	(291,	9) C0	2.90	(1,	9) C0	2.70	(353,	9) C0
11	6.70	(338,	21) C0	5.20	(153,	8) C0	5.20	(359,	8) C0	5.10	(26,	19) C0	5.10	(40,	8) C0
12	4.30	(7,	18) C0	4.30	(53,	18) C0	4.30	(69,	19) C0	4.30	(83,	19) C0	4.30	(228,	19) C0
13	5.80	(362,	8) C0	5.60	(361,	19) C0	5.60	(363,	19) C0	5.50	(362,	10) C0	5.40	(360,	9) C0
14	2.40	(53,	9) C0	2.40	(333,	8) C0	2.40	(348,	9) C0	2.30	(50,	8) C0	2.30	(58,	8) C0
15	9.00	(42,	8) C0	8.90	(265,	8) C0	8.90	(304,	9) C0	8.70	(74,	8) C0	8.70	(307,	8) C0
16	2.40	(9,	9) C0	2.40	(68,	8) C0	2.40	(274,	10) C0	2.40	(278,	8) C0	2.40	(289,	8) C0
17	8.70	(1,	18) C0	8.70	(2,	18) C0	8.70	(3,	9) C0	8.70	(10,	17) C0	8.70	(17,	18) C0
18	2.30	(5,	8) C0	2.30	(6,	19) C0	2.30	(79,	8) C0	2.30	(129,	8) C0	2.30	(134,	8) C0
19	6.00	(21,	8) C0	5.90	(18,	9) C0	5.90	(290,	8) C0	5.80	(306,	8) C0	5.80	(320,	8) C0
20	2.30	(295,	8) C0	2.30	(303,	19) C0	2.20	(33,	8) C0	2.20	(72,	8) C0	2.20	(318,	19) C0

MAXIMUM 8-HOUR AVERAGED LINK CONTRIBUTIONS
IN PARTS PER MILLION (ppm)
EXCLUDING AMBIENT BACKGROUND CONCENTRATIONS.

Rcptr No.	Total Conc	Ending Day Hr	Ambient Backgnd	Total Link	Link +1	Link +2	Link +3	Link +4	Link +5	Link +6	Link +7	Link +8	Link +9
1	4.18	(354,12)	.00	4.18	.08	1.30	.40	.03	.08	.05	1.87	.07	.30
2	10.94	(362,14)	.00	10.94	.38	2.64	6.50	.01	.20	.00	.10	.20	.91
3	5.78	(157,12)	.00	5.77	.00	.00	.00	.08	1.33	.00	.03	.83	3.48
4	6.30	(318,24)	.00	6.23	.00	.00	.01	.39	5.43	.00	.40	.00	.00
5	6.74	(55,13)	.00	5.31	.20	4.14	.21	.01	.15	.00	.06	.06	.47
6	2.33	(230,14)	.00	2.27	.02	1.82	.02	.00	.15	.00	.17	.02	.08
7	2.90	(354,11)	.00	2.90	.05	.87	.18	.15	.63	.00	.62	.05	.35

8	.70 (354,11)	.00	.70	.00	.22	.02	.00	.30	.00	.10	.00	.07
9	5.82 (290,24)	.00	5.77	.02	.25	.10	.22	4.53	.00	.40	.07	.18
10	.88 (354,11)	.00	.88	.00	.22	.02	.02	.48	.00	.03	.02	.10
11	3.65 (338,22)	.00	3.03	.22	1.25	.25	.05	.50	.00	.38	.12	.27
12	1.75 (345,19)	.00	1.68	.02	1.43	.02	.00	.10	.00	.10	.00	.02
13	3.68 (362,14)	.00	3.67	.20	1.15	1.04	.04	.28	.00	.21	.13	.64
14	1.10 (362,13)	.00	1.10	.03	.21	.05	.01	.24	.00	.39	.04	.14
15	4.92 (354,11)	.00	4.92	.07	.98	.22	.02	.05	.05	3.30	.03	.20
16	.97 (317,10)	.00	.93	.02	.22	.03	.02	.15	.00	.35	.03	.12
17	5.91 (149,15)	.00	5.90	.01	.01	.01	.13	1.24	.00	.16	.72	3.61
18	.70 (318,24)	.00	.69	.01	.13	.01	.01	.19	.00	.07	.03	.23
19	2.97 (6,24)	.00	2.96	.03	.36	.07	.16	1.46	.00	.27	.16	.46
20	.63 (270,11)	.00	.63	.02	.13	.02	.00	.18	.00	.07	.02	.20

SECOND HIGHEST 8-HOUR AVERAGED LINK CONTRIBUTIONS
IN PARTS PER MILLION (ppm)
EXCLUDING AMBIENT BACKGROUND CONCENTRATIONS.

Rcptr No.	Total Conc	Ending Day Hr	Ambient Backgnd	Total Link	Link +1	Link +2	Link +3	Link +4	Link +5	Link +6	Link +7	Link +8	Link +9
1	4.06 (323,13)	.00	3.59	.04	.71	.20	.03	.51	.01	1.97	.03	.07	
2	9.61 (364,13)	.00	9.61	.26	2.44	5.71	.04	.30	.00	.11	.13	.61	
3	5.50 (230,13)	.00	5.50	.00	.00	.00	.13	1.73	.00	.00	.73	2.90	
4	5.93 (62, 1)	.00	5.85	.00	.03	.03	.43	4.90	.00	.45	.00	.00	
5	6.66 (272,13)	.00	5.41	.28	3.71	.26	.03	.34	.00	.03	.13	.65	
6	2.17 (157,12)	.00	2.13	.00	1.70	.03	.00	.15	.00	.13	.02	.10	
7	2.58 (288,11)	.00	2.48	.00	.18	.05	.17	1.25	.00	.50	.05	.28	
8	.41 (8, 9)	.00	.41	.00	.10	.00	.00	.20	.00	.07	.00	.04	
9	5.79 (40,12)	.00	5.74	.00	.03	.01	.04	5.50	.00	.16	.00	.00	
10	.73 (353, 9)	.00	.73	.00	.17	.03	.02	.37	.00	.10	.00	.05	
11	3.30 (324,21)	.00	3.27	.19	1.19	.20	.07	.73	.00	.31	.16	.43	
12	1.73 (265,21)	.00	1.67	.02	1.40	.02	.00	.10	.00	.12	.00	.02	
13	3.27 (364,13)	.00	3.27	.10	1.16	.80	.04	.34	.00	.36	.09	.39	
14	.86 (27,14)	.00	.83	.01	.24	.04	.00	.13	.00	.26	.01	.13	
15	4.43 (42,11)	.00	4.04	.09	.83	.27	.06	.34	.03	2.06	.07	.30	
16	.85 (362,13)	.00	.85	.00	.08	.03	.03	.31	.00	.31	.01	.09	
17	5.80 (299,23)	.00	5.80	.03	.10	.07	.15	1.27	.00	.25	.67	3.27	

18	.70 (6,23)	.00	.69	.01	.11	.01	.00	.20	.00	.10	.03	.21
19	2.87 (40,12)	.00	2.84	.01	.20	.04	.10	2.13	.00	.16	.07	.13
20	.55 (72,10)	.00	.53	.00	.13	.03	.00	.10	.00	.07	.02	.18

MAXIMUM 1-HOUR AVERAGED LINK CONTRIBUTIONS
IN PARTS PER MILLION (ppm)
EXCLUDING AMBIENT BACKGROUND CONCENTRATIONS.

Rcptr No.	Total Conc	Ending Day Hr	Ambient Backgnd	Total Link	Link +1	Link +2	Link +3	Link +4	Link +5	Link +6	Link +7	Link +8	Link +9
1	8.80	(32, 8)	.00	8.40	.10	3.90	1.20	.00	.00	.10	3.10	.00	.00
2	17.50	(362, 9)	.00	17.50	.60	3.10	11.60	.00	.10	.00	.00	.40	1.70
3	8.00	(49,18)	.00	8.00	.00	.00	.00	.30	3.80	.00	.00	.90	3.00
4	7.50	(61,19)	.00	7.40	.00	.00	.00	1.10	5.40	.00	.90	.00	.00
5	10.00	(10, 9)	.00	8.00	.80	5.30	.00	.00	.10	.00	.00	.30	1.50
6	7.30	(249,10)	.00	7.30	.10	6.00	.10	.00	.50	.00	.10	.10	.40
7	5.30	(32, 8)	.00	5.00	.10	3.00	.70	.00	.00	.00	1.20	.00	.00
8	2.70	(32, 8)	.00	2.60	.00	.80	.10	.10	1.10	.00	.30	.00	.20
9	8.80	(52, 9)	.00	8.60	.00	.30	.30	1.00	5.90	.00	1.10	.00	.00
10	3.50	(304,19)	.00	3.40	.00	.80	.10	.10	1.90	.00	.20	.10	.20
11	6.70	(338,21)	.00	2.90	.20	1.90	.30	.00	.00	.00	.50	.00	.00
12	4.30	(7,18)	.00	4.10	.00	3.40	.10	.00	.20	.00	.40	.00	.00
13	5.80	(362, 8)	.00	5.80	.40	2.00	1.90	.00	.10	.00	.00	.20	1.20
14	2.40	(53, 9)	.00	2.30	.00	.30	.10	.10	.50	.00	.90	.10	.30
15	9.00	(42, 8)	.00	8.10	.20	2.90	.90	.00	.00	.10	4.00	.00	.00
16	2.40	(9, 9)	.00	2.30	.10	.50	.10	.00	.30	.00	.90	.10	.30
17	8.70	(1,18)	.00	8.70	.00	.00	.00	.20	2.80	.00	.00	1.40	4.30
18	2.30	(5, 8)	.00	2.20	.10	.40	.10	.00	.30	.00	.30	.10	.90
19	6.00	(21, 8)	.00	5.80	.20	2.40	.00	.00	.00	.00	.00	1.10	2.10
20	2.30	(295, 8)	.00	2.20	.00	.40	.10	.10	.40	.00	.30	.10	.80

SECOND HIGHEST 1-HOUR AVERAGED LINK CONTRIBUTIONS
IN PARTS PER MILLION (ppm)
EXCLUDING AMBIENT BACKGROUND CONCENTRATIONS.

Rcptr No.	Total Conc	Ending Day Hr	Ambient Backgnd	Total Link	Link +1	Link +2	Link +3	Link +4	Link +5	Link +6	Link +7	Link +8	Link +9
1	8.70	(1, 9)	.00	8.20	.10	3.60	1.20	.00	.00	.10	3.20	.00	.00
2	16.80	(362,10)	.00	16.80	.70	3.70	10.40	.00	.00	.00	.00	.30	1.70
3	8.00	(111,19)	.00	8.00	.00	.00	.00	.20	3.70	.00	.00	1.00	3.10
4	7.50	(70, 8)	.00	7.20	.00	.00	.00	1.00	4.70	.00	1.50	.00	.00
5	9.90	(6, 9)	.00	7.90	.70	5.30	.00	.00	.10	.00	.00	.30	1.50

6	7.20	(32,19)	.00	7.20	.10	6.00	.10	.00	.50	.00	.10	.10
.30												
7	5.20	(1, 9)	.00	4.80	.10	2.80	.60	.00	.00	.00	1.30	.00
.00												
8	2.40	(1, 9)	.00	2.30	.00	.80	.10	.10	.90	.00	.30	.00
.10												
9	8.80	(322, 9)	.00	8.60	.00	.20	.30	1.00	5.90	.00	1.20	.00
.00												
10	3.30	(354, 9)	.00	3.30	.00	.80	.10	.10	1.80	.00	.10	.10
.30												
11	5.20	(153, 8)	.00	5.10	.70	2.70	.70	.00	.00	.00	1.00	.00
.00												
12	4.30	(53,18)	.00	4.20	.00	3.50	.10	.00	.20	.00	.40	.00
.00												
13	5.60	(361,19)	.00	5.60	.40	2.30	1.70	.00	.00	.00	.00	.20
1.00												
14	2.40	(333, 8)	.00	2.30	.00	.30	.10	.10	.50	.00	.90	.10
.30												
15	8.90	(265, 8)	.00	8.00	.20	2.70	.90	.00	.00	.10	4.00	.00
.10												
16	2.40	(68, 8)	.00	2.30	.10	.50	.10	.00	.30	.00	.90	.10
.30												
17	8.70	(2,18)	.00	8.70	.00	.00	.00	.20	2.80	.00	.00	1.40
4.30												
18	2.30	(6,19)	.00	2.20	.10	.50	.10	.00	.30	.00	.30	.10
.80												
19	5.90	(18, 9)	.00	5.80	.20	2.40	.10	.00	.00	.00	.00	1.10
2.00												
20	2.30	(303,19)	.00	2.20	.10	.50	.10	.00	.30	.00	.30	.10
.80												

Appendix IV: Control File for Dropping All the Separate Left- and Right-Turn Lanes

```
'EXAMPLE - TWO WAY INTERSECTION (EX-1)'  60. 321.  0. 0.  20 0.3048 1
 1 1 81  12  31 81
  52158 81  91919 81
 1 0 'U'
'REC   1   (SE   CORNER)   '    -48.571587  -29.679636  6.0
'REC   2   (SW   CORNER)   '    -42.679848  37.663116  6.0
'REC   3   (NW   CORNER)   '    48.571598  29.679619  6.0
'REC   4   (NE   CORNER)   '    42.679836  -37.663132  6.0
'REC   5   (1ST   WB-EB)   '    -38.304623  87.672096  6.0
'REC   6   (2nd   WB-EB)   '    -4.662333  472.203247  6.0
'REC   7   (3rd   WB-EB)   '    -52.946835  -79.688606  6.0
'REC   8   (4th   WB-EB)   '    -86.588997  -464.219757  6.0
'REC   9   (5th   WB-EB)   '    38.304634  -87.672089  6.0
'REC   10   (6th   WB-EB)   '    4.662404  -472.203247  6.0
'REC   11   (7th   WB-EB)   '    52.946846  79.688591  6.0
'REC   12   (8th   WB-EB)   '    86.589066  464.219757  6.0
'REC   13   (1ST   SB-NB)   '    -92.688805  42.038372  6.0
'REC   14   (2ND   SB-NB)   '    -456.299866  73.850334  6.0
'REC   15   (3RD   SB-NB)   '    -98.580566  -25.304392  6.0
'REC   16   (4TH   SB-NB)   '    -462.19162  6.507519  6.0
'REC   17   (5TH   SB-NB)   '    100.572952  25.130087  6.0
'REC   18   (6TH   SB-NB)   '    477.134552  -7.814862  6.0
'REC   19   (7TH   SB-NB)   '    94.681206  -42.212669  6.0
'REC   20   (8TH   SB-NB)   '    471.242798  -75.157677  6.0
2 'C'
1 1 1 1 1 1 1
'MAIN ST. AND THIRD     INTERSECTION'       12
1 2
'EB   ALLTURNS   '   'AG'   -15.839744  25.477489  69.22467  997.763489  0.   36.0   3
2 2
'WB   ALLTURNS   '   'AG'   15.83976  -25.47748  -69.224525  -997.763489  0.   36.0   3
3 2
'NB   ALLTURNS   '   'AG'   -37.431816  -14.793883  -997.763489  69.224449  0.   24.0   2
4 2
'SB   ALLTURNS   '   'AG'   37.43182  14.793878  997.763489  -69.224838  0.  24.0   2
5 1
'EB APPROACH '  'AG'  69.22  997.76  -17.93  1.57  0.  55.6
6 1
'EB DEPARTURE'  'AG' -17.93  1.57  -105.07  -994.63 0.  55.6
7 1
'WB APPROACH '  'AG' -69.22  -997.76  17.93  -1.57  0.  55.6
8 1
'WB DEPARTURE'  'AG' 17.93  -1.57  105.09   994.63  0.  55.6
9 1
'NB APPROACH '  'AG' -997.76  69.22  -1.05  -11.95  0.  43.6
10 1
'NB DEPARTURE'  'AG' -1.05  -11.95  995.15  -99.15  0.  43.6
11 1
'SB APPROACH '  'AG' 997.23  -69.22  1.05  11.95    0.  43.6
12 1
'SB DEPARTURE'  'AG' 1.05  11.95  -995.15  99.15    0.  43.6
1        0
        1       96      71      1       194     426     0       0       0
        2       96      71      1       184     426     0       0       0
        3       96      80      1       74      426     0       0       0
        4       96      82      1       62      426     0       0       0
5      194   23
6      174   23
7      194   23
8      188   23
9      74    23
10     84    23
11     62    23
12     84    23
2       0
        1       96      71      1       97      426     0       0       0
        2       96      71      1       97      426     0       0       0
        3       96      80      1       37      426     0       0       0
        4       96      82      1       31      426     0       0       0
5      97    23
6      87    23
```

```
7      97    23
8      92    23
9      37    23
10     42    23
11     31    23
12     42    23
3       0
        1       96      71      1       97      426     0       0       0
        2       96      71      1       97      426     0       0       0
        3       96      80      1       37      426     0       0       0
        4       96      82      1       31      426     0       0       0
5      97    23
6      87    23
7      97    23
8      92    23
9      37    23
10     42    23
11     31    23
12     42    23
4       0
        1       96      71      1       97      426     0       0       0
        2       96      71      1       97      426     0       0       0
        3       96      80      1       37      426     0       0       0
        4       96      82      1       31      426     0       0       0
5      97    23
6      87    23
7      97    23
8      92    23
9      37    23
10     42    23
11     31    23
12     42    23
5       0
        1       96      71      1       97      426     0       0       0
        2       96      71      1       97      426     0       0       0
        3       96      80      1       37      426     0       0       0
        4       96      82      1       31      426     0       0       0
5      97    23
6      87    23
7      97    23
8      92    23
9      37    23
10     42    23
11     31    23
12     42    23
6       0
        1       96      71      1       388     426     0       0       0
        2       96      71      1       388     426     0       0       0
        3       96      80      1       148     426     0       0       0
        4       96      82      1       124     426     0       0       0
5     388    23
6     348    23
7     388    23
8     364    23
9     148    23
10    168    23
11    124    23
12    168    23
7       0
        1       96      71      1       388     426     0       0       0
        2       96      71      1       388     426     0       0       0
        3       96      80      1       148     426     0       0       0
        4       96      82      1       124     426     0       0       0
5     388    23
6     348    23
7     388    23
8     364    23
9     148    23
10    168    23
11    124    23
12    168    23
8       0
        1       96      71      1       970     426     0       0       0
        2       96      71      1       970     426     0       0       0
        3       96      80      1       370     426     0       0       0
        4       96      82      1       310     426     0       0       0
```

```
5     970    23
6     870    23
7     970    23
8     910    23
9     370    23
10    420    23
11    310    23
12    420    23
9       0
        1       96      71      1       970     426     0       0       0
        2       96      71      1       970     426     0       0       0
        3       96      80      1       370     426     0       0       0
        4       96      82      1       310     426     0       0       0
5     970    23
6     870    23
7     970    23
8     910    23
9     370    23
10    420    23
11    310    23
12    420    23
10      0
        1       96      71      1       970     426     0       0       0
        2       96      71      1       970     426     0       0       0
        3       96      80      1       370     426     0       0       0
        4       96      82      1       310     426     0       0       0
5     970    23
6     870    23
7     970    23
8     910    23
9     370    23
10    420    23
11    310    23
12    420    23
11      0
        1       96      71      1       728     426     0       0       0
        2       96      71      1       728     426     0       0       0
        3       96      80      1       278     426     0       0       0
        4       96      82      1       234     426     0       0       0
5     728    23
6     653    23
7     728    23
8     683    23
9     278    23
10    315    23
11    233    23
12    315    23
12      0
        1       96      71      1       728     426     0       0       0
        2       96      71      1       728     426     0       0       0
        3       96      80      1       278     426     0       0       0
        4       96      82      1       234     426     0       0       0
5     728    23
6     653    23
7     728    23
8     683    23
9     278    23
10    315    23
11    233    23
12    315    23
13      0
        1       96      71      1       728     426     0       0       0
        2       96      71      1       728     426     0       0       0
        3       96      80      1       278     426     0       0       0
        4       96      82      1       234     426     0       0       0
5     728    23
6     653    23
7     728    23
8     683    23
9     278    23
10    315    23
11    233    23
12    315    23
14      0
        1       96      71      1       728     426     0       0       0
        2       96      71      1       728     426     0       0       0
```

```
        3       96      80      1       278     426     0       0       0
        4       96      82      1       234     426     0       0       0
5     728     23
6     653     23
7     728     23
8     683     23
9     278     23
10    315     23
11    233     23
12    315     23
15      0
        1       96      71      1       728     426     0       0       0
        2       96      71      1       728     426     0       0       0
        3       96      80      1       278     426     0       0       0
        4       96      82      1       234     426     0       0       0
5     728     23
6     653     23
7     728     23
8     683     23
9     278     23
10    315     23
11    233     23
12    315     23
16      0
        1       96      71      1       970     426     0       0       0
        2       96      71      1       970     426     0       0       0
        3       96      80      1       370     426     0       0       0
        4       96      82      1       310     426     0       0       0
5     970     23
6     870     23
7     970     23
8     910     23
9     370     23
10    420     23
11    310     23
12    420     23
17      0
        1       96      71      1       970     426     0       0       0
        2       96      71      1       970     426     0       0       0
        3       96      80      1       370     426     0       0       0
        4       96      82      1       310     426     0       0       0
5     970     23
6     870     23
7     970     23
8     910     23
9     370     23
10    420     23
11    310     23
12    420     23
18      0
        1       96      71      1       970     426     0       0       0
        2       96      71      1       970     426     0       0       0
        3       96      80      1       370     426     0       0       0
        4       96      82      1       310     426     0       0       0
5     970     23
6     870     23
7     970     23
8     910     23
9     370     23
10    420     23
11    310     23
12    420     23
19      0
        1       96      71      1       970     426     0       0       0
        2       96      71      1       970     426     0       0       0
        3       96      80      1       370     426     0       0       0
        4       96      82      1       310     426     0       0       0
5     970     23
6     870     23
7     970     23
8     910     23
9     370     23
10    420     23
11    310     23
12    420     23
20      0
```

```
        1       96      71      1       582     426     0       0       0
        2       96      71      1       582     426     0       0       0
        3       96      80      1       222     426     0       0       0
        4       96      82      1       186     426     0       0       0
5     582     23
6     522     23
7     582     23
8     546     23
9     222     23
10    252     23
11    186     23
12    252     23
21      0
        1       96      71      1       582     426     0       0       0
        2       96      71      1       582     426     0       0       0
        3       96      80      1       222     426     0       0       0
        4       96      82      1       186     426     0       0       0
5     582     23
6     522     23
7     582     23
8     546     23
9     222     23
10    252     23
11    186     23
12    252     23
22      0
        1       96      71      1       388     426     0       0       0
        2       96      71      1       388     426     0       0       0
        3       96      80      1       148     426     0       0       0
        4       96      82      1       124     426     0       0       0
5     388     23
6     348     23
7     388     23
8     364     23
9     148     23
10    168     23
11    124     23
12    168     23
23      0
        1       96      71      1       388     426     0       0       0
        2       96      71      1       148     426     0       0       0
        3       96      80      1       148     426     0       0       0
        4       96      82      1       124     426     0       0       0
5     388     23
6     348     23
7     388     23
8     364     23
9     148     23
10    168     23
11    124     23
12    168     23
24      0
        1       96      71      1       194     426     0       0       0
        2       96      71      1       194     426     0       0       0
        3       96      80      1       74      426     0       0       0
        4       96      82      1       62      426     0       0       0
5     194     23
6     174     23
7     194     23
8     182     23
9      74     23
10     84     23
11     62     23
12     84     23
```

Appendix V: Detailed Statistics of MODEL7

```
Call: gam(formula = sqrt(CO) ~ TVRT * ffef * qef * I(1/ws) * s(deg))
Deviance Residuals:
        Min          1Q     Median         3Q       Max
 -0.3377383 -0.05327348 0.01145361 0.06911144 0.2462609

(Dispersion Parameter for Gaussian family taken to be 0.010225 )

    Null Deviance: 530.8084 on 2915 degrees of freedom

Residual Deviance: 9.45834 on 2881.002 degrees of freedom

Number of Local Scoring Iterations: 1

DF for Terms and F-values for Nonparametric Effects

                             Df Npar Df  Npar F Pr(F)
                  (Intercept)  1
                         TVRT  1
                         ffef  1
                          qef  1
                       I(1/ws)  1
                         s(deg)  1       3 428.221     0
                      TVRT:ffef  1
                       TVRT:qef  1
                       ffef:qef  1
                    TVRT:I(1/ws)  1
                    ffef:I(1/ws)  1
                     qef:I(1/ws)  1
                     TVRT:s(deg)  1
                     ffef:s(deg)  1
                      qef:s(deg)  1
                   I(1/ws):s(deg)  1
                    TVRT:ffef:qef  1
               TVRT:ffef:I(1/ws)  1
                TVRT:qef:I(1/ws)  1
                ffef:qef:I(1/ws)  1
                TVRT:ffef:s(deg)  1
                 TVRT:qef:s(deg)  1
                 ffef:qef:s(deg)  1
            TVRT:I(1/ws):s(deg)  1
            ffef:I(1/ws):s(deg)  1
             qef:I(1/ws):s(deg)  1
          TVRT:ffef:qef:I(1/ws)  1
           TVRT:ffef:qef:s(deg)  1
      TVRT:ffef:I(1/ws):s(deg)  1
       TVRT:qef:I(1/ws):s(deg)  1
       ffef:qef:I(1/ws):s(deg)  1
TVRT:ffef:qef:I(1/ws):s(deg)  1
```

Coefficients(MODEL7)

```
(Intercept)         TVRT      ffef         qef   I(1/ws)       s(deg)
TVRT:ffef      TVRT:qef
   0.5057894 0.0001620727 0.0024598 0.001367051 0.5653725 0.0003296539
0.00001220306 2.876189e-007
       ffef:qef TVRT:I(1/ws) ffef:I(1/ws) qef:I(1/ws)    TVRT:s(deg)
ffef:s(deg)     qef:s(deg)
 -4.718339e-006 0.0001403846  0.006767998 0.001235776 -4.638322e-007 -
9.702114e-006 -6.375061e-007
 I(1/ws):s(deg)  TVRT:ffef:qef TVRT:ffef:I(1/ws) TVRT:qef:I(1/ws)
ffef:qef:I(1/ws) TVRT:ffef:s(deg)
  -0.0005905532 -7.326684e-009     3.097587e-006    5.964968e-007   -
5.582865e-006    6.518139e-009
 TVRT:qef:s(deg) ffef:qef:s(deg) TVRT:I(1/ws):s(deg) ffef:I(1/ws):s(deg)
qef:I(1/ws):s(deg)
   4.299014e-010   1.988366e-008       6.091722e-007       5.556044e-006
1.015428e-006
 TVRT:ffef:qef:I(1/ws) TVRT:ffef:qef:s(deg) TVRT:ffef:I(1/ws):s(deg)
TVRT:qef:I(1/ws):s(deg)
        -9.013931e-010       -1.203309e-011           -6.876637e-009
-1.152603e-009
 ffef:qef:I(1/ws):s(deg) TVRT:ffef:qef:I(1/ws):s(deg)
          -7.935235e-009                1.996407e-012
```